DETERMINATION OF COEFFICIENT OF RATE OF HORIZONTAL CONSOLIDATION OF PEAT SOIL

NURLY GOFAR

Laporan Projek Penyelidikan Fundamental
Vot 75210

Faculty of Civil Engineering
Universiti Teknologi Malaysia

JUNE 2006

IN THE NAME OF ALLAH THE BENEFICENT THE MERCIFUL.

ACKNOWLEDGEMENT

The author would like to convey her sincere appreciation to the Research Management Center (RMC) of Universiti Teknologi Malaysia for the support to carry out this fundamental research (vot 75210). Special gratitude is dedicated to the Faculty of Civil Engineering and the staff of the Geotechnical Laboratory for their support and encouragement. The author is also indebted to her research assistants (Yulindasari and Wong Leong Sing) for conducting the laboratory work and analysis. Appreciations are also conveyed to those who contributed in one way or the other to finish this research.

ABSTRACT

Encountered extensively in wetlands, fibrous peat is considered as problematic soil because it exhibits unusual compression behavior. When a mass of fibrous peat soil with both vertical and horizontal drainage boundaries is subjected to a consolidation pressure, rate of excess pore water dissipation from the soil in the horizontal direction (c_h) is expected to be higher than that in the vertical direction (c_v). c_h/c_v of two is commonly used in practice for estimation of consolidation in soft clay improved by vertical drain whereas published data showed that the c_h/c_v ratio for fibrous peat could be as high as 300.

This research focused on the consolidation behavior of fibrous peat from Kampung Bahru, Pontian, Johor with respect to one-dimensional vertical and horizontal consolidation. The result is useful for evaluation of the utilization of some type of vertical drainage for soil improvement to accelerate the settlement of fibrous peat soil.

Results from constant head permeability reveal that the soil is almost isotropic as indicated by equal initial permeability in horizontal and vertical direction. Hydraulic consolidation tests in Rowe cell, the coefficient of rate of horizontal consolidation increases significantly with consolidation pressure, while the increase in the coefficient of rate of vertical consolidation does not increase as much. The c_h/c_v ratio increase from 3.5 to 6 for consolidation pressure of 25 to 200 kPa. The ratio of coefficient of permeability k_h/k_v under a consolidation pressure of 200 kPa is about 5. This finding implies that the utilization of horizontal drain maybe suitable for accelerating settlement and reducing the effect of secondary consolidation.

ABSTRAK

Ditemui secara meluas di kawasan paya, tanah gambut gentian adalah tanah bermasalah kerana mempunyai sifat pengukuhan yang luar biasa. Apabila sesuatu jisim tanah gambut berfiber yang terdedah kepada sistem saliran air secara menegak dan mendatar dikenakan tekanan pengukuhan, kadar lesapan air terlebih secara mendatar (c_h) pada amnya adalah lebih tinggi berbanding dengan kadar lesapan air terlebih secara menegak (c_v). Nisbah c_h/c_v sebesar dua biasa digunakan untuk pengiraan pengukuhan tanah liat lembut yang dibaiki dengan menggunakan saliran menegak. Bahkan data yang sudah dipublikasikan sebelum ini menunjukkan bahawa nisbah tersebut dapat meningkat sehingga 300 untuk tanah gambut gentian.

Projek penyelidikan ini membincangkan hasil kajian makmal tentang sifat pengukuhan tanah secara menegak dan mendatar bagi sampel-sampel tanah gambut gentian yang didapati dari kampung Bahru, Pontian, Johor. Hasil kajian akan berguna untuk mengevaluasi kesesuaian kaedah saliran menegak untuk pembaikan tanah gambut gentian.

Keputusan ujian keboleh telapan dengan tekanan tetap yang ditunjukkan dari cirri keboleh telapan menegak (k_v) dan mendatar (k_h) menunjukan bahawa tanah adalah isotropik. Walau bagaimanapun ciri keboleh telapan ini berkurang selepas berlakunya tekanan. Keputusan ujian pengukuhan hidraulik dengan sel Rowe menunjukkan bahawa ciri keboleh telapan dalam arah mendatar meningkat dengan cepat berbanding tekanan pengukuhan. Nisbah c_h/c_v meningkat dari 3.5 kepada 6 untuk peningkatan tekanan pengukuhan dari 25 kepada 200 kPa. Nisbah k_h/k_v adalah 5 untuk tekanan pengukuhan sebesar 200 kPa. Ini menandakan bahawa penggunaan sistem saliran air secara mendatar mungkin sesuai bagi mempercepatkan proses pemendapan tanah gambut gentian.

TABLE OF CONTENTS

LIST OF TABLES

LIST OF FIGURES

LIST OF SYMBOLS

A	-	Area of sample
AC	-	Ash content
B	-	Pore pressure parameter
c_c	-	Compression index
c_h	-	Horizontal coefficient of consolidation
c_r	-	Recompression index
c_v	-	Vertical coefficient of consolidation
c_α, $c_{\alpha 1}$	-	Coefficient of secondary compression
$c_{\alpha 2}$	-	Coefficient of tertiary compression
D	-	Diameter of sample
e	-	Void ratio
e_o	-	Initial void ratio
FC	-	Fiber content
G_s	-	Specific gravity
H, H_o	-	Initial thickness of consolidating soil layer
h	-	Head loss due to the height of water in the burette
i	-	Hydraulic gradient
k_h	-	Horizontal coefficient of permeability
k_{ho}	-	Initial horizontal coefficient of permeability
k_v	-	Vertical coefficient of permeability
k_{vo}	-	Initial vertical coefficient of permeability

L	-	Longest drainage path in consolidating soil layer; equal to half of H with top and bottom drainage, and equal to H with top drainage only
m	-	Secondary compression factor
m_v	-	Coefficient of volume compressibility
OC	-	Organic content
p	-	Consolidation pressure
p_o	-	Initial pressure
p_1	-	Inlet pressure
p_2	-	Outlet pressure
Q	-	Cumulative flow
q	-	Rate of flow
r	-	Radius of sample
T_r	-	Radial theoretical time factor
T_v	-	Vertical theoretical time factor
t	-	Time
t_s	-	Time to reach end of secondary compression
t_p	-	Time to reach end of primary consolidation
U_r	-	Average degree of consolidation due to radial drainage
U_v	-	Average degree of consolidation due to vertical drainage
u	-	Excess pore water pressure at any point and any time
u_o	-	Initial excess pore water pressure
w	-	Natural moisture content
ΔH_s	-	Change in height of soil layer due to secondary compression from time, t_1 to time, t_2
ΔH_t	-	Change in height of soil layer due to tertiary compression from time, t_3 to time, t_4

Δp	-	Pressure difference
ε_i	-	Instantaneous strain
ε_p	-	Primary strain
ε_s	-	Secondary strain
ε_t	-	Tertiary strain
γ_w	-	Unit weight of water
σ'_v	-	Effective vertical stress
δ	-	Total compression
δ_p	-	Primary consolidation settlement
δ_s	-	Secondary compression

LIST OF APPENDICES

CHAPTER 1

INTRODUCTION

1.1 Background

Peat is usually found as an extremely loose, wet, unconsolidated surface deposit which forms as an integral part of a wetland system, therefore; access to the peat deposit is usually very difficult as the water table exists at, near or above the ground surface. This type of soil covers large area in West Johore including Pontian, Batu Pahat and Muar. As part of the development in this area, many civil engineering structures have to be constructed over peat deposit. Replacing the peat with good quality soil is common practice when construction has to take place on peat deposit even though most probably this will lead to uneconomical design.

Alternative construction and stabilization methods were discussed in literatures (Noto, 1991; Hartlen and Wolsky, 1996; Huat, 2004, and others) such as: surface reinforcement, preloading, chemical stabilization, sand or stone column, pre-fabricated vertical drains, and pile. The selection of the most appropriate method should be based on the examination of the index and engineering characteristics of the soil. Researchers have examined peat soils from different parts of the world and their findings differ from one and another mainly due to different characteristics of peat soils. This indicates that the behavior of peat soil is site specific. Thus assessment on the response of peat deposit to loading should be done before the any construction has to take place at a particular site.

Peat is known for low shear strength and high compressibility characteristics, both are actually interrelated. The compressibility of peat depends not only on the

deformation of the material and rearrangement of solid particles, but also on the dissipation of pore water pressure from the soil in response to loading and decomposition of the fiber content. The deformation of peat may continue for a long time due to creep. The shear strength is initially low but may increase as the soil is deforming and consolidating under application of load. The rate of strength increase to the increase in load is almost one-fold for peat as compared to soft clay with a rate of strength increase of 0.3 (Noto, 1991).

In general, elastic deformation of a soil is influenced by the fabric or the arrangement of solid particles in the soil. The soil phase of peat is formed by organic materials derived mainly from plant which is highly compressible. The fabric or arrangement of the particles is controlled the way the particle is deposited. For most transported soil, the particle arrangement was formed such that the flow in horizontal direction is more dominant as compared to the vertical direction. The formation of peat deposit led to a pronounced structural anisotropy in which the fibers tend to have horizontal orientation. Thus, under a consolidation pressure, water tends to flow faster from the soil in the horizontal direction than in the vertical direction.

The particle arrangement will also influence the rate of flow as water tries to dissipate from soil under loading. General practice is to use coefficient of rate of horizontal consolidation (c_h) twice the coefficient of rate of vertical consolidation (c_v) for clay and the ratio is much higher for peat soil. Parallel to the coefficient of rate of consolidation, Dhowian and Edil (1980) and Colley (1950) suggested that for predominantly fibrous peat soils, the horizontal hydraulic conductivity (k_h) is greater than that in vertical direction (k_v) by an order of magnitude. The subsequent research by Edil et al. (2001) has shown that for peat with high fiber content, the ratio of c_h/c_v could be as high as 300. Thus, it is believe that the compression of fibrous peat soil is much faster in horizontal direction compared to vertical direction.

1.2 Objectives of study

The project focuses on the study of compressibility of fibrous peat due to primary consolidation or dissipation of excess pore water pressure in horizontal

direction, and the effect of secondary consolidation on the horizontal coefficient of consolidation, c_h. In order to achieve the aim of the project, the following objectives are set forth:

1. To study the rate of vertical and horizontal consolidation of fibrous peat through hydraulic consolidation tests.
2. To study the effect of secondary compression on the determination of vertical and horizontal coefficient of consolidation (c_v and c_h) of fibrous peat soil
3. To compare the vertical and horizontal coefficient of consolidation (c_v and c_h) of fibrous peat soil under a range of consolidation pressures
4. To compare the vertical and horizontal coefficient of permeability, (k_h and k_v) of fibrous peat soil under a consolidation pressure
5. To outline the use of knowledge of horizontal coefficient of consolidation, c_h on the development of soil improvement method for construction on fibrous peat soil

1.3 Scope of study

The study covers the determination of coefficient of rate of consolidation and coefficient of permeability of fibrous peat in vertical and horizontal direction. The interpretation of the results of the study should be limited to:

1. Peat soil found in Kampung Bahru, Pontian, West Johore.
2. Samples were obtained using block sampling method (refer to procedure outlined in research report for UTM Fundamental vot 75137)
3. Identification of index properties, classification, and engineering properties of the soil was done in the previous research (UTM Fundamental vot 75137)
4. Evaluation of coefficient of rate of consolidation in horizontal and vertical directions was made based on the results of Hydraulic consolidation test (Rowe Cell).
5. Evaluation of vertical and horizontal permeability of soil based on constant head permeability test and hydraulic consolidation equipment.

CHAPTER 2

LITERATURE REVIEW

2.1 Fibrous Peat

2.1.1 Definition

Peat is a mixture of fragmented organic material formed in wetlands under appropriate climatic and topographic conditions. The deposit is generally found in thick layers on limited areas. The soil is known for its low shear strength and high compressibility which often results in difficulties when construction work has to take place on peat deposit. The low strength often causes stability problem and consequently the applied load is limited or the load has to be placed in stages. Large deformation may occur during and after construction period both vertically and horizontally, and the deformation may continue for a long time due to creep.

The classification of peat soil is developed based on (1) decomposition of fiber (2) the vegetation forming the organic content, and (3) organic content and fiber content. The classification based on the degree of decomposition was proposed by Von Post (1922) in which the degree of decomposition is grouped into H_1 to H_{10}: the higher the number, the higher the degree of decomposition (Table A.1). Fibrous peat with more than 60% fiber content is usually in the range of H_1 to H_4 (Halten and Wolski, 1996). The classification based on the vegetation forming the organic material is not usually adopted in engineering practice. The most widely used classification system in engineering practice is based on organic content. A soil with organic content of more than 75% is classified as peat.

The peat is further classified based on fiber content because the presence of fiber alters the consolidation process of fibrous peat from that of organic soil or amorphous peat. Amorphous peat is the peat soil with fiber content less than 20%. It contains mostly particles of colloidal size (less than 2 microns), and the pore water is absorbed around the particle surface. The behavior of amorphous granular peat is similar to clay soil. Fibrous peat is the one having fiber content more than 20% and posses two types of pore i.e.: macro-pores (pores between the fibers) micro-pores (pores inside the fiber itself). The behavior of fibrous peat differs from amorphous peat in that it has a low degree of decomposition, fibrous structure, and easily recognizable plant structure (Karlson and Hansbo, 1981). The compressibility of fibrous peat is very high and it is due to both primary consolidation and secondary compression of the soil. In some cases, tertiary compression follows the secondary compression.

Fibrous peat soil has many void spaces existing between the solid grains. Due to the irregular shape of individual particles, fibrous peat soil deposits are porous and the soil is considered a permeable material. Therefore; the rate of consolidation of fibrous peat is high, however; the rate decreases significantly due to consolidation. Ajlouni (2000) pointed out a pronounced decrease in c_v with load during consolidation due to large reduction in permeability.

2.1.2 Structural Arrangement

Fibrous peat has essentially an open structure with interstices filled with a secondary structural arrangement of nonwoody, fine fibrous material (Dhowian and Edil, 1980), thus; physical properties of fibrous peat soil differ markedly from those of mineral soils. Kogure *et al.* (1993) presented the idea of multi-phase system of fibrous peat which consists of organic bodies and organic space. The organic body consists of organic matter and water in inner voids, while the organic space consists of water in outer voids and the soil particles. The solid organic matter can be drained under consolidation pressure. The cross section of deposition and diagram of the multi-phase system of fibrous peat are schematically shown in Figure 2.1(a) and (b).

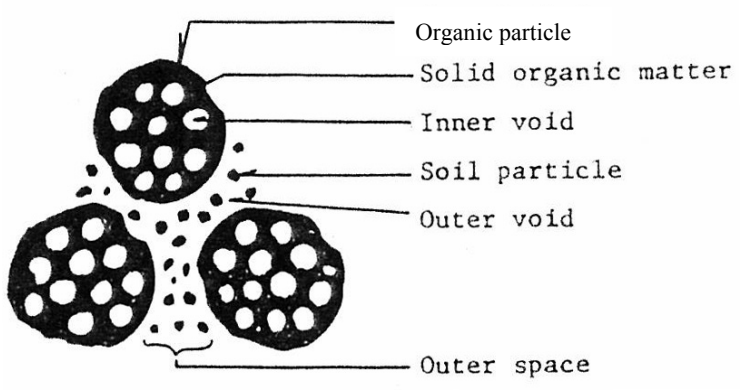

(a)

Organic bodies	Organic matters (Solids)
	Water (Inner voids)
Organic spaces	Water (Outer voids)
	Soil particles (Solids)

(b)

Figure 2.1: Schematic diagram of (a) deposition and (b) multi-phase system of fibrous peat (Kogure *et al.*, 1993)

It can be observed from Figure 2.1(a) that organic particles consist of solid organic matter and inner voids. The solid organic matter is flexible with the inner voids, which are filled with water that can be drained under consolidation pressure. The spaces between the organic bodies, called outer voids are filled with solid particles (solids) and water.

Dhowian and Edil (1980) showed that fiber arrangement appears to be a major compositional factor in determining the way in which peat soils behave. Figure 2.2 shows a scanning electron micrograph of Middleton fibrous peat specimen under 400 kPa vertical consolidation pressures (Fox and Edil, 1996). The photograph was taken in vertical and horizontal planes. Comparison of the two micrographs indicates a pronounced structural anisotropy for the fibrous peat with the void spaces in the horizontal direction larger than those in the vertical direction resulting from the fiber orientation within the soil. Individual microstructures remained essentially intact after compression under high-stress conditions. This implies that for the fibrous peat

soil, horizontal rates of permeability and consolidation are larger than their respective vertical rates of permeability and consolidation.

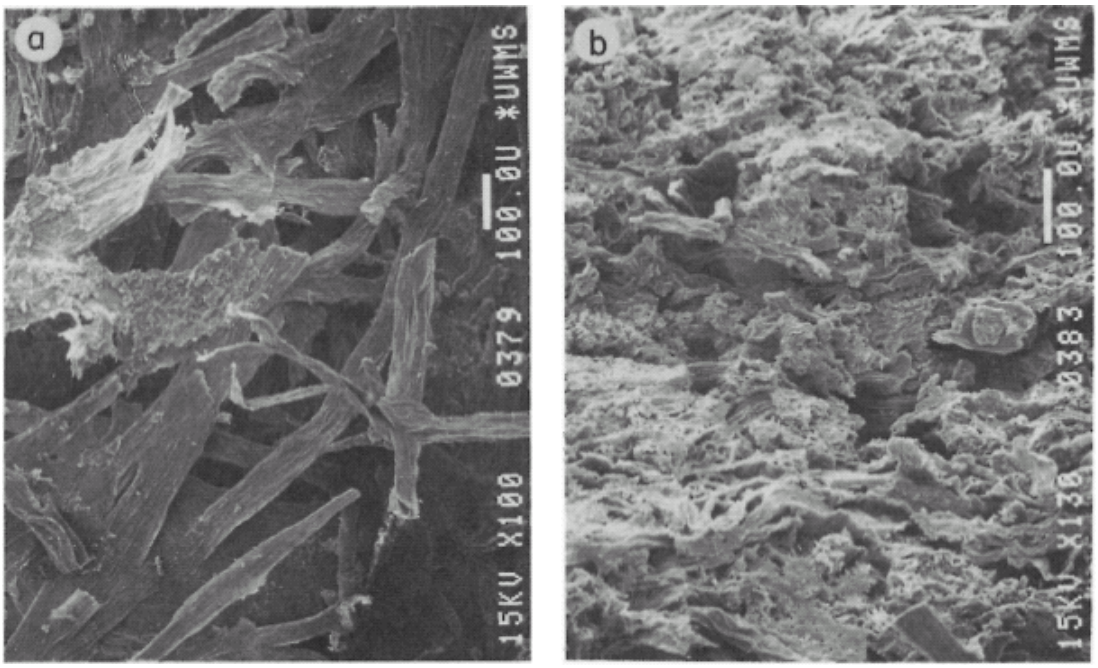

Figure 2.2: Scanning Electron Micrographs of Middleton fibrous peat; (a) horizontal plane, (b) vertical plane (Fox and Edil, 1996)

2.1.3 Physical and Chemical Properties

Fibrous peat owns a wide range of physical properties such as texture, color, water content, density, and specific gravity. The texture of fibrous peat is coarse when compared to clay. This has an implication on the geotechnical properties of peat related to the particle size and compressibility behavior of peat. Soil fabric characterized by organic coarse particles hold a considerable amount of water because they are generally very loose, and the organic particle itself is hollow and largely full of water. Previous researches have indicated that the water content of peat researched in West Malaysia ranges from 200 to 700 % (Huat, 2004). High water content results in high buoyancy and high pore volume leading to low bulk density and low bearing capacity. Unit weight of peat is typically lower compared to inorganic soils. The average unit weight of fibrous peat is about equal to or slightly

higher than the unit weight of water. A range of 8.3–11.5 kN/m^3 is common for unit weight of fibrous peat in West Malaysia (Huat, 2004).

Specific gravity of fibrous peat soil ranges from 1.3 to 1.8 with an average of 1.5 (Ajlouni, 2000). The low specific gravity is due to low mineral content of the soil. Natural void ratio of peat is generally higher than that of inorganic soils indicating their higher capacity for compression. Natural void ratio of 5-15 is common and a value as high as 25 have been reported for fibrous peat (Hanharan, 1954). Peat will shrink extensively when dried. The shrinkage could reach 50% of the initial volume, but the dried peat will not swell up upon re-saturation because dried peat cannot absorb water as much as initial condition; only 33% to 55% of the water can be reabsorbed (Mokhtar, 1998).

Generally, peat soils are very acidic with low pH values, often lies between 4 and 7 (Lea, 1956). Peat existing in Peninsular Malaysia is known to have very low pH values ranging from 3.0 to 4.5, and the acidity tends to decrease with depth (Muttalib et.al., 1991). The submerged organic component of peat is not entirely inert but undergoes very slow decomposition, accompanied by the production of methane and less amount of nitrogen and carbon dioxide and hydrogen sulfide. Gas content affects all physical properties measured and field performance that relates to compression and water flow. A gas content of 5 to 10% of the total volume of the soil is reported for peat and organic soils (Muskeg Engineering Handbook 1969).

2.1.4 Engineering Properties

Most fibrous peat is considered frictional or non-cohesive material (Adam, 1965) due to the fiber content, thus the shear strength of peat is determined based on drained condition. The friction is mostly due to the fiber and the fiber is not always solid because it is usually filled with water and gas, thus; the high friction angle does not actually reflect the high shear strength of the soil. Shear box is the most common test for determining the drained shear strength of fibrous peat, while triaxial test is frequently used for laboratory evaluation of shear strength of peat under consolidated-undrained condition (Noto, 1991).

Previous studies indicated that the effective internal friction ϕ' of peat is generally higher than inorganic soil i.e: 50^o for amorphous granular peat and in the range of 53^o–57^o for fibrous peat (Edil and Dhowian, 1981). Landva (1983) indicated the range of 27^o–32^o under a normal pressure of 30 to 50 kPa. The range of internal friction angle of peat in West Malaysia is 3^o–25^o (Huat, 2004).

Considering the presence of peat soil is almost always below the groundwater level, the determination of undrained shear strength is also important. This is usually done in-situ because sampling of peat for laboratory evaluation of undrained shear strength of fibrous peat is almost impossible. An undrained shear strength of peat soil (S_u) obtained by vane shear test was in range of 3 –15 kPa, which is much lower than that of the mineral soils. A correction factor of 0.5 is suggested for the test results on organic soil with a liquid limit of more than 200% (Hartlen and Wolsky, 1996). Some approaches to in situ testing in peat deposits are: vane shear test, cone penetration test, pressure-meter test, dilatometer test, plate load test and screw plate load tests (Edil, 2001). Among them, the vane shear test is the most commonly used; however, the interpretation of the test results must be handled with caution.

The compression behavior of fibrous peat is controlled by the fiber content. Secondary compression is generally found as the more significant part of compression because the time rate is much slower than the primary consolidation. Determination of compressibility of fibrous peat is usually based on the standard consolidation test.

Peat soils have a unit weight close to that of water; thus, the in-situ effective stress (σ'_o) is very small and sometimes cannot be detected from the results of consolidation test. It is also very difficult to obtain the beginning of secondary consolidation (t_p) from consolidation curve because the preliminary consolidation occurs rapidly. Natural void ratio (e_o) is very high due to large pores, consequently; the e-log p' curves showed a steep slope indicating a high value of a_v and c_c. The compression index of peat soil ranges from 2 to 15. Furthermore, the secondary consolidation may start before the dissipation of excess pore water pressure is completed.

Compression of fibrous peat continues at a gradually decreasing rate under constant effective stress, and this is termed as the secondary compression. The secondary compression of peat is thought to be due to further decomposition of fiber which is conveniently assumed to occur at a slower rate after the end of primary consolidation. The rate of secondary compression is conveniently defined by the slope (c_α) of the final part of the void ratio versus log time curve. This estimate is based on assumptions that c_α is independent of time, thickness of compressible layer and applied pressure. Ratio of c_α/c_c has been used widely to study the behavior of peat. Mesri et al. (1994) reported a range between 0.05 and 0.07 for c_α/c_c.

2.1.5 Permeability

Permeability is one of the most important properties of peat because it controls the rate of consolidation and increase in the shear strength of soil (Hobbs, 1986). Previous studies on physical and hydraulic properties of fibrous peat soil indicate that the soil is averagely porous, and this certifies the fact that fibrous peat soil has a medium degree of permeability. A range of the coefficient of permeability of 10^{-5} to 10^{-8} m/s was obtained from previous studies (Colley, 1950 and Miyakawa, 1960).

Constant head permeability and Rowe consolidation cells have been used to determine the vertical and horizontal coefficient of permeability of fibrous peat soil. The permeability of peat depends on the void ratio, mineral content, degree of decomposition of the peat, chemistry and the presence of gas. Mesri *et al*. (1997) carried out permeability measurements during the secondary compression stage of oedometer tests on Middleton peat. The study showed that a typical void ratio of 12, Middleton peat is anisotropic with a value of $k_{ho}/k_{vo} = 10$.

The change in permeability as a result of compression is drastic for fibrous peat soils (Dhowian and Edil, 1980). Research on Portage fibrous peat shows the soil initially has a relatively high permeability comparable to fine sand or silty sand,

as shown in Figure 2.3. However, as compression proceeds and void ratio decreases rapidly, permeability is greatly reduced (about 10,000-fold) to a value comparable to that of clay. The fact is supported by the finding of Colleselli *et al*. (2000), which stated that the initial permeability of peats is 100 –1000 times that of soft clays and silts. Also shown in Figure 2.3, at a given void ratio, the horizontal coefficient of permeability, k_h is higher (by about 300-fold) than its vertical coefficient of permeability, k_v. This also indicates that horizontal coefficient of consolidation of Portage peat is greater than its vertical coefficient of consolidation.

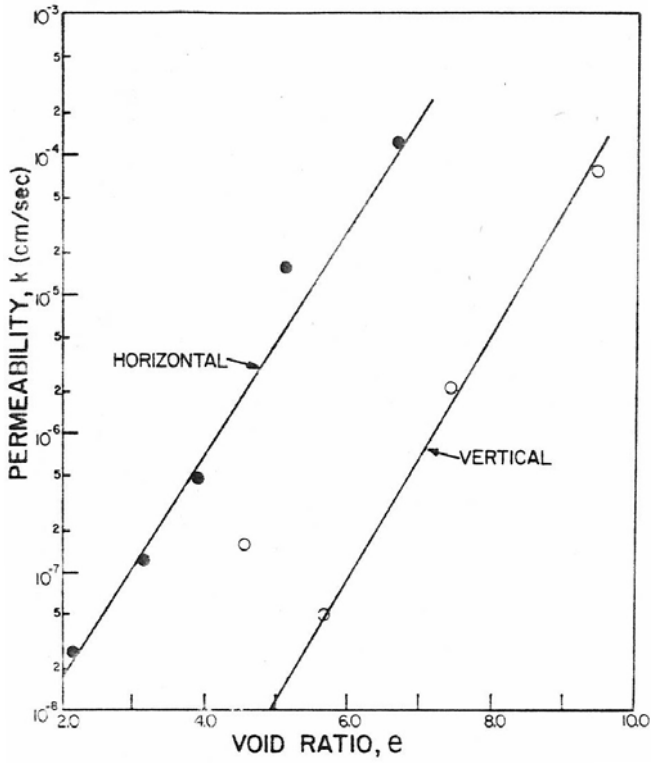

Figure 2.3: Coefficient of permeability versus void ratio for vertical and horizontal specimens of Portage peat (Dhowian and Edil, 1980)

The dominant factors, in addition to the original structure and material characteristics that control hydraulic conductivity of peat, are density (or degree of consolidation) and extent of decomposition. These factors can change with time and result in a change in hydraulic conductivity. In its natural state, peat can have a hydraulic conductivity as high as sand, i.e., 10^{-5} to 10^{-4} m/s. Hydraulic conductivity

decreases markedly under load down to the level of silt or clay hydraulic conductivity i.e., 10^{-8} to 10^{-9} m/s or even lower (Hillis and Brawner, 1961; Dhowian and Edil, 1980; Lea and Brawner, 1963). According to Edil (2003), the rate of decrease of hydraulic conductivity with decreasing void ratio is usually higher than that in clays. The large decrease in hydraulic conductivity under continuous compression implies that large strain theory of consolidation may be appropriate for high water content fibrous peat (Lan, 1992).

2.2 Soil Compressibility

In general, the compressibility of a soil consists of three stages, namely initial compression, primary consolidation and secondary compression. While initial compression occurs instantaneously after the application of load, the primary and secondary compressions are time dependent. The initial compression is due partly to the compression of small pockets of gas within the pore spaces, and partly to the elastic compression of soil grains. Primary consolidation is due to dissipation of excess pore water pressure caused by an increase in effective stress whereas secondary compression takes place under constant effective stress after the completion of dissipation of excess pore water pressure.

The time required for the water to dissipate from the soil depends on the permeability of the soil itself. In granular soil, the process is rapid and hardly noticeable due to its high permeability. On the other hand, the consolidation process may take years in clay soil. For peat, the primary consolidation occurs rapidly due to high initial permeability and secondary compression takes a significant part of compression.

2.2.1 Primary Consolidation

One-dimensional theory of consolidation developed by Terzaghi in 1925 carries an assumption that primary consolidation is due to dissipation of excess pore

water pressure caused by an increase in effective stress whereas secondary compression takes place under constant effective stress after the completion of the dissipation of excess pore water pressure. Other important assumptions attached to the Terzaghi consolidation theory are that the flow is one-dimensional and the rate of consolidation or permeability is constant throughout the consolidation process.

Consolidation characteristics of soil can be represented by consolidation parameters such as coefficient of axial compressibility a_v, coefficient of volume compressibility m_v, compression index c_c, and recompression index c_r. Another important characteristic of soil compressibility is the pre-consolidation pressure (σ_c'). The soil that has been loaded and unloaded will be less compressible when it is reloaded again, thus; settlement will not usually be great when the applied load remains below the pre consolidation pressure. These parameters can be estimated from a curve relating void ratio (e) at the end of each increment period against the corresponding load increment in linear scale (Figure 2.4) or log scale (Figure 2.5).

As shown in Figure 2.4, the coefficient of axial compressibility a_v is the slope of the e–p' curve for a certain range of stress while the coefficient of volume compressibility m_v can be computed as:

$$m_v = \frac{a_v}{1 + e_o} \tag{2.1}$$

The compression index c_c, and recompression index c_r are the slope of the e–log p' curve (Figure 2.5) for loading and unloading stages.

The soil that has been loaded and unloaded will be less compressible when it is reloaded again. Thus, it is also necessary to estimate the pre consolidation pressure (the stress carried by soil in the past, σ_c') because consolidation settlement will not usually be great when the applied load remains below the pre consolidation pressure. The pre-consolidation pressure can be obtained from the consolidation curve by procedure suggested by Cassagrande.

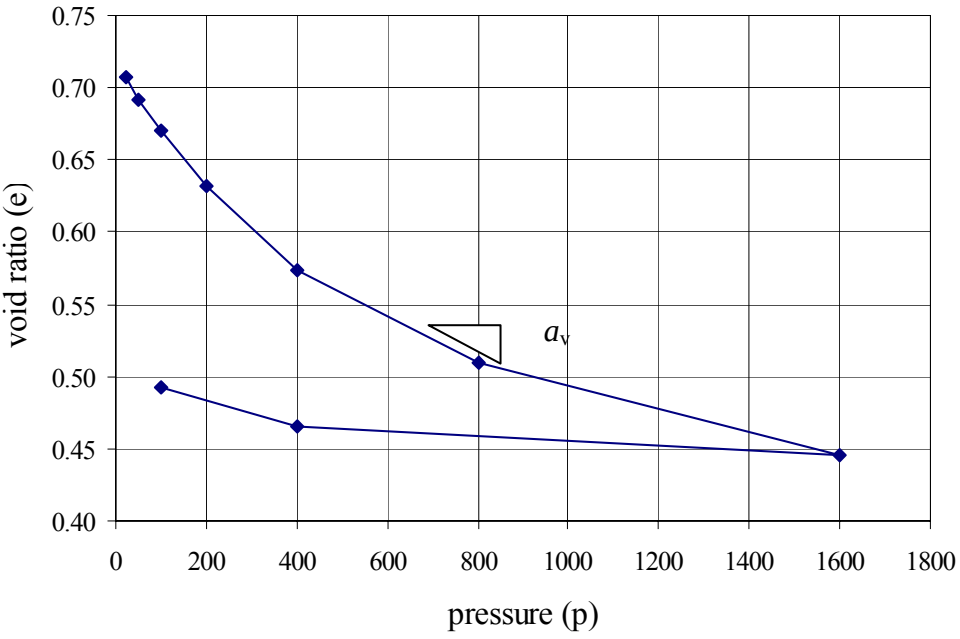

Figure 2.4 Plot of Void ratio vs. pressure in linear scale

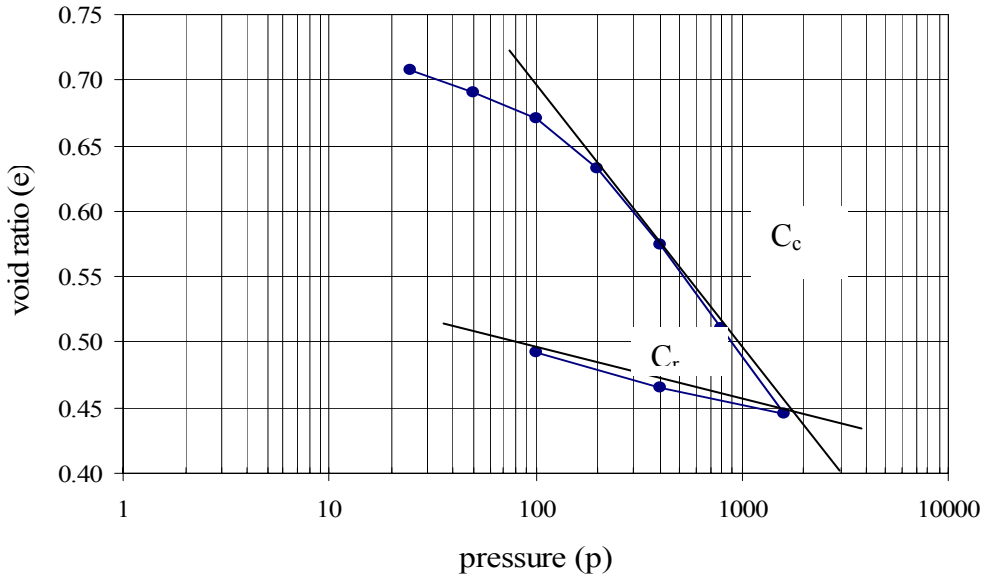

Figure 2.5 Plot of void ratio vs. pressure in logarithmic scale

The time rate of consolidation, and subsequently the time required for a certain degree of consolidation to take place, can be obtained based on plot of compression against time for each load increment. The Hydrodynamic equation governing the Terzaghi one-dimensional consolidation is:

$$c_v \frac{\partial^2 u_e}{\partial z^2} = \frac{\partial u_e}{\partial t} \tag{2.2}$$

where u_e is the excess pore water pressure at time t and depth z, and c_v is the coefficient of rate of consolidation (m^2/year or m^2/sec) which contains the material properties that govern the consolidation process.

$$c_v = \frac{k_v}{\gamma_w} \frac{1+e_o}{a_v} = \frac{k_v}{m_v \gamma_w} \tag{2.3}$$

General solution to Equation 2.2 is given by Taylor (1948) in terms of a Fourier series expansion of the form:

$$\mu = (\sigma_2' - \sigma_1') \sum_{n=0}^{n=\infty} f_1(Z) f_2(T_v) \tag{2.4}$$

where Z and T_v are non-dimensional parameters. Z is geometry factor, which is equal to z/H, and T_v is Time factor, in which:

$$T_v = \frac{c_v \, t}{H_d^{\,2}} \tag{2.5}$$

The relationship between the average degree of consolidation U_{avg} and T_v can be observed from Figure 2.6.

The coefficient of rate of consolidation for a particular pressure increment in oedometer test can be determined by curve fitting methods. There are two methods commonly used to determine the value of c_v i.e the logarithmic time (Cassagrande's) method, and the square root time (Taylor's) method. These empirical procedures were developed to fit approximately the observed laboratory test data to the Terzaghi theory of consolidation.

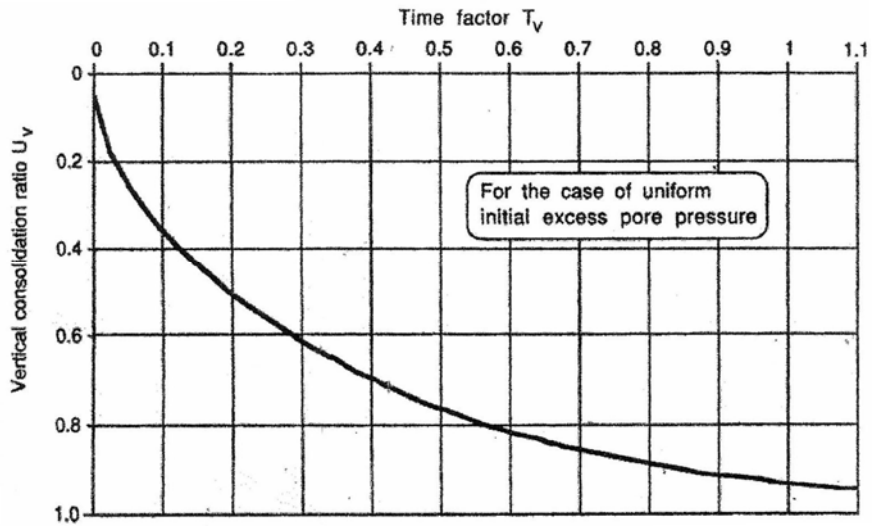

Figure 2.6 Consolidation curve for two-way vertical drainage (Head, 1982)

The Cassagrande methods use the plot of dial readings versus the logarithmic of time (log t). The idea is to find the reading at t_{50} or the time for 50% consolidation (Figure 2.7). The procedure is as follows:

1. Plot a graph relating dial reading (mm) versus log time
2. Produce a straight line for primary consolidation and secondary consolidation part of the graph. The two lines will meet at point C.

3. The ordinate of point C is D_{100} = the deformation corresponds to U = 100%
4. Choose time t_1 (point A), $t_2 = 4t_1$ (point B). The difference in the dial reading is equal to x.
5. An equal distance x set off above point A fixes the point D_0 = the deformation corresponds to U =0%. Notes that Ro is not essentially equal to the initial reading may be due to small compression of air within the sample.
6. The compression between D_0 and D_{100} is called the primary consolidation.
7. A point corresponding to U = 50% can be located midway between D_0 and D_{100}. The value of T corresponds to U = 50% is 0.196.
8. Thus
$$c_v = \frac{0.196\, H_d^{\,2}}{t_{50}} \qquad (2.6)$$

where H_d is half the thickness of specimen for a particular pressure increment.

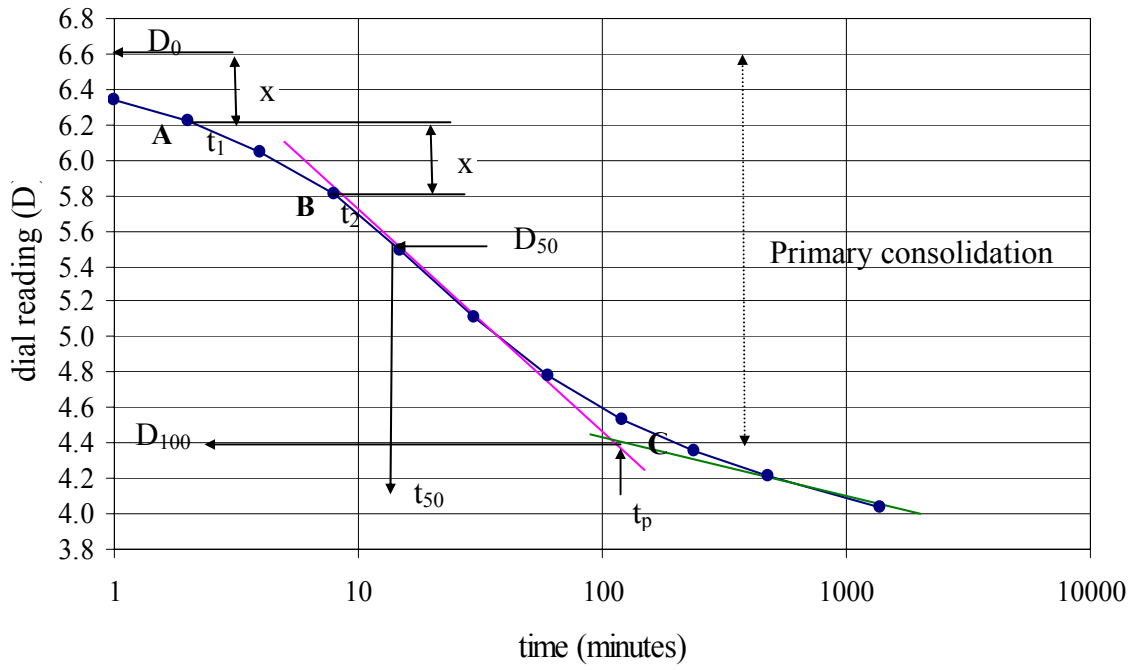

Figure 2.7 Determination of c_v by Cassagrande method

The square root of time methods developed by Taylor is based on the similarity of the shapes of experimental and theoretical curves when plotted versus the square root of time (Figure 2.8). The following procedure was recommended:

1. Extent the straight line part of the curve to intersect the ordinate (t = 0) at point D. The point shows the initial reading (D_o). The intersection of this line with the abscissa is P.
2. Take point Q such that OQ = 1.15 OP.
3. The intersection of line DQ and the curve is called point G
4. Draw horizontal line from G to the ordinate (D_{90}). The point shows the value of $\sqrt{t_{90}}$. The value of T corresponds to U = 90% is 0.848.
5. Thus

$$c_v = \frac{0.848\ H_d^{\ 2}}{t_{90}} \qquad (2.7)$$

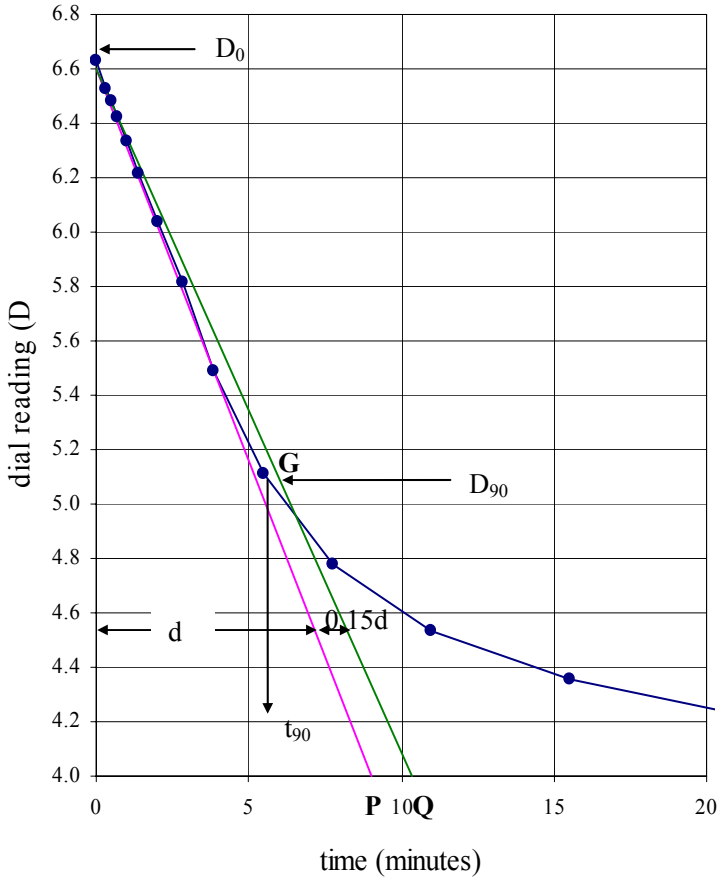

Figure 2.8 Determination of c_v by Taylor method

2.2.2 Secondary Compression

For some soils, especially those containing organic material, the compression does not cease when the excess pore water pressure has completely dissipated but continues at a gradually decreasing rate under constant effective stress. Thus, it is common to differentiate the two processes as primary and secondary compression. Secondary compression, also referred as creep, is thought to be due to the gradual readjustment of the clay particles into a more stable configuration following the structural disturbance caused by the decrease in void ratio, especially if the clay is laterally confined.

Previous researchers have shown that both primary and secondary compressions can take place simultaneously. However, it is assumed that the secondary compression is negligible during primary compression, and is identified after primary consolidation is completed. Secondary compression of soil is conveniently assumed to occur at a slower rate after the end of primary consolidation. The rate of secondary compression in the oedometer test can be defined by the slope (c_α) of the final part of the void ratio versus log time curve (Figure 2.9).

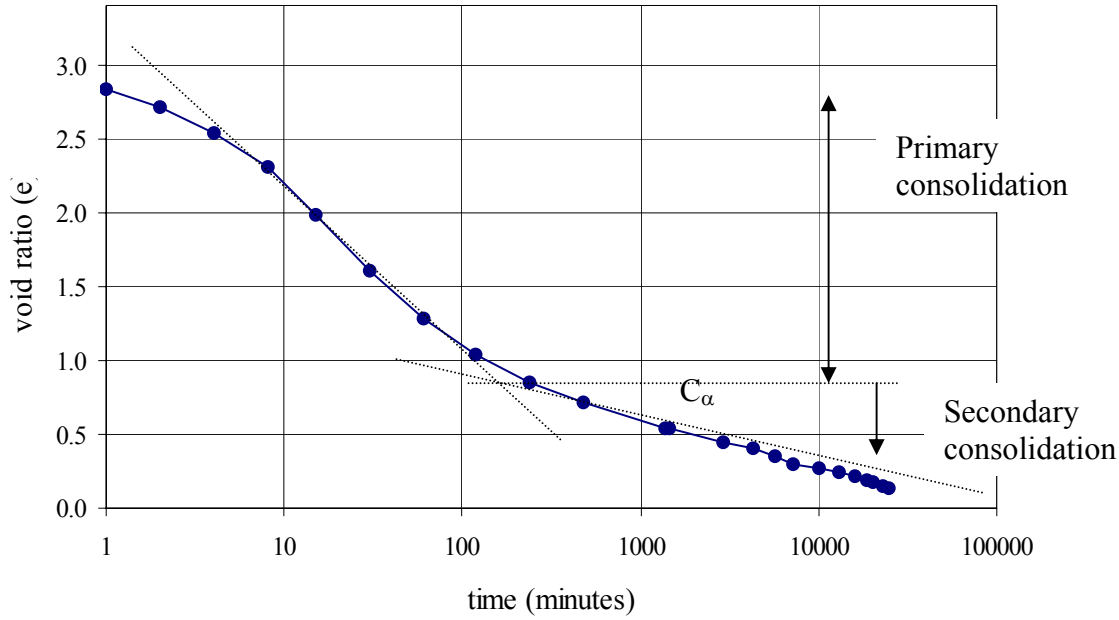

Figure 2.9 Determination of the coefficient of rate of secondary compression from consolidation curve (Cassagrande)

The axial rate of consolidation can be obtained from Figure 2.9 as the ratio of change on the void ratio to the change on the logarithmic of time.

$$C_\alpha = \frac{\Delta e}{\Delta \log t} = \frac{\Delta e}{\log \frac{t_f}{t_p}} \qquad (2.8)$$

the rate of secondary compression can be expressed as:

$$C_{\alpha\varepsilon} = \frac{C_\alpha}{1+e_o} \qquad (2.8)$$

in which Δe is the change of void ratio from t_p to t_f. t_p denotes the time of the completion of primary consolidation, while t_f is the time for which the secondary consolidation settlement is required. The void ratio at time t_p is denoted as e_o. This estimate is based on assumptions that c_α is independent of time, thickness of compressible layer and applied pressure. Research showed that the ratio of c_α/c_c is almost constant and varies from 0.025 to 0.06 for inorganic soil, while a slightly high range was obtained for organic soils and peats (Holtz and Kovacs, 1981).

2.3 Large Strain Consolidation Test

The compressibility characteristics of a soil are usually determined from consolidation tests. General laboratory tests for measurement of compression and consolidation characteristics of a soil are: Oedometer consolidation test, Constant Rate of Strain (CRS) test, and Rowe Cell test. The procedures for these tests are fully described in BS 1377-6 and Head (1982, 1986).

2.3.1 Problems Related to Conventional Test

Although more sophisticated consolidation tests are now available, the oedometer test is still recognized as the standard test for determining the consolidation characteristics of soil. Oedometer cell can accommodate 50 mm diameter and 20 mm thick samples (Figure 2.10). Due to the relatively small specimen thickness, testing time is not excessively long and the test can be extended to a long-term test if secondary characteristics are required.

The test provides a reasonable estimate of the amount of settlement of structure on inorganic clay deposits. However, the rate of settlement is often underestimated, that is, the total settlement is reached in a shorter time than that predicted from the test data. This is largely due to the size of sample which does not represent soil fabric and its profound effect on drainage conditions. Besides the

natural condition of the sample, sampling disturbance will have a more pronounced effect on the results of the test done on small samples. Furthermore, the boundary effect from the ring enhances the friction of the sample. Friction reduces the stress acted on the soil during loading and reduces swelling during unloading.

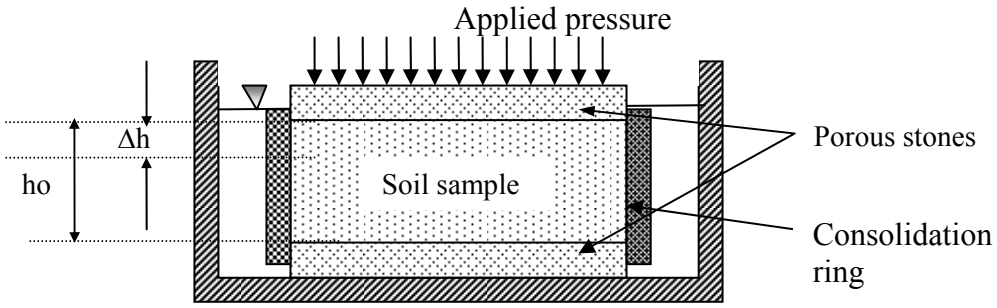

Figure 2.10 Schematic diagram of Oedometer Cell

For standard test, the samples were subjected to consolidation pressures with load increment ratio of one. The load is applied through a mechanical lever arm system, thus: measurement can be easily affected by sudden shock. Excessive disturbance affects the e - log p' plot and tends to obscure the effect of stress history; gives low values of pre-consolidation pressure and over-consolidation ratio, and gives high coefficient of volume compressibility at low stresses. Excessive disturbance also reduces the effect of secondary compression which is a very important characteristic of fibrous peat.

The other limitation of oedometer test is that there is no means of measuring excess pore-water pressures, the dissipation of which control the consolidation process. Therefore the estimation of compressibility is based solely on the change of height of the specimen.

2.3.2 Large Strain Test (Rowe Cell)

Rowe consolidation cell (Figure 2.11) was introduced by Rowe and Barden in 1966 to overcome the disadvantages of the conventional oedometer apparatus when performing consolidation tests on non-uniform deposits such as fibrous peat. Rowe cell has many advantages over the conventional Oedometer consolidation apparatus. The main features responsible for these improvements are the hydraulic loading system; the control facilities and ability to measure pore water pressure, and the capability of testing samples of large diameter.

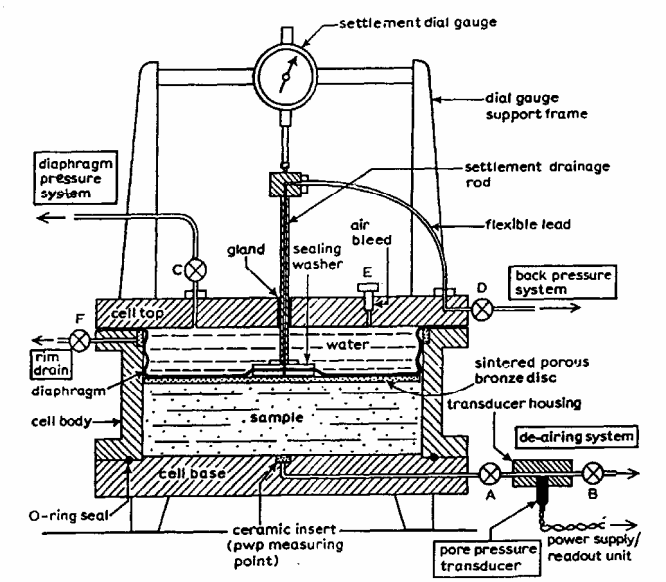

Figure 2.11 Schematic diagram of Rowe Consolidation cell

Through hydraulic loading system, the sample is less susceptible to vibration effects and higher pressures can be applied easily due to large sample size. The hydraulic loading system enables samples of large diameter up to 254 mm diameter to be tested for practical purposes and allows for large settlement deformations. The use of large samples enables the effect of the soil fabric (laminations, fissures, bedding planes) to be taken into account in the consolidation process, thereby enabling a realistic estimate of the rate of consolidation to be made. Large samples have been found to give higher and more reliable values of c_v, especially under low stresses, than conventional oedometer test samples (Head, 1986). Better agreement has been reported between predicted and observed rates of settlement, as well as their magnitude, may be partly due to the relatively smaller effect of structural viscosity

and fabric in larger samples. Tests on high quality large diameter samples minimize the effect of sample disturbance and therefore provide more reliable data for settlement analysis than conventional one-dimensional oedometer tests on small samples.

The most important feature of Rowe cell is the ability to control drainage and to measure pore water pressure during the course of consolidation tests. Drainage of the sample can be controlled, and several different drainage conditions can be imposed on the sample. Figure 2.12 shows different drainage conditions that can be applied to the consolidation tests using Rowe consolidometer. Control of drainage enables loading to be applied to the sample in the undrained condition, allowing full development of pore pressure. Consequently the initial immediate settlement can be measured separately from the consolidation settlement, which starts when the drainage line is opened.

Pore water pressure can be measured accurately at any time and with immediate response. Pore pressure readings enable the beginning and end of the primary consolidation phase to be positively established. The volume of water draining from the sample can be measured, as well as surface settlement.

The sample can be saturated by applying increments of back pressure until a B value of unity is obtained, or by controlling the applied effective stress, before starting consolidation. Tests can be carried out under an elevated back pressure, which ensures fully saturated conditions, gives a rapid pore water pressure response, and ensures reliable time relationships.

The sample can be loaded either by applying a uniform pressure over the surface (free strain), or through a rigid plate which maintains the loaded surface plane (equal strain). Fine control of loadings, including initial loads at low pressures, can be accomplished easily. Several drainage conditions (vertical or horizontal) are possible, and back pressure can be applied to the sample. In this test, samples can be saturated and then tested under the application of back pressure. Consolidation and permeability tests can be successively conducted in Rowe cell providing data over a range of void ratios or strain.

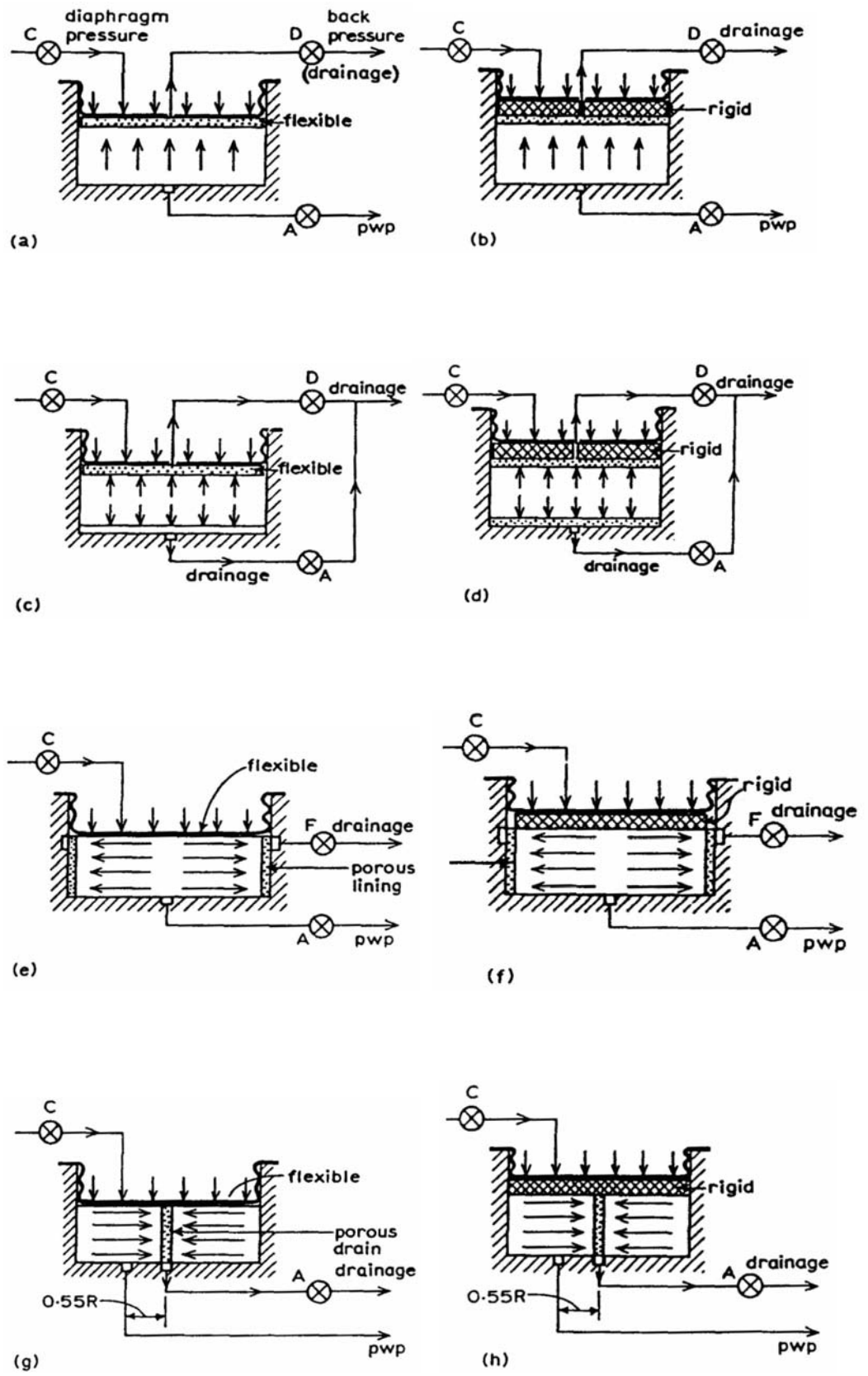

Figure 2.12 : Drainage and loading conditions for consolidations tests in Rowe cell: (a),(c), (e), (g) with 'free strain' loading, (b), (d), (f), (h) with 'equal strain' loading (Head, 1986)

2.4 Analysis of Time-Compression curve

Figure 2.13 shows three types of time-compression curve derived from laboratory consolidation test on different types of soil (Leonards and Girault, 1961). Type I curve is defined by Terzaghi's theory with S-shaped curve. The separation of primary and secondary compression from Type I curve is relatively easy because it follows that the secondary compression occurs at a slower rate after the dissipation of pore water pressure. Identification of the beginning of secondary consolidation (t_p) and the rate of secondary compression (c_α) for type I curve can be estimated based on Cassagrande method as explained in Section 2.2.2.

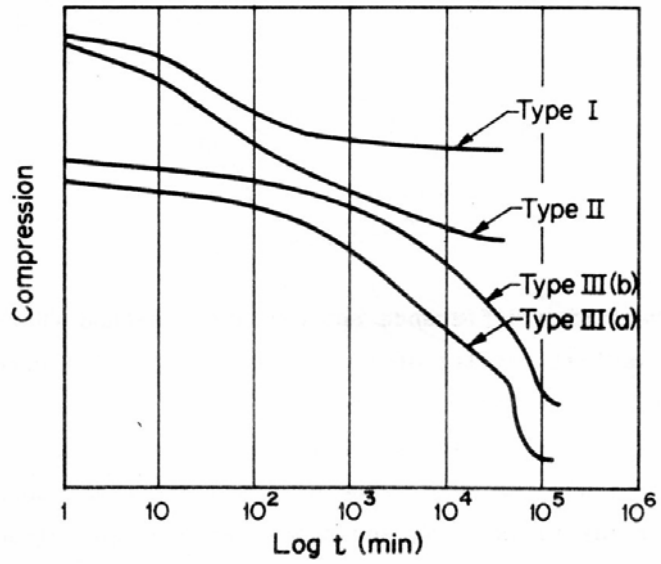

Figure 2.13 Types of time-compression curve derived from consolidation test (Leonards and Girault, 1961)

Researches showed that the time compression curves derived from results of one-dimensional consolidation test on fibrous peat soil do not follow the type I curve. They resemble the type II curve in which the primary consolidation is very rapid and secondary compression does not vary linearly with logarithmic of time and tertiary compression is actually observed after secondary compression. Therefore the quantification of secondary compression based on conventional (Cassagrande) method frequently under-estimate the settlement. Dhowian and Edil (1980) extended the Cassagrande method to include the nonlinearity of secondary compression of

fibrous peat by a coefficient of secondary compression, $c_{\alpha 1}$, and coefficient of tertiary compression, $c_{\alpha 2}$ (Figure 2.13). In this case, time of secondary compression (t_s) should be identified in addition to the time for primary consolidation (t_p). The term 'tertiary strain' is introduced as a soil strain to designate the increasing coefficient of secondary compression with time.

It is evident that the conventional method assumes that the secondary compression begins at the completion of pore-water pressure ($t_p = t_{100}$), and this can be evaluated from time–settlement curve. The methods also assumed that the secondary compression occurs at a slower rate then the primary consolidation, thus t_p is obtained at the inflexion point in the curve. The method cannot evaluate secondary compression of soils exhibiting Type III curve (Figure 2.13) because the curve does not show an inflection point.

Previous researcher (Robinson, 1997) have pointed out that the full dissipation of pore water pressure cannot be predicted based on settlement curve because based on his findings on consolidation test with measurement of pore water pressure, the pore water pressure dissipation is completed earlier than the time predicted from the inflection point of the settlement curve. Further analysis by the same researcher (Robinson, 2003) revealed that the secondary compression actually starts during the dissipation of excess pore-water pressure from the soil. This observation was based on Terzaghi's one dimensional consolidation theory, whereby the relationship between dissipation of excess pore water pressure and compression during primary consolidation can be represented by a straight line while the actual curve derived from laboratory consolidation test on peat soil was not actually follows a straight line. Thus, the settlement was actually due to combination of pore water pressure dissipation on primary consolidation and secondary compression.

Robinson (2003) suggested a method for separating the primary consolidation and secondary compression that occur during the consolidation process. The method was developed based on time–compression and the time–pore water pressure curves (Figure 2.14).

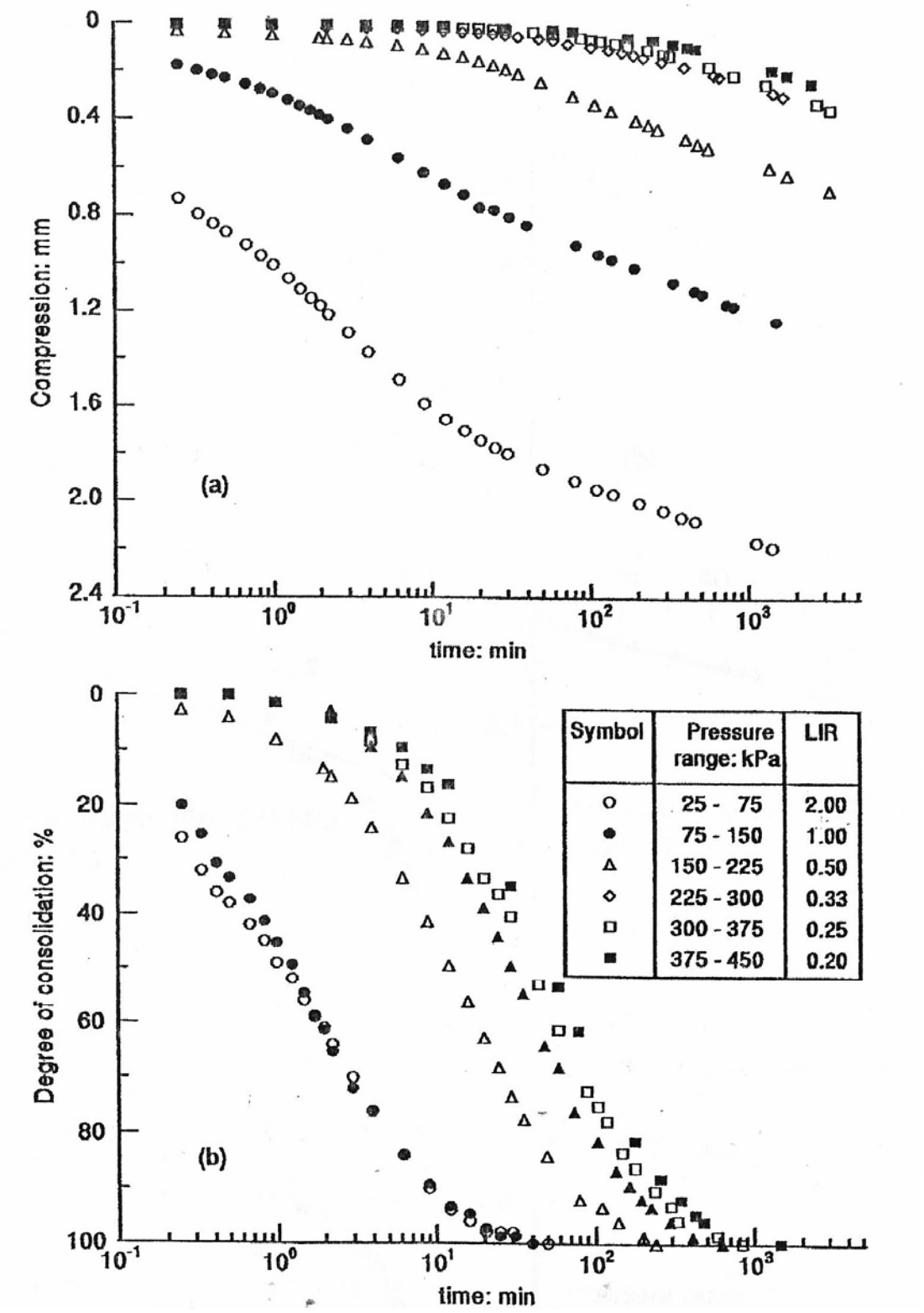

Figure 2.14: (a) Time-compression curves, and (b) time-degree of consolidation from the measured pore water pressure dissipation curves for peat (Robinson, 2003)

It can be observed that the dissipation of pore water pressure dissipation (Figure 2.14(b)) is actually completed earlier than predicted by the settlement curve (Figure 2.14(a)). Some settlement curves do not exhibit the inflection point, that the end of primary consolidation cannot be predicted based on Cassagrande method. According to Robinson (2003), the data from Figure 2.14(a) and 2.14(b) can be plotted as degree of consolidation measured from the dissipation of excess pore water pressure versus total compression of the soil in Figure 2.15(a)-(f).

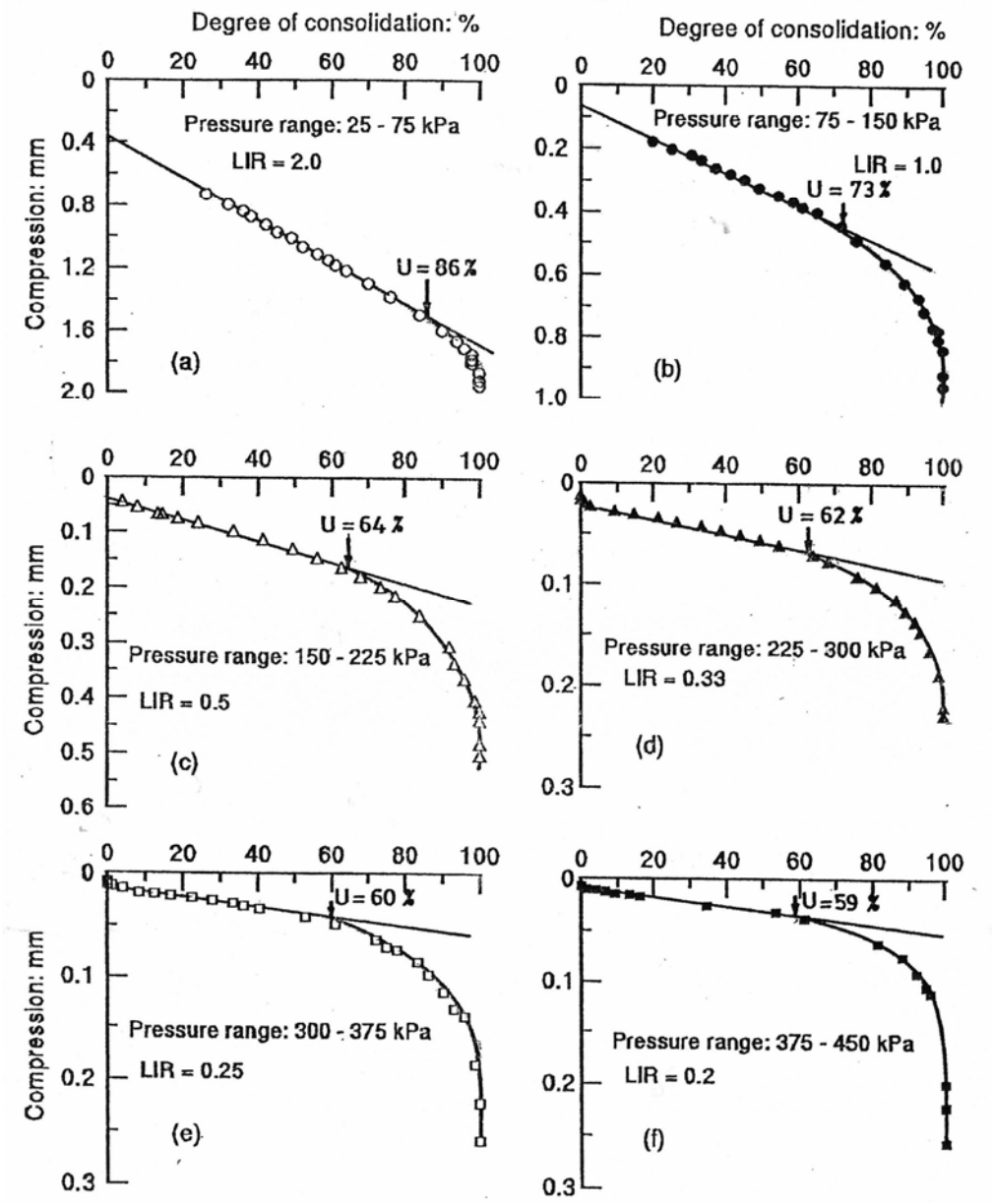

Figure 2.15: Degree of consolidation from the pore water pressure dissipation curves plotted against compression for several consolidation data for peat (Robinson, 2003)

Figure 2.15 (a) to (f) show similar trend in which the curve deviate from a straight line at a certain degree of consolidation. The point where the curve diverges from linearity is identified as the beginning of secondary compression. The compression corresponding to the point where the straight line meets the U = 100% axis is the total primary consolidation settlement (δ_p), while the compression below the extrapolated line is the secondary compression (δ_s). Thus, using this procedure, it is possible to separate the primary consolidation settlement and secondary compression from time-compression data obtained from the laboratory one-dimensional consolidation test. Figure 2.16 (a) and (b) show the total and primary consolidation settlement after the removal of secondary compression respectively. A clear S or Type I curve is obtained which is the shape expected if only the primary consolidation is considered (Figure 2.16 (b)).

The secondary compression-time relationship is commonly represented by a logarithmic function. Instead of using the consolidation curve derived directly from test results, the evaluation of the coefficient of consolidation of peat soil should be based on the primary consolidation versus logarithmic of time curve (Figure 2.16(b)). This figure is redrawn in Figure 2.17 for the purpose of describing the evaluating the coefficient of consolidation. The starting and ending ordinates of the primary consolidation curve are regarded as the beginning and ending of primary consolidation (D_0 and D_{100}) of soil respectively. The corresponding times are denoted by t_0 and t_{100} respectively. The time for 50% primary consolidation can be obtained from D_{50} which is the midpoint between d_0 and d_{100}. For one-dimensional two-way vertical drainage, coefficient of consolidation (c_v) can be calculated by Equation 2.6.

For Robinson's method, as long as the secondary compression varies linearly with logarithmic of time, the time-secondary compression relationship is satisfactorily represented by the coefficient of secondary compression. The plot can be obtained by subtracting the primary consolidation from total settlement. Note that zero secondary settlement was obtained for t equal to t_o, where t_o is the beginning of secondary consolidation. Figure 2.18 shows the plot of the secondary compression (δ_s) against their corresponding time ($t–t_o$). The coefficient of secondary compression of soil (c_α) is the slope of the line shown in Figure 2.18.

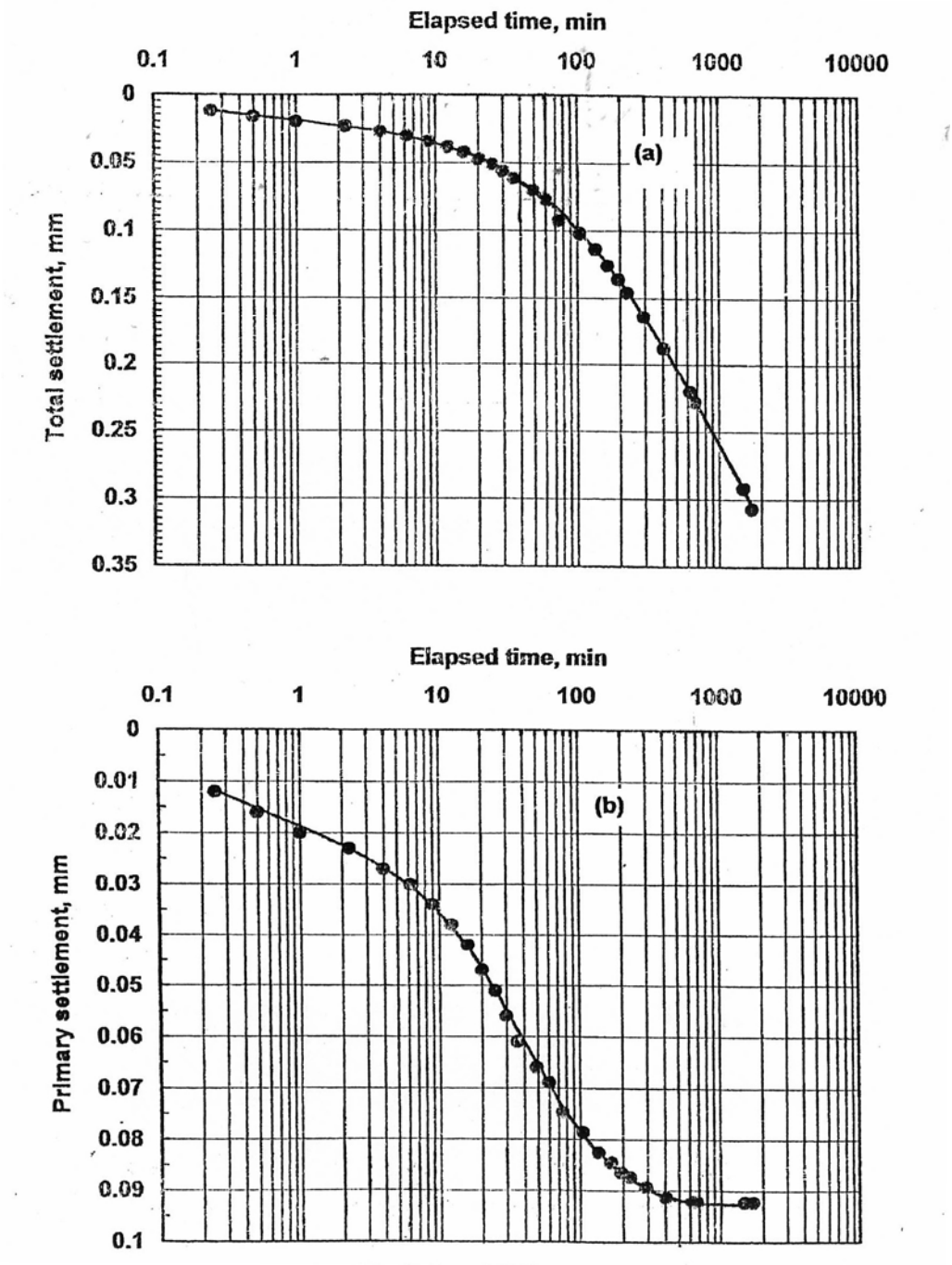

Figure 2.16: (a) Time-total settlement curves for peat and (b) Time-settlement curve after removing the secondary compression (Robinson, 2003)

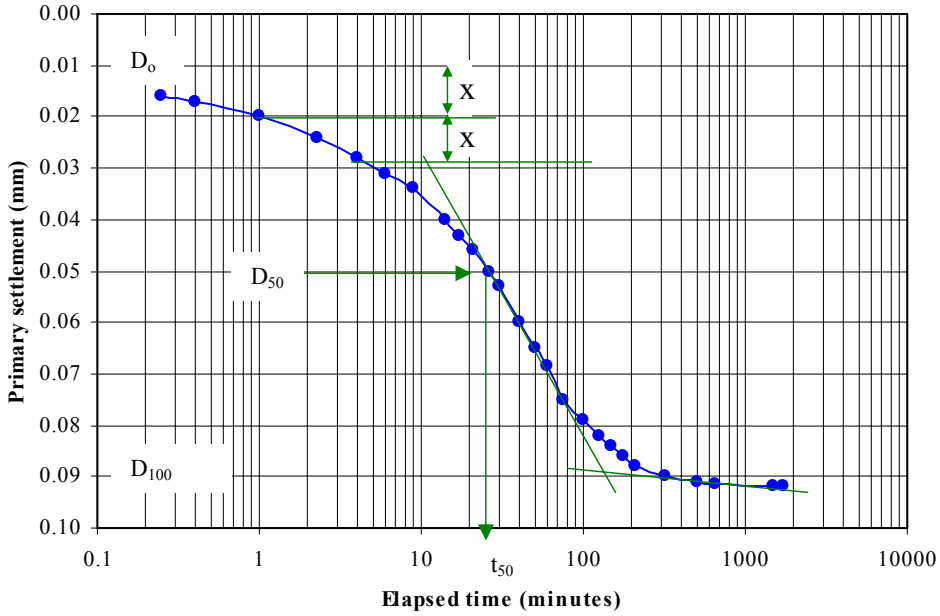

Figure 2.17: Primary consolidation versus log time curve for evaluation of coefficient of consolidation

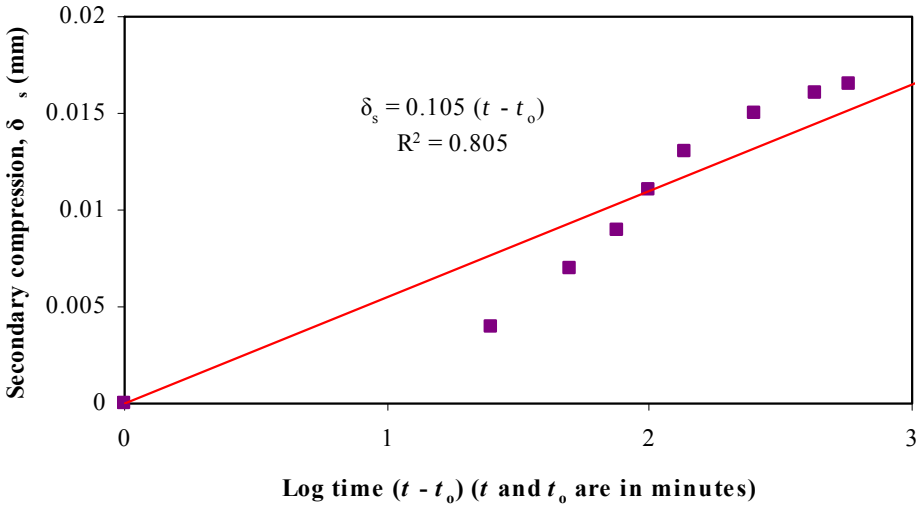

Figure 2.18: Secondary compression versus log time curve for evaluation of coefficient of secondary consolidation

2.5 Measurement of Horizontal Coefficient of Consolidation

Several laboratory and field tests have been used to evaluate horizontal coefficient of consolidation, c_h of fibrous peat soil. This parameter can be measured in field by piezocone test (e.g. Tortesson, 1975), in situ permeability test (e.g. Wilkinson, 1968), in situ consolidation test (e.g. Clarke et al., 1979), and trial embankment test (e.g. Asaoka (1978) and others). In laboratory, horizontal coefficient of consolidation, c_h of the soil is measured by standard consolidation using Oedometer cell or triaxial test (Escario and Uriel (1961)) and Rowe consolidation test developed by Rowe and Barden, 1966.

The measurement of horizontal consolidation of soil in standard consolidation test was achieved by modifying the equipment to provide radial drainage or by cutting the specimen appropriately in the respective direction (Ajlouni, 2000). In Rowe consolidation cell, the horizontal consolidation of soil can be evaluated by performing the test with radial drainage. There are two types of test: central or radial inward drainage and periphery or radial outward drainage. These tests are presented in Figures 2.9 (e), (f), (g) and (h). The estimation of the horizontal coefficient of consolidation based on this test is similar to that done for vertical consolidation except for the time factor. The time factor (T_v) for 50 and 90% degree of consolidation for periphery drainage with average drainage condition are 0.0866 and 0.288 respectively (Head, 1986).

CHAPTER 3

METHODOLOGY

3.1 Introduction

The study was an experimental research, which concentrate on the evaluation of coefficient of rate of horizontal consolidation of fibrous peat. The methodology of the research is summarized in the flowchart shown in Figure 3.1. Literature study was made to provide rationale of the research and to gather sufficient information on the consolidation behavior of fibrous peat. The samples of fibrous peat were obtained from Kampung Bahru, Pontian, Johor from depth of 1 to 2 m below the ground surface, thus, the sample is considered as surface peat. The sampling method is described in report for UTM fundamental research vot 75137 (2006). The organic and fiber content of the peat as well as the degree of humification obtained from previous research have shown that the soil can be classified as fibrous peat.

The scanning Electron Micrograph was performed to evaluate the structural arrangement of the peat. Engineering characteristics evaluated in this research include consolidation and permeability test. Preliminary evaluation of the consolidation characteristics of the soil is based on the standard consolidation test. Constant-head permeability tests were carried out to determine initial hydraulic conductivity of the peat. All laboratory test procedures are based on the manual of soil laboratory testing (Head, 1981, 1982, 1986) in accordance with the British Standards (BS) and American Standard Testing Methods (ASTM).

The focus of the research was to evaluate consolidation parameters (c_h, c_v, c_α, k_h, and k_v) of the fibrous peat under a range of consolidation pressures. The evaluation is based on the hydraulic consolidation tests (Rowe Cell), and the time–compression curve obtained from the test. Comparison between c_h and c_v as well as comparison between k_h, and k_v under various consolidation pressure was evaluated to confirm the hypothesis developed for the study that the dissipation of pore water pressure in horizontal direction is actually faster that that in vertical direction. Evaluation of the effect of secondary compression on the consolidation of fibrous peat was also performed.

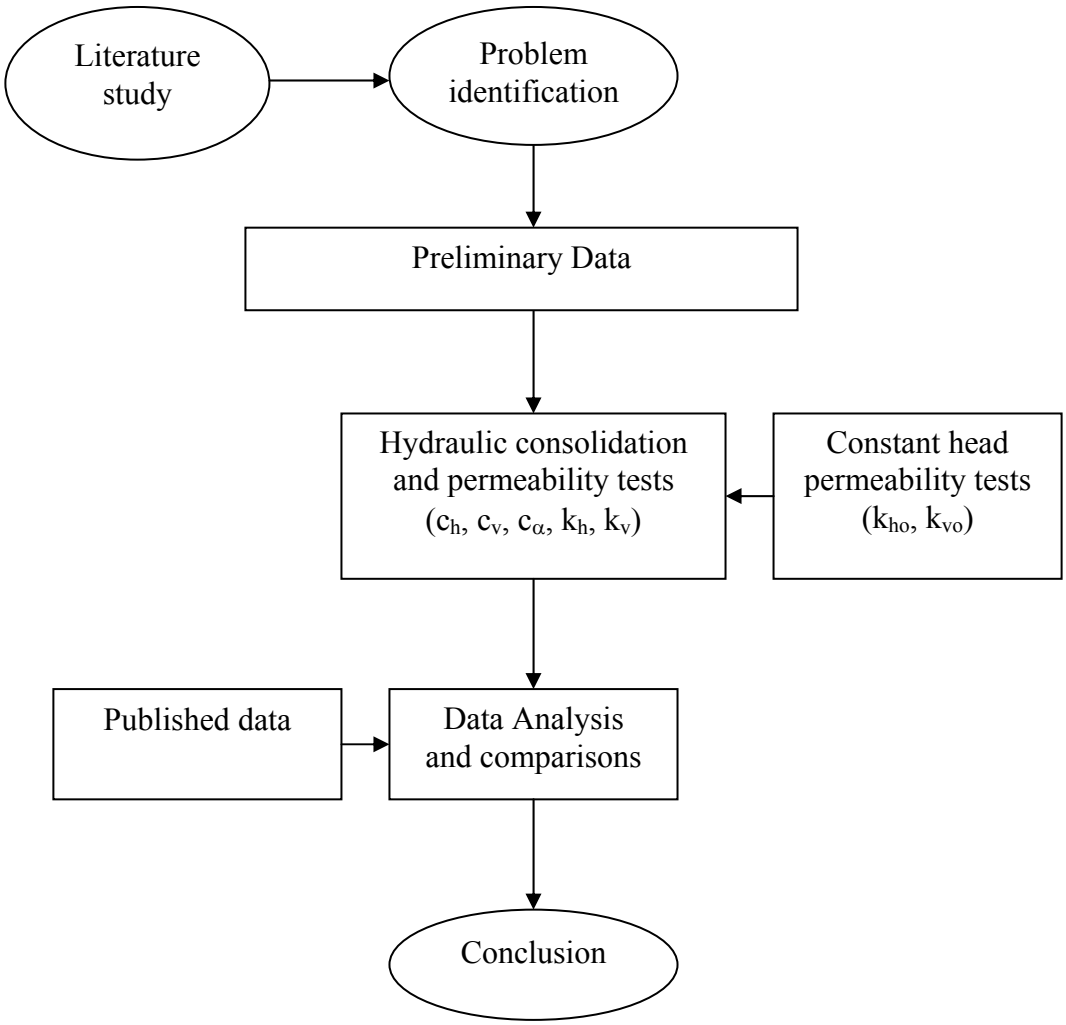

Figure 3.1 Flow chart of the study

3.2 Preliminary data

Most of the preliminary data for the research such as physical and chemical characteristics and classification of the peat under study were acquired from report for fundamental research vot 75137 (2006). Standard consolidation test data useful for establishing the rate of consolidation pressure to be used in the large strain consolidation test was also obtained from the report.

Considering the published range of initial permeability of fibrous peat, constant head permeability test was adopted in this study to determine the initial permeability of the soil in horizontal and vertical directions. The constant head permeability test was done on sample obtained vertically and horizontally using piston sampler. The tests are done following standard procedures of ASTM D2434.

Scanning Electron Micrograph were done in this research to determine the structural arrangement of the soil as the basis for the analysis on the horizontal coefficient of consolidation and the effect of secondary compression on the consolidation of the peat. The test follows the standard procedure outlined in ASTM F 1392-93.

3.3 Large Strain Consolidation Test

Evaluation of the coefficient of consolidation in vertical and horizontal direction was performed on large strain consolidation tests using Rowe consolidation cell (Figure 3.2) with internal diameter of 150 mm and height of 50 mm. The vertical consolidation was tested under two-way vertical drainage, while the horizontal consolidation was evaluated by horizontal drainage to periphery. Under both conditions, the soil samples were subjected to hydraulic consolidation pressures of 25, 50, 100, and 200 kPa.

The effect of consolidation pressure on fabric arrangement and therefore the permeability of the peat were studied by carrying out permeability test on Rowe cell under consolidation pressure of 100 and 200 kPa for vertical and horizontal drainage.

The setting up the apparatus and the procedures for both consolidation and permeability tests are outlined in Appendix B.

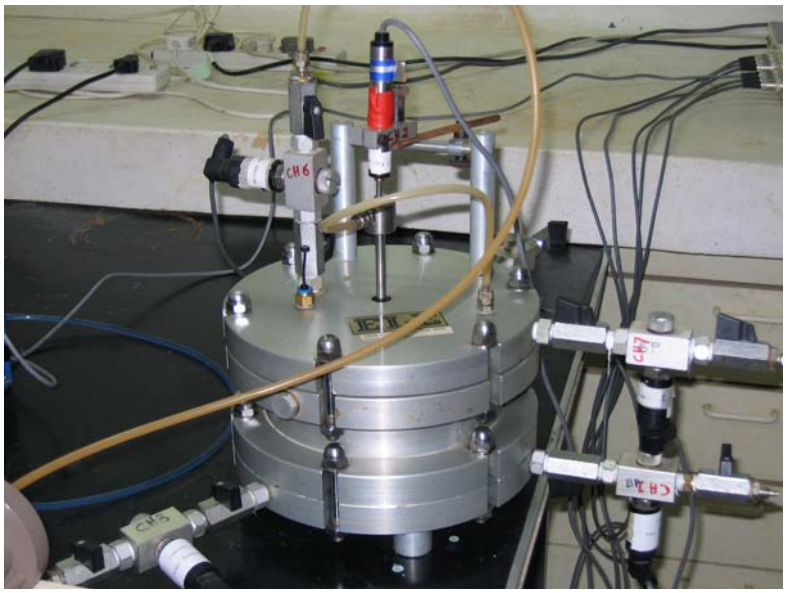

Figure 3.2 Rowe Consolidation cell

3.4 Data Analysis

3.4.1 Analysis of Test Results

Graphical plots of settlement, volume change, and pore-water pressure as a function of time were obtained from each loading stage of a Rowe cell consolidation test. The graph was kept up to date during each loading stage to monitor the progress of primary consolidation to reach 100%. These graphs are used to determine the time corresponding to primary consolidation and secondary compression, from which the coefficient of consolidation can be calculated by using an equation with the appropriate multiplying factor.

Wherever possible, it is better to use the pore pressure dissipation graph rather than the settlement or volume change curve because the end points (0% and 100% dissipation) are both clearly defined and t_{50} or t_{90} can be read directly from the graph. The t_{50} point is preferable because the mid portion of the curve best fit to the theoretical curve. Settlement and volume-change measurements are governed by the deformation of the sample as a whole, and analysis is dependent on an overall 'average' behavior.

Besides the time compression curve, a graph relating the void ratio at the end of each loading stage with the effective pressure on a linear or logarithmic scale was plotted for a complete set of consolidation test data. The e–p' curve is used to obtain coefficient of axial compressibility a_v and thus the coefficient of volume compressibility m_v, while the e–log p' is used to obtain compression and recompression indexes, c_c and c_r respectively. Pre-consolidation pressure can also be obtained if possible. These data are required for evaluation of the magnitude of primary settlement and to obtain the ratio of c_α/c_c for calculation of secondary compression.

3.4.2 Analysis of Time-Compression Curve

The time-compression curves derived from test results were analyzed based on Cassagrande and Robinson methods. The secondary compression index as well as the beginning and end of secondary compression are among the parameters required for the analysis of secondary compression. Furthermore the settlement and the coefficient of rate of consolidation c_v was calculated based on the curve.

Cassagrande method requires a compression–log time curve to evaluate the parameters. The detailed procedure for analysis of time–compression curve by Cassagrande method is outlined in Sections 2.2.1 and 2.2.2. Besides the compression–log time curve, the pore-water pressure–log time curve is required for evaluation of the parameters by Robinson's method. These plots are used to develop compression–degree of consolidation graph as the basis for determination of

settlement and c_v. The procedures for evaluation of settlement and coefficient of consolidation c_v by Robinson's method is outlined in Section 2.4.

3.4.3 Analysis of output

As pointed out in the beginning, the output of the study is presented in terms of coefficient of consolidation and permeability in horizontal and vertical directions c_h, c_v, k_h, k_v, as well as the effect of secondary compression c_α, These values were evaluated and compared. The ratios of c_h/c_v and k_h/k_v can be used for analysis on the effect of fabric on the properties. The ratio of c_α/c_c can be used as a basis for evaluation of secondary compression of the peat. These results were compared to the published data on similar type of soil.

CHAPTER 4

RESULTS AND DISCUSSION

4.1 Introduction

The discussion in this chapter will follow the stated objectives of the study mentioned in Chapter 1. Section 4.2 presents the results of the laboratory test on the soil identification and consolidation characteristics based on the standard Oedometer test obtained from previous research (UTM Fundamental vot 75137). Section 4.3 deals with the study on the fiber orientation of the soil sample which is very useful on the analysis of horizontal coefficient of consolidation.

The main focus of the study is to determine the horizontal coefficient of consolidation on Rowe consolidation test, and the results are compared with the vertical coefficient of consolidation. The results of the test and the analysis of the compression curves obtained from the tests are given in Section 4.4. Effect of secondary compression on the consolidation behavior in both directions is discussed in Section 4.5.

Fiber orientation influences the permeability of soil and application of pressure affects the fiber orientation, thus; permeability characteristics are evaluated in the study. Section 4.6 presents the analysis on the initial

permeability obtained from constant head permeability test, permeability obtained from consolidation test and the permeability calculated from the coefficient of consolidation. Comparisons on the horizontal and vertical permeability are also subject of analysis.

4.2 Soil identification

As mentioned previously, data on the fundamental properties of the peat soil is obtained from previous research and summarized in Table 4.1. As shown in Table 4.1, the peat soil is acidic with high organic and fiber contents which are typical of peat soil in West Malaysia (Muttalib, 1991 and Huat, 2004). Thus, based on the fiber and organic content, the soil can be identified as Fibrous peat. Moisture content of 608 % indicates that the peat soil has a high water-holding capacity. Based on von Post humification scale, the peat can be classified as H_4 or low to medium degree of decomposition.

Table 4.1: Basic properties of the peat soil

	Parameters	**Results**	**Published data (ranges)**
Index properties	Von Post humification of peat	H_4	H_1- H_4
	Natural water content (%)	608	200 – 700
	Bulk unit weight (kN/m^3)	10.02	8.30 – 11.50
	Dry unit weight (kN/m^3)	1.40	
	Specific Gravity (G_s)	1.47	1.30 – 1.80
	Initial void ratio (e_o)	8.92	3 – 15
	Acidity (pH)	3.24	3.0 – 4.5
Classification	% < 0.063 mm	2.74	
	Organic content (%)	97	> 90
	Ash content (%)	3	< 10
	Fiber content (%)	90	> 20

Standard Oedometer test was conducted on 12 samples. Each of the samples has a thickness of 20.13 mm, a diameter of 50.23 mm, and was subjected to consolidation pressures of 12.5 kPa, 25 kPa, 50 kPa, 100 kPa, 200 kPa, and 400 kPa. The results indicate that primary consolidation and secondary compression characteristics of the soil can be easily identified from consolidation curves.

Typical log time-compression curve from Oedometer test is shown in Figure 4.1. It can be observed from the Figure that the primary consolidation is still dominant in the compression of the peat, but the consolidation occur in a relatively short time as compared to clay. Secondary compression, even though less significant than the primary consolidation in term of magnitude, could be very important in term of the design life of a structure. Tertiary compression was observed from the test results, but may not be very significant in term of the design life of a structure because as shown in Figure 4.1, the secondary compression takes a significant amount of time.

The e-log p' curve obtained from the set of data shows that the pre-consolidation pressure is about 45 kPa and the compression index is 3.772. Based on the oedometer data, the range of consolidation pressure to be used in large strain consolidation test is 25, 50, 100, and 200 kPa.

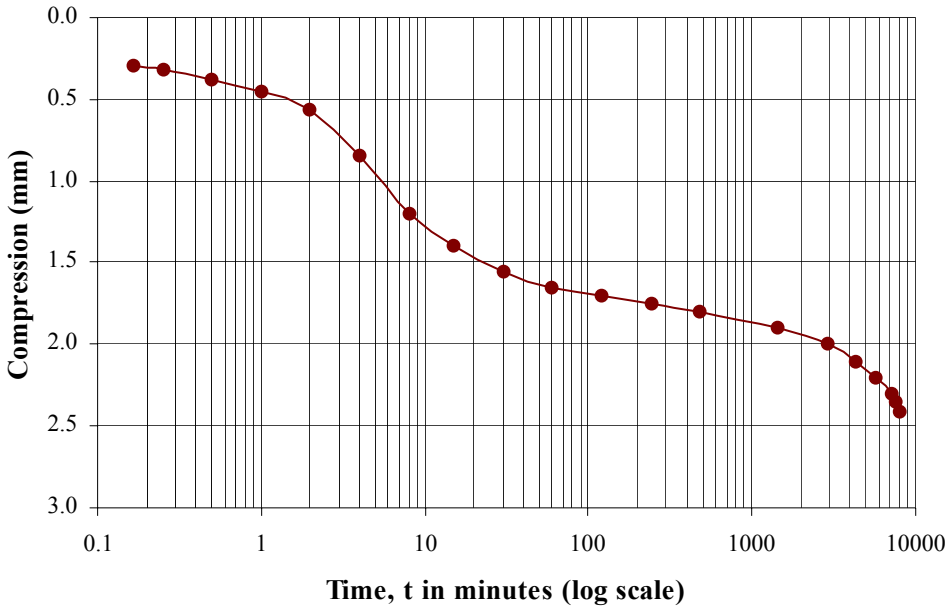

Figure 4.1: Typical log time-compression curves from oedometer test

4.3 Fiber Orientation

Fiber orientation is identified as a dominant factor is the structure of fibrous peat soil. The presence of the fiber induces the natural soil imperfections or discontinuities such as, fissures, cracks, rootlets and pockets of organic material may results in the high initial permeability of the soil. The application of consolidation pressure may induce a rearrangement of fiber orientation and drastically reduces the void, causing a significant reduction in the vertical permeability.

Even though most of the features of anisotropy of the fibrous peat are visible to the naked eye, a more detailed analysis on the microstructure of the fiber and the fiber content can be examined under a Scanning Electron Microscope (SEM). The examination is important because research have shown that the fiber content appears to be a major compositional factor in determining the way in which peaty soils behave (Dhowian and Edil 1980).

Figure 4.2 and 4.3 show the typical fiber orientation obtained by Scanning Electron Microscope for the fibrous peat obtained from Kampung Bahru, Pontian at initial state and under consolidation pressure of 200 kPa. The samples were cut in vertical and horizontal sections to enable the observation of the rearrangement of the fiber due to application of consolidation pressure. Comparison of the two pictures indicates a pronounced structural anisotropy for the fibrous peat with the void spaces in the horizontal direction larger than those in the vertical direction resulting from the fiber orientation within the soil. Individual microstructures remained essentially intact after compression under high-stress conditions. This implies that for the fibrous peat soil, horizontal rates of permeability and consolidation are larger than their respective vertical rates of permeability and consolidation. The results of Scanning Electron Microscope of Fibrous peat samples under various consolidation pressure and drainage are given in Appendix B.

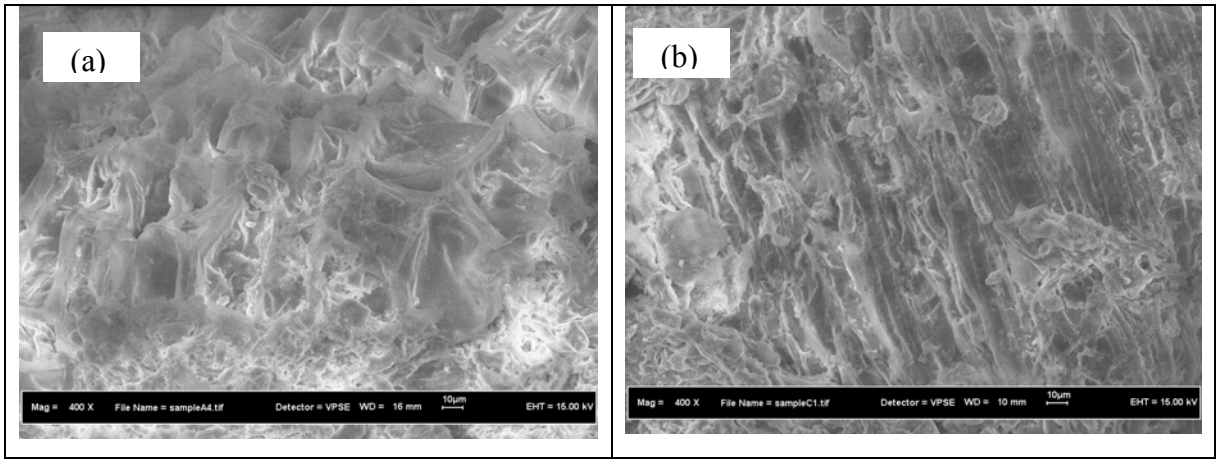

Figure 4.2 SEM of fibrous peat samples at initial state (a) horizontal section x 400, (b) vertical section x 400

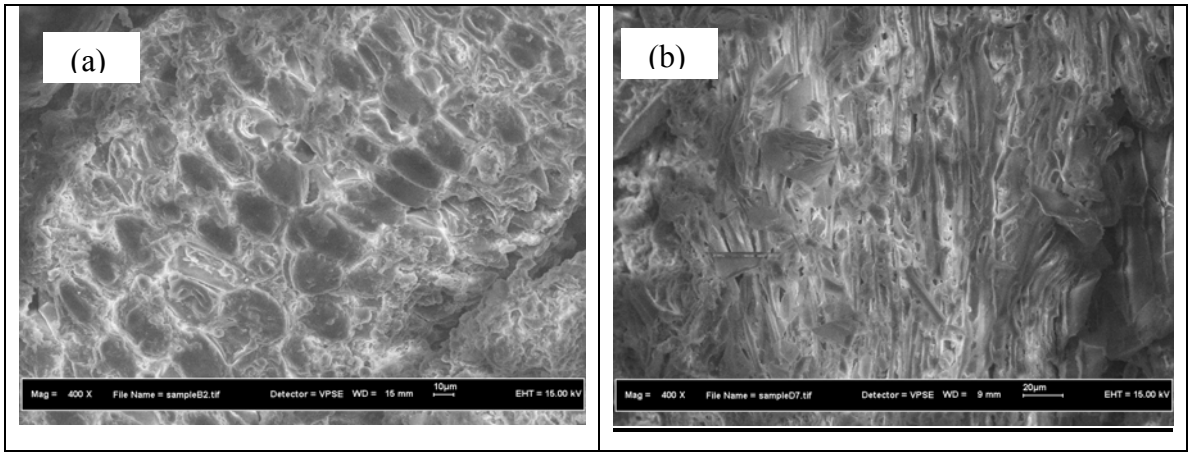

Figure 4.3 SEM of fibrous peat samples under consolidation pressure of 200 kPa (a) horizontal section x 400 (b) vertical section x 400

4.4 Analysis of Compression Curves from Consolidation Tests (Rowe Cell)

Hydraulic vertical and radial consolidation tests were conducted on 'identical' fibrous peat soil sample in order to evaluate secondary compression characteristics of the soil with respect to periphery and two-way vertical drainages. The sample was placed on a Rowe consolidation cell with diameter of 151.4 mm and height of 48.78 mm. Each sample was subjected to hydraulic consolidation pressures of 25, 50, 100, and 200 kPa during the test. Complete data on the results of consolidation test is given in Appendix D and Appendix E for samples subjected to vertical and horizontal drainage respectively.

Figure 4.4 and Figure 4.5 show the typical time–compression and time–pore water pressure dissipation curves obtained from the results of consolidation test for samples subjected to vertical drainage, while Figure 4.6 and 4.7 show similar plots for samples subjected to horizontal drainage. It can be seen from the Figures 4.4 and 4.6 that the time–compression curves obtained from large strain test are similar in shape with the results of Oedometer test (Figure 4.1), except that the tertiary consolidation appeared earlier than those observed in Oedometer test.

The shape of log time-compression curve indicates that deformation process of fibrous peat often strongly deviates from the simple model used in Terzaghi's consolidation equation, which is the basis for the Casagrande and Taylor's evaluations of primary consolidation and estimation of the coefficient of rate of consolidation. The time compression curves obtained from both Oedometer and Rowe cell did not give a clear indication of an inflection point where the primary consolidation is assumed to end and the secondary consolidation is assumed to start. Thus, the secondary consolidation may have started during the process of pore water pressure dissipation. Furthermore, the figures show that the secondary consolidation does not occur at a constant rate. However, comparison of Figure 4.4 and 4.6 indicated that the consolidation test on Rowe cell with horizontal drainage give a better curves in terms of inflection point and rate of secondary consolidation. This may be due to the fact that the primary consolidation occurred more rapidly with the implementation of perimeter drainage in the Rowe cell.

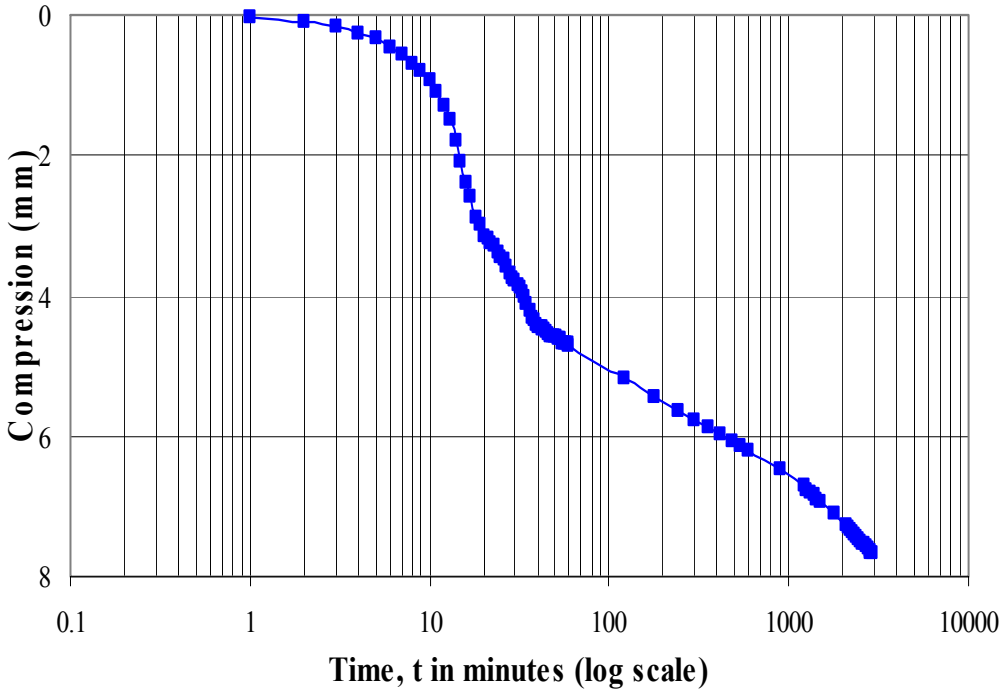

Figure 4.4: Log time-compression curves from hydraulic consolidation test with vertical drainage for consolidation pressure 50 kPa.

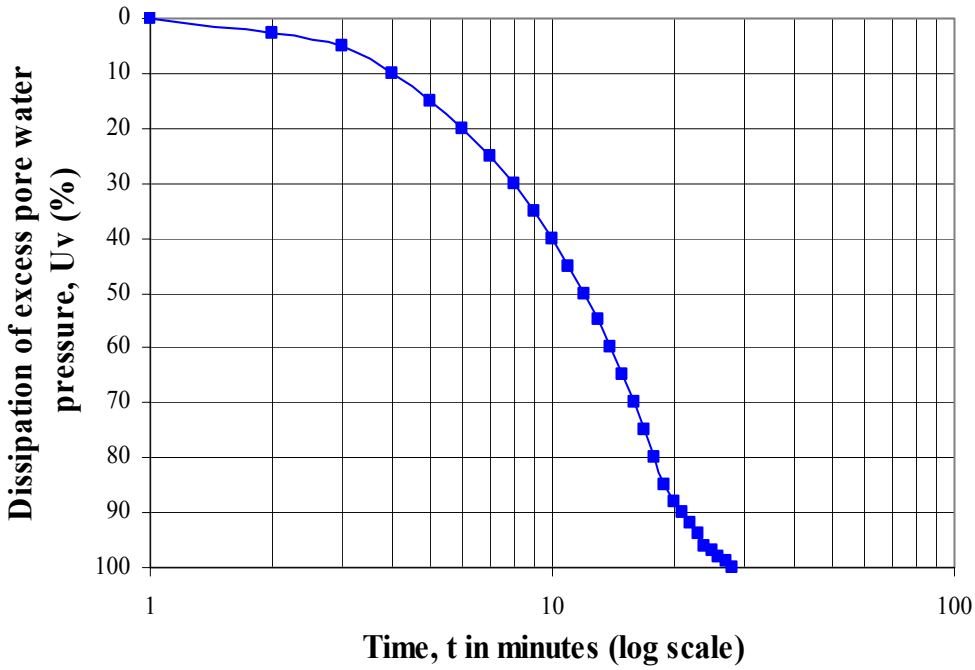

Figure 4.5: Log time-pore water pressure curve from hydraulic consolidation test with vertical drainage for consolidation pressure 50 kPa.

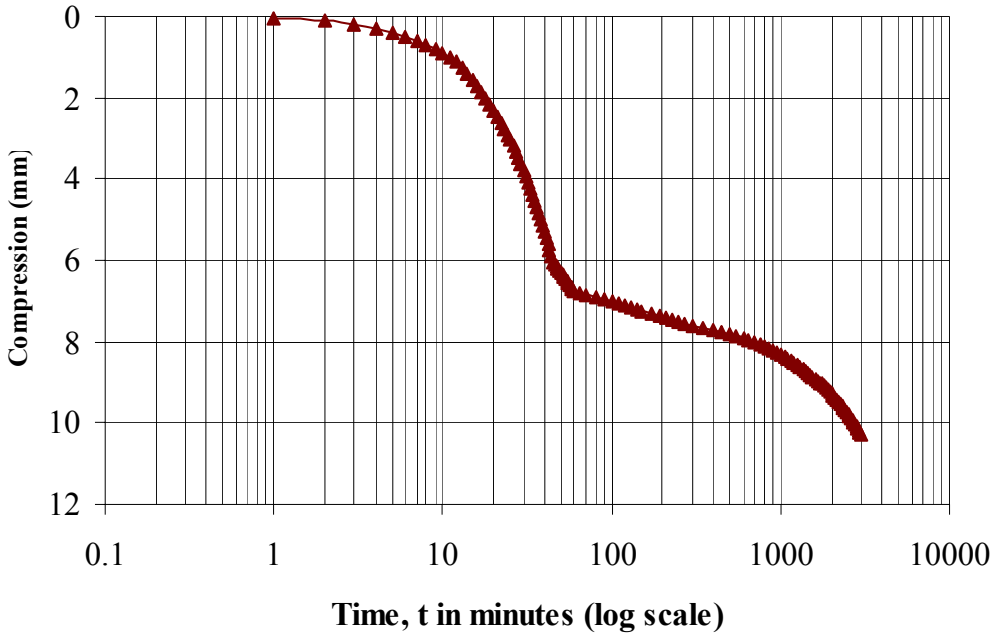

Figure 4.6: Log time-compression curves from hydraulic consolidation test with horizontal drainage for consolidation pressure 50 kPa.

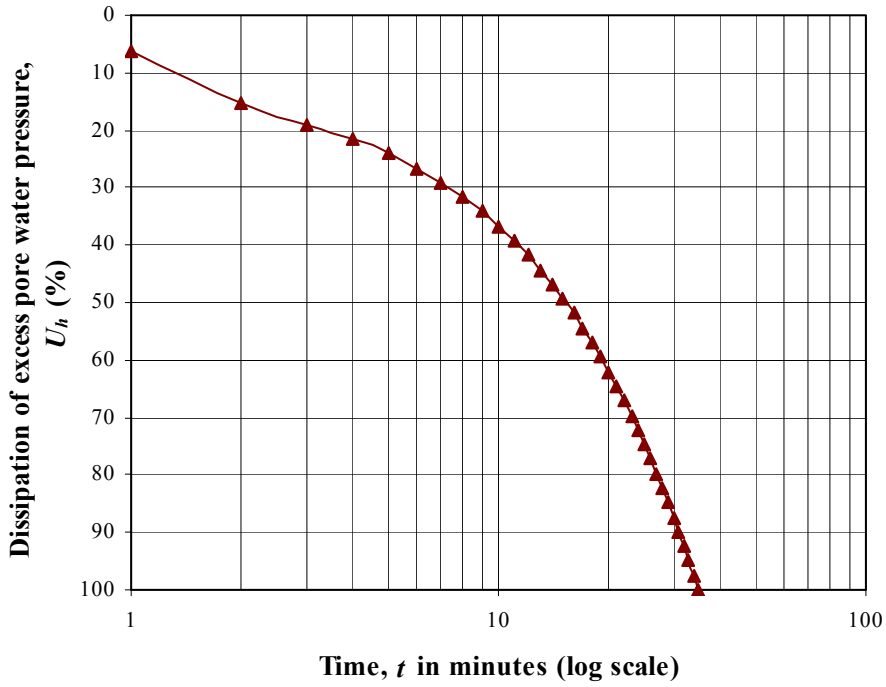

Figure 4.7: Log time-pore water pressure curve from hydraulic consolidation test with horizontal drainage for consolidation pressure 50 kPa.

Figure 4.6 shows that the consolidation test with horizontal drainage gave a distinctive curve and a clear inflection point when compared with Figure 4.4. Furthermore, the end of primary consolidation is also easier to obtain from Figure 4.7 as compared to Figure 4.5. This might be due to the fact that the fiber tends to rearrange in horizontal direction during primary consolidation that the end of the primary consolidation with horizontal drainage is more visible when compared to the consolidation with two ways vertical drainage. Comparison of Figure 4.4 and 4.6 also show that the secondary consolidation seems to be more dominant when the soil is subjected to consolidation pressure with vertical drainage. In this case, the secondary compression started during the dissipation of excess pore-water pressure, and the secondary consolidation started earlier when subjected to two-way vertical drainage.

The time-compression curves and the time-pore water pressure dissipation curves derived from each test were evaluated using Robinson's (2003) method to obtain the compressibility characteristics i.e. the coefficient of consolidation and the coefficient of secondary consolidation both in vertical and horizontal directions.

Figures 4.8 and Figure 4.9 show the relationship between the degree of consolidation and the compression for samples subjected to vertical and horizontal drainage respectively. The curves are useful for separating the primary consolidation from the secondary compression. The degree of primary consolidation where the secondary compression started can be identified from the figures as the point where the curve deviates from a straight line. Primary and secondary compression occurred beyond this point should be separated and the curves were used to develop a primary consolidation and secondary compression curves. The primary consolidation cuve was used for the evaluation of coefficient of consolidation (c_v and c_h), while the secondary compression part was used for evaluation of coefficient of secondary consolidation ($c_{\alpha v}$ and $c_{\alpha h}$). The procedure is presented in Section 2.4 while the analysis for a typical set of data are given in Appendix D and E for the results of consolidation test on Rowe Cell with two-way vertical and radial drainage respectively.

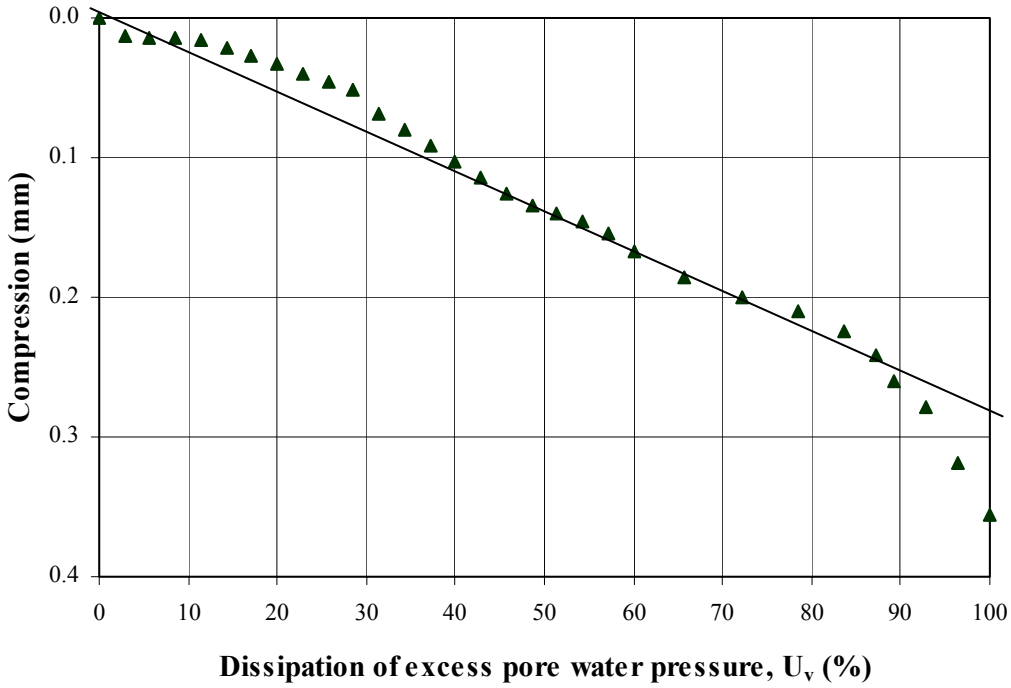

Figure 4.8: Typical degree of consolidation - compression curve from hydraulic consolidation test with two-way vertical drainage.

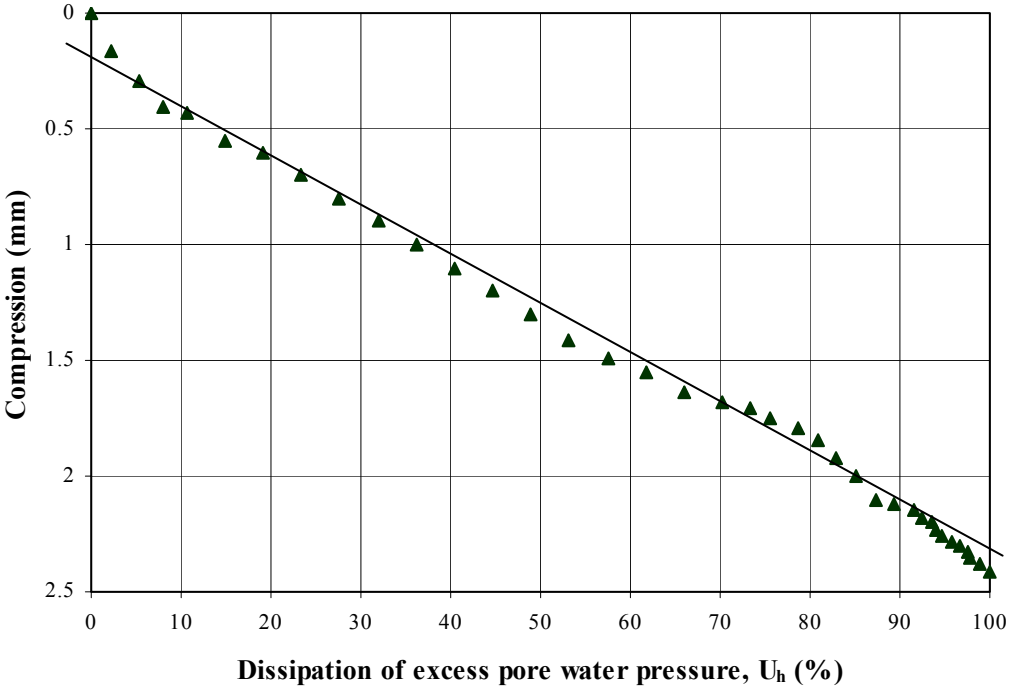

Figure 4.9: Typical degree of consolidation - compression curve from hydraulic consolidation test with horizontal drainage.

In accordance with Figures 4.4 and 4.6, Figure 4.8 and 4.9 shows that the secondary consolidation is more dominant when the soil is subjected to consolidation pressure with vertical drainage. It seems that the horizontal drainage have the effect of eliminating the secondary consolidation, and increasing the primary consolidation. Figure 4.8 and 4.9 shows that the primary consolidation of the identical sample subjected to horizontal drainage is almost ten times of the primary settlement when the sample subjected to vertical drainage even-though the final settlement is almost equal.

Time compression analysis gives the time of the completion of primary consolidation (t_{100}) which is an important parameter for evaluation of consolidation behavior of fibrous peat. The average time needed for complete dissipation of pore water pressure (t_{100}) and the variation with consolidation pressure Table 4.2.

Figure 4.10 and Figure 4.11 shows the variation of the completion of primary consolidation with consolidation pressure. The curves show a clear indication that t_{100} decreases non-linearly with increasing consolidation pressure. The higher the consolidation pressure, the faster the dissipation of pore-water pressure and the shorter the time needed for primary consolidation. Comparison of Figure 4.10 and 4.11 shows that: the t_{100} for horizontal consolidation is generally higher than that obtained from vertical consolidation due to the length of drainage path. For vertical consolidation the length of drainage path is half the thickness of sample, while the drainage path for horizontal consolidation is the radius of the sample.

Table 4.2: Average time for completion of primary consolidation (t_{100}) obtained from Rowe test results

No	Consolidation Pressure (kPa)	Vertical consolidation (min)	Horizontal consolidation (min)
1.	25	27.4	41.3
2.	50	25.6	37.0
3.	100	23.0	34.3
4.	200	22.6	31.3

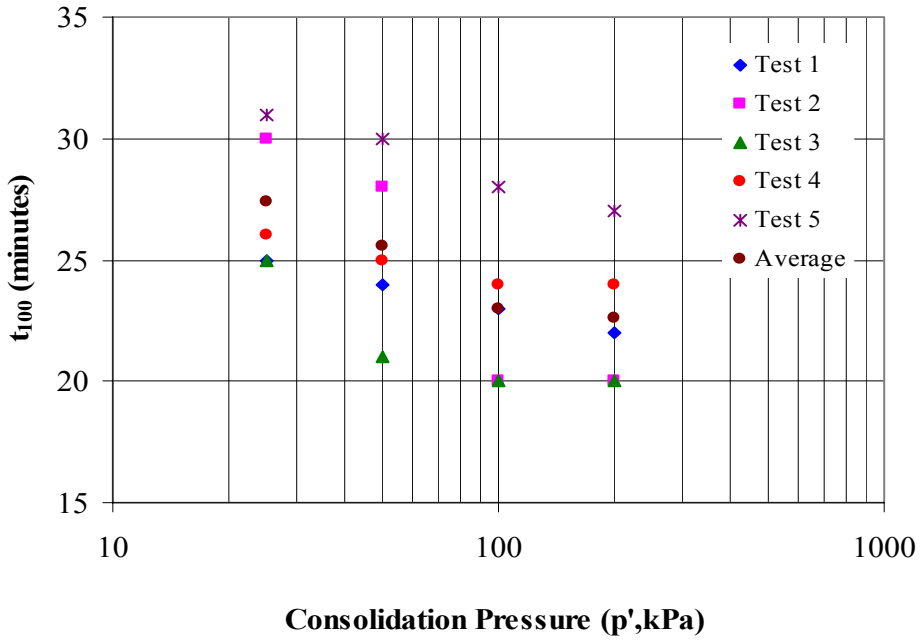

Figure 4.10 Variation of the beginning of secondary consolidation with consolidation pressure for sample tested under vertical consolidation

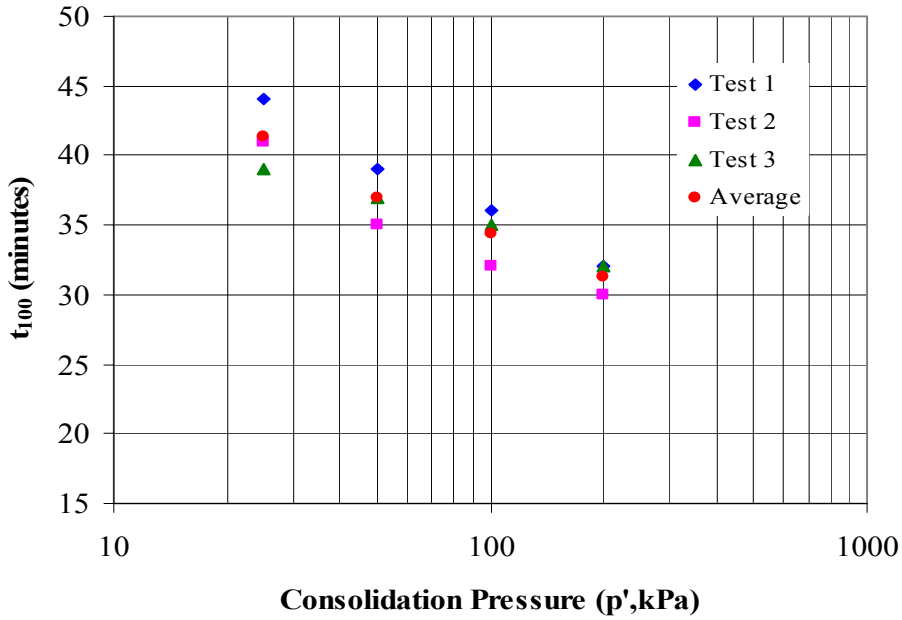

Figure 4.11 Variation of the beginning of secondary consolidation with consolidation pressure for sample tested under horizontal consolidation

The end of primary consolidation (t_{100}) is used for evaluation of the coefficient of rate of consolidation. Figure 4.12 and Figure 4.13 show the variation of the coefficient of consolidation obtained from the tests with consolidation pressure subjected to vertical and horizontal drainage respectively.

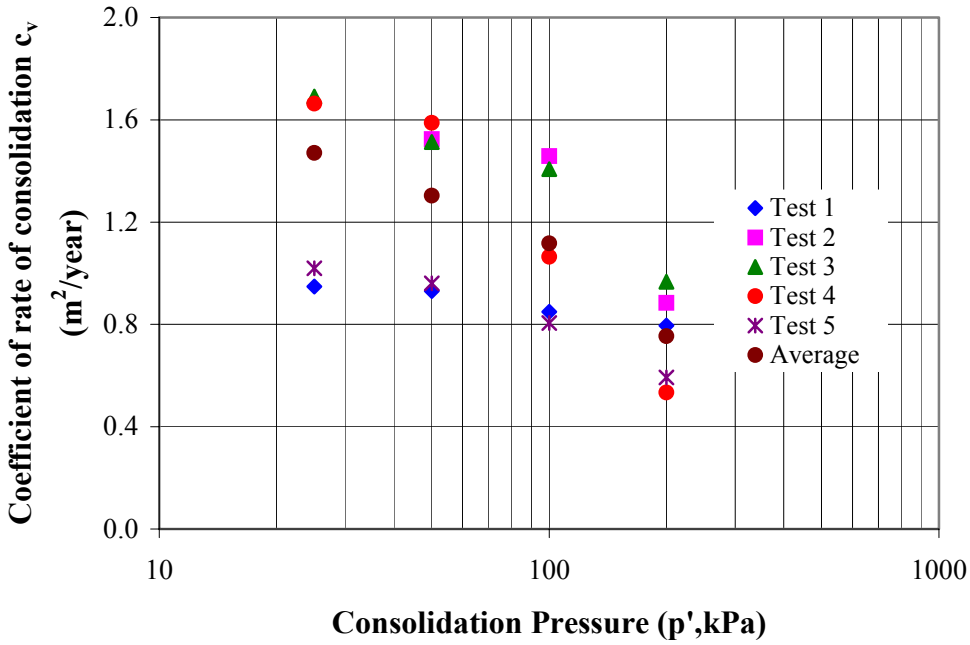

Figure 4.12: Variation of coefficient of secondary consolidation with consolidation pressure for sample tested under vertical consolidation

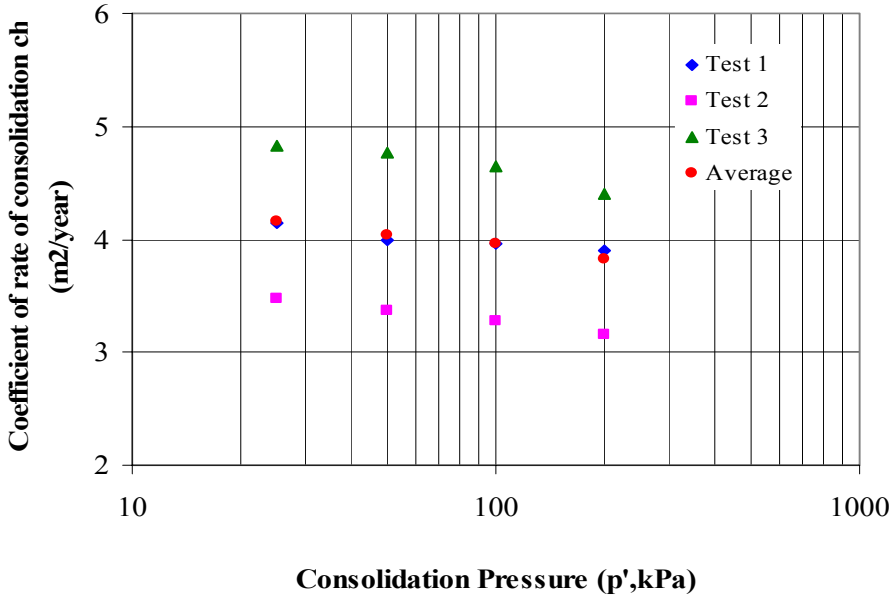

Figure 4.13: Variation of coefficient of secondary consolidation with consolidation pressure for sample tested under horizontal consolidation

It is clear from the Figures 4.12 and 4.13 that the coefficient of consolidation decreases almost linearly with increasing consolidation pressure, however the effect is more significant for samples subjected to vertical consolidation, may be due to the rearrangement of fiber. This finding is in agreement with the theory of consolidation which stated that the coefficient of rate of consolidation decreases with increasing consolidation pressure. However, comparison of Figures 4.12 and 4.13 indicates that the decrease is more significant for the sample subjected to vertical drainage.

The average coefficient of rate of consolidation obtained from Rowe consolidation test with vertical and horizontal drainage are shown in Table 4.3. The ratio of c_h/c_v obtained based on the average values are shown in the last column of the Table. The ratio of c_h/c_v increases as the consolidation pressure increases. This findings demonstrate that the effect of consolidation pressure is more significant to the pore water pressure dissipation in vertical direction.

Table 4.3: Average coefficient of consolidation obtained from Rowe test results

No	Consolidation Pressure (kPa)	Coefficient of vertical consolidation, c_v (m^2/yr)	Coefficient of horizontal consolidation c_h (m^2/yr)	Ratio c_h/c_v based on average values
1.	25	1.47	5.22	3.55
2.	50	1.30	5.07	3.90
3.	100	1.12	4.89	4.37
4.	200	0.76	4.48	5.89

The results on the analysis of time-compression curve for each test based on Robinson (2003) method are given in Appendix D and E for vertical and horizontal consolidation respectively.

4.5 Effect of Secondary Compression on Rate of Consolidation

The preceding discussion has shown that the secondary consolidation is more significant when the sample is subjected to consolidation pressure with vertical drainage as compared to horizontal drainage. The completion of dissipation of pore water pressure as indicated in Table 4.2 does not necessarily represent the beginning of secondary consolidation. Thus evaluation of Figure 4.8 and 4.9 for all results of consolidation tests are required to obtain the degree of consolidation indicating the beginning of secondary compression. The figures indicate that the secondary compression started during the primary consolidation. However, comparison of Figure 4.8 and 4.9 shows that the secondary consolidation started earlier when subjected to two-ways vertical drainage.

Table 4.4 shows the average degree of consolidation for which the secondary consolidation started and the time of the beginning of secondary consolidation obtained from all consolidation test data.

Table 4.4: Average degree of consolidation (U%) and the time for the beginning of secondary compression (t_p) obtained from Rowe test results

No	Consolidation Pressure (kPa)	Vertical consolidation		Horizontal consolidation	
		U(%)	t_p (min)	U(%)	t_p (min)
1.	25	64.6	17.7	80.6	33.3
2.	50	60.1	15.4	76.5	28.3
3.	100	56.1	12.9	66.2	22.7
4.	200	53.1	12.0	61.4	19.3

Figure 4.14 and Figure 4.15 shows the variation of the beginning of secondary consolidation with consolidation pressure. The curves show a clear indication that t_p decreases non-linearly with increasing consolidation pressure. The higher the consolidation pressure, the faster the dissipation of pore-water pressure and the shorter the time needed for primary consolidation.

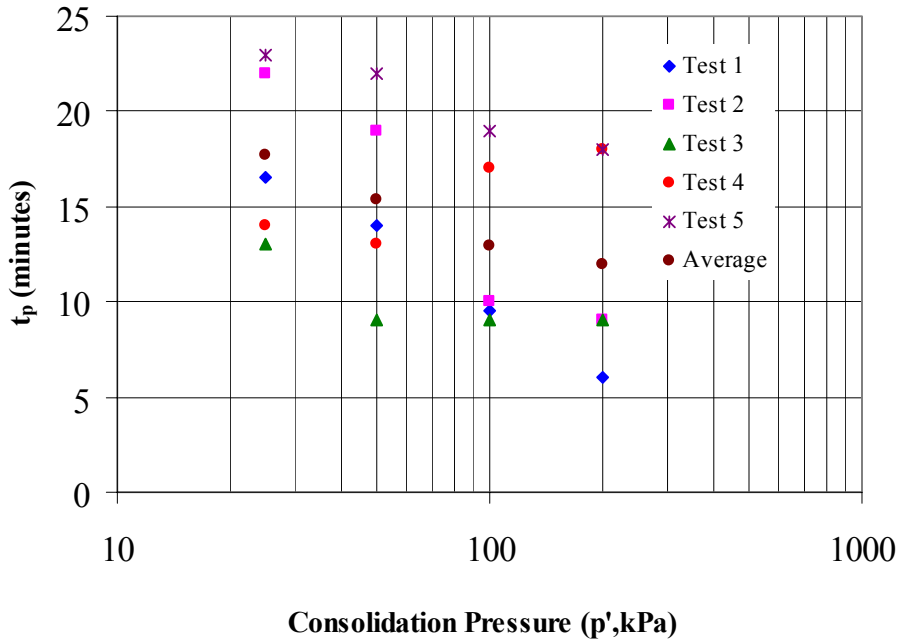

Figure 4.14 Variation of the beginning of secondary consolidation with consolidation pressure for sample tested under vertical consolidation

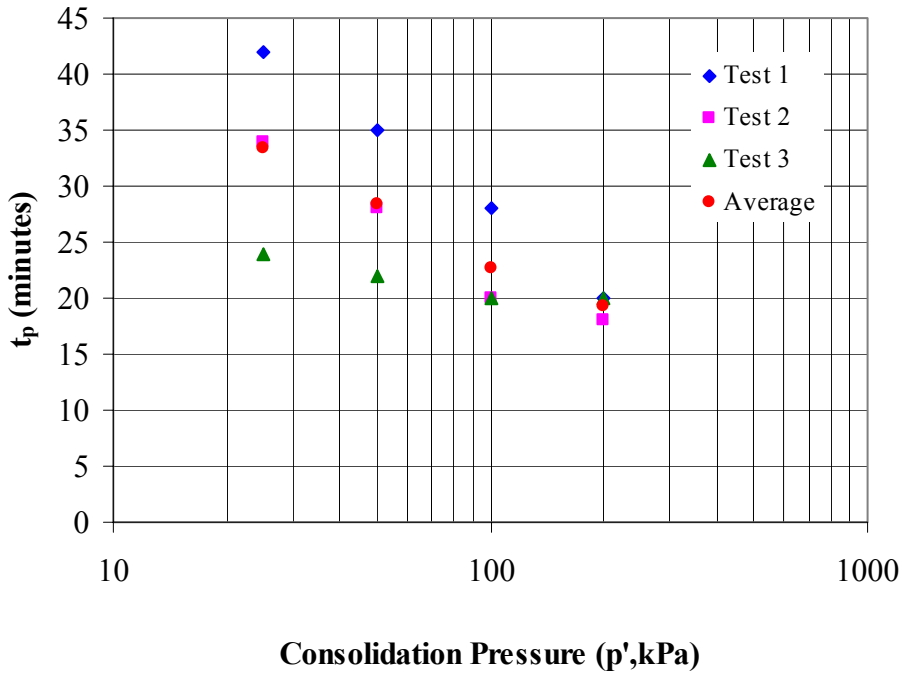

Figure 4.15 Variation of the beginning of secondary consolidation with consolidation pressure for sample tested under horizontal consolidation

The secondary consolidation is evaluated from the second part of Figure 4.8 and 4.9 for samples subjected to vertical and horizontal consolidation respectively. Figure 4.16 and Figure 4.17 show the variation of the coefficient of secondary compression c_α with consolidation pressure. As expected, there is no clear trend on the relationship between the coefficients of secondary consolidation with consolidation pressure, thus; the mean and standard deviation were obtained for the coefficient of secondary compression over the whole range of pressure. The analysis yields the coefficient of secondary consolidation in vertical direction is 0.261 while the secondary consolidation in horizontal direction is 0.226. Given the c_c value obtained from previous research (Research Report for UTM Fundamental vot 75137) equal to 3.128 and 2.879 respectively, the ratio of c_α/c_c for Pontian Peat are 0.083 and 0.078 for vertical and horizontal consolidation respectively or average c_α/c_c value is 0.08. This finding supports the previous researches that the coefficient of secondary consolidation is constant and the ratio of c_α/c_c could be used as a basis for the calculation of secondary consolidation of soil. This value is in slightly higher than published data on different type of peat (Mesri, 1997).

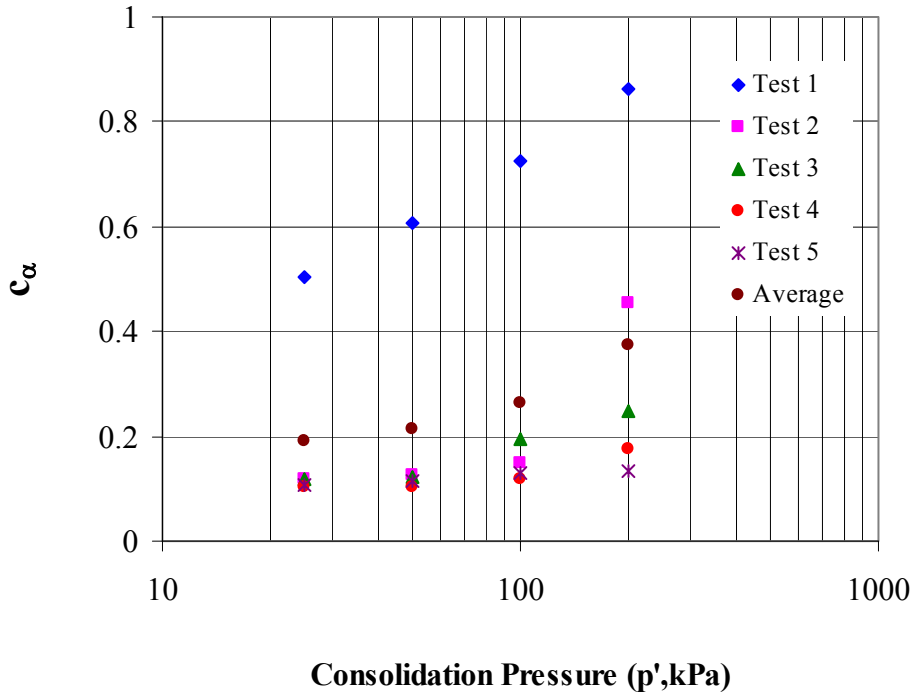

Figure 4.16 Variation of coefficient of secondary consolidation with consolidation pressure for sample tested under vertical consolidation

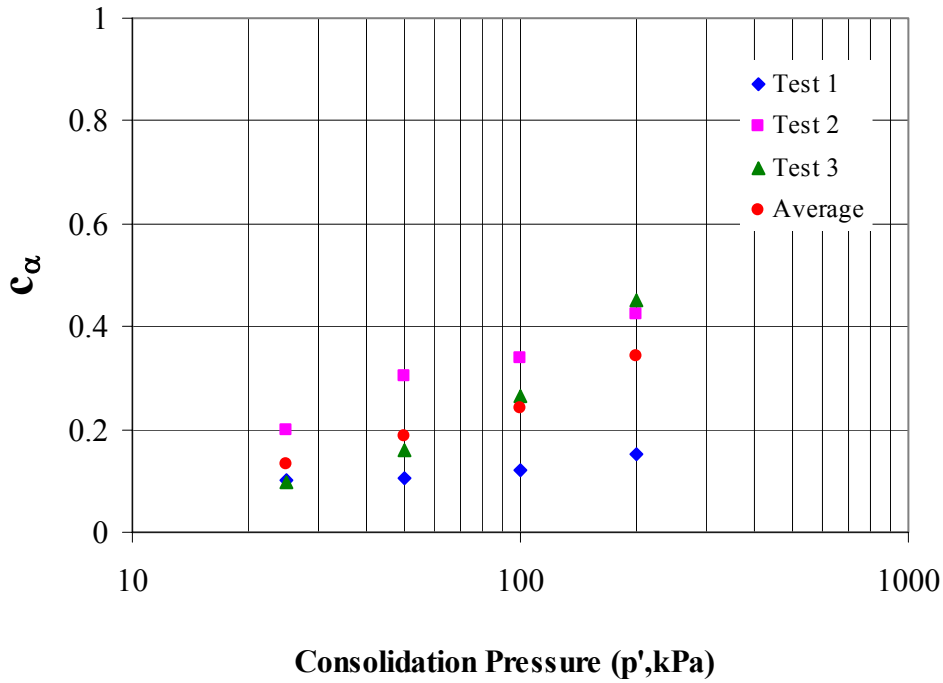

Figure 4.17 Variation of coefficient of secondary consolidation with consolidation pressure for sample tested under horizontal consolidation

4.6 Permeability

The rate of consolidation of the fully saturated and undisturbed fibrous peat soil is affected primarily by the permeability of the soil. Compression of the soil occurs rapidly when a new loading is applied and this is directly related to the high permeability of the soil. As such, it is important to evaluate the permeability of the soil, which is defined as the ability of water to flow through the soil. The permeability of the soil is characterized by the soil's permeability parameters, namely vertical coefficient of permeability, k_v, and horizontal coefficient of permeability, k_h. Evaluation of permeability is made in this research for evaluation of the effect of fiber on the initial permeability and effect of application of consolidation pressure on the reorientation of the fiber and permeability of the soil. The procedures and results of the permeability tests are given in Appendix F.

4.6.1 Initial Permeability

The initial permeability of the soil is observed through constant head permeability test. The samples for the test were obtained by piston sampler pushed into the soil in horizontal and vertical directions. The sample was transferred directly to the permeameter for the test to ensure minimum disturbance. The test were performed on four undisturbed horizontal soil samples, which were cut with their axes perpendicular to the vertical direction of the in situ soil, and three undisturbed vertical soil samples, which were cut with their axes parallel to the vertical direction of the in situ soil. The purpose of the tests was to determine the initial rate of permeability of the soil with respect to horizontal and vertical directions.

The results of the test revealed that at initial state, the average horizontal coefficient of permeability of the soil at standard temperature of 20°C, k_{ho} (20°) is 9.48 x 10^{-5} m/s whereas, the average vertical coefficient of permeability of the soil at standard temperature of 20°C, k_{vo} (20°) is 1.20 x 10^{-4} m/s. This indicates that at initial state, the average horizontal coefficient of permeability, k_{ho} is actually slightly lower than the average vertical coefficient of permeability, k_{vo}. The ratio of k_{ho} / k_{vo} is 0.79. With the average value of k_{ho} (20°C) = 9.48 x 10^{-5} m/s and k_{vo} (20°C) = 1.20 x 10^{-4} m/s, the initial permeability of the soil is classified as medium and the soil has a good drainage characteristic.

From results of Scanning Electron Microscope (Figure 4.2), it can be observed that the initial arrangement of fiber is somewhat uniform and the effect or roots is visible. Thus, at initial stage the water may take an erratic drainage path resulting in almost uniform permeability.

The relationship between the coefficient of permeability of the soil in it's initial state at standard temperature, k_o (20°C) and it's initial void ratio, e_o is plotted in Figure 4.18. It can be observed from Figure 4.18 that the fibrous peat soil samples have high initial void ratios with the void ratios range from 8 to 12. At a typical initial void ratio, e_o of 10, the vertical coefficient of permeability of the soil, k_{vo} is

about 1.32 times higher than the horizontal coefficient of permeability, k_{ho}. It can also be observed from Figure 4.16 that initial permeability of the soil varies from sample to sample. This shows that the soil is anisotropic and the anisotropy in initial permeability of the soil results from the natural soil imperfections or discontinuities, such as root holes, animal burrows, joints, fissures, seams, and soil cracks, that significantly contribute to high initial permeability of the soil. A significant visual observation on all the soil samples after the tests is the presence of horizontal as well as vertical rootlets that create many open voids and channels, and that explain why the fibrous peat soil is as porous as clean sand.

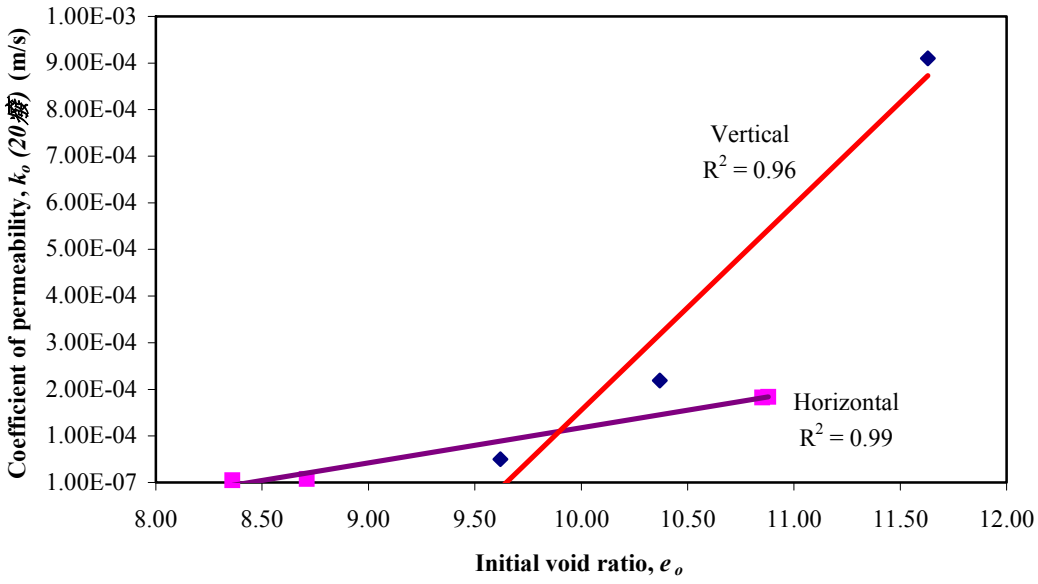

Figure 4.18: Graph of coefficient of permeability at standard temperature of 20°C, k_o (20°C) versus initial void ratio, e_o of the fibrous peat soil samples

4.5.2 Effect of Consolidation Pressure on Permeability

Hydraulic permeability test was carried out at a consolidation pressure of 100 and 200 kPa and an inlet pressure of 90 and 180 kPa on the soil sample. The outlet pressure was determined by the height of the water collected by a burette connected to the outlet of water flow from the Rowe consolidometer. The burette has an internal diameter of 12.19 mm, an external diameter of 15.15 mm and a maximum

volume capacity of 100 ml. All hydraulic permeability tests were conducted at a room temperature of 25°C.

Effect of consolidation pressure on permeability is studied for consolidation pressure of 100 kPa and 200 kPa with vertical drainage. The result shows a significant decrease in the permeability in which the coefficient of permeability under 100 kPa is 2.71 x 10^{-9} m/s, and under 200 kPa is 5.07 x 10^{-10} m/s. This coefficient of permeability is within the range of the permeability of clay.

Coefficient of permeability obtained from hydraulic consolidation test under 200 kPa consolidation pressure is much higher in horizontal direction than that in vertical direction. As shown in the Table 4.5, at a consolidation pressure of 200 kPa, the horizontal coefficient of permeability of the soil is higher than the vertical coefficient of permeability. The data also shows that the ratio of k_h/k_v increase significantly as consolidation pressure increases.

Table 4.5: Effect of consolidation pressure on coefficient of permeability

Type of permeability test / Coefficient of permeability	Constant-head permeability test	Hydraulic permeability test (under 200 kPa consolidation pressure)
k_h (20°C) (m/s)	9.48 x 10^{-5}	2.60 x 10^{-9}
k_v (20°C) (m/s)	1.20 x 10^{-4}	5.07 x 10^{-10}
k_h/k_v	0.79	5.13

4.5.3 Coefficient of Permeability based on Consolidation Test

Coefficient of permeability can be evaluated based on the coefficient of consolidation obtained from consolidation test through Equation 2.3. Given the m_v value shown in Table 4.6, and the unit weight of water 9.8 kN/m^3, the coefficient of permeability for the range of consolidation pressure used in the test is summarized in Table 4.7.

Table 4.6: Coefficient of volume compressibility m_v

No	Consolidation Pressure (kPa)	Coefficient of volume compressibility m_v (1/kPa)	Coefficient of volume compressibility m_h (1/kPa)
1.	50	$3.31x10^{-3}$	$2.43x10^{-3}$
2.	100	$2.05x10^{-3}$	$1.40x10^{-3}$
3.	200	$1.40x10^{-3}$	$0.91x10^{-3}$

Table 4.7 Coefficient of permeability based on hydraulic consolidation test

No	Consolidation Pressure (kPa)	Coefficient of vertical permeability k_v (m/s)	Coefficient of horizontal permeability k_h (m/sec)	Ratio k_h/k_v
1.	50	$1.460x10^{-10}$	$3.732x10^{-10}$	2.56
2.	100	$0.739x10^{-10}$	$2.112x10^{-10}$	2.86
3.	200	$0.335x10^{-10}$	$1.276x10^{-10}$	3.81

The data shown in Table 4.7 indicated that: the application of consolidation pressure has the effect of decreasing the coefficient of permeability of fibrous peat soil. As for the coefficient of consolidation the effect of consolidation pressure is more significant on the vertical coefficient of permeability as compared to the horizontal one, thus: the ratio of k_h/k_v is higher for higher consolidation pressure.

The data obtained from constant head permeability, permeability test on hydraulic consolidation test, and the data calculated from the results of consolidation test are plotted in Figure 4.19 and 4.20. It can be observed from the Figures that all test suggested a significant decrease in permeability as consolidation pressure increases. However, the effect is more dominant to the permeability in vertical direction and the ratio of k_h/k_v is increasing as the consolidation pressure increases. This indicates that the utilization of perimeter drainage have a positive effect on speeding up the settlement of construction on peat soil by encouraging primary consolidation.

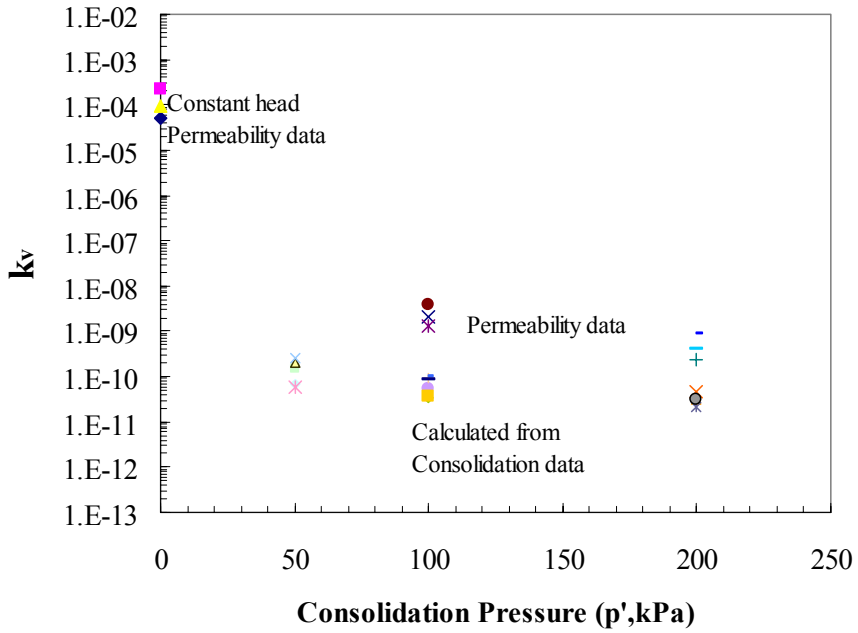

Figure 4.19 Relationship between Vertical Coefficient of Permeability and Consolidation Pressure obtained from all tests

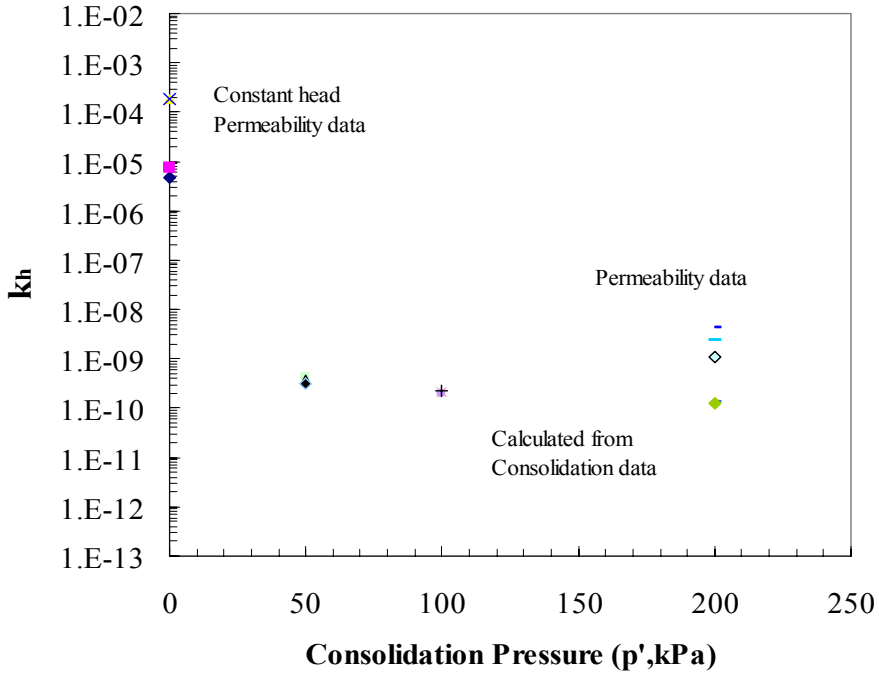

Figure 4.20 Relationship between Horizontal Coefficient of Permeability and Consolidation Pressure obtained from all tests.

4.7 Discussion

The previous study (UTM Fundamental Research vot 75137) concluded that that the peat obtained from Kampung Bahru, Pontian is typical of peat in West Malaysia with high water content (608%), a very high organic and fiber content (97 and 90% respectively), and low to medium degree of composition (H_4). The soil is acidic with pH of 3.24. The initial undrained shear strength of the soil is very low, but it is expected to increase with compression.

The compression behavior can be analyzed based on time-compression curve. The results showed that the soil has a high compressibility with significant secondary compression stage, which is not constant with the logarithmic of time in some cases. The primary consolidation is quite dominant in the compression of the peat in term of magnitude due to high initial void ratio. Even though it is observed that the duration of primary consolidation is short compared to clay soil, the time required to finish the consolidation is also quite long compared to construction time. The secondary compression stage is less significant than the primary consolidation in term of magnitude, but could be very important in term of the design life of a structure. Tertiary compression is observed but negligible in term of time because the secondary consolidation takes a long time to finish.

This research covers the determination of coefficient of rate of consolidation and coefficient of permeability of fibrous peat in vertical and horizontal direction on the peat soil obtained from the same location as previous research. The evaluation of coefficient of rate of consolidation in horizontal and vertical directions was made based on the results of consolidation test done on Rowe cell, while the assessment of vertical and horizontal permeability of soil based on constant head permeability test, the permeability test done on the consolidation equipment, and the calculation based on the coefficient of rate of consolidation. The results of the tests and analysis are presented in Table 4.8.

Table 4.8 Compressibility parameters and permeability obtained from consolidation tests with vertical and horizontal drainage

Consolidation Parameters	Vertical drainage	Horizontal drainage
Compression index, c_c	3.128	2.879
*Coefficient of volume compressibility m_v	0.0020	0.0014
*End of primary consolidation, t_{100} (min)	22.6	31.3
*Beginning of secondary consolidation, t_p (min)	12.0	19.3
Coefficient of secondary compression c_α	0.261	0.226
Ratio of secondary consolidation c_α / c_c	0.08	0.08
*Coeff. of rate of consolidation (m^2/yr)	0.76	4.48
Initial coefficient of permeability, k (m/s)	12×10^{-5}	9.48×10^{-5}
* Coefficient of permeability, k (m/s)	5.07×10^{-10}	26×10^{-10}

*) under consolidation pressure of 200 kPa, if applicable

The rate of vertical and horizontal consolidation of fibrous peat is analyzed based on the results of consolidation tests using Rowe cell and analysis based on Robinson (2003) method. As indicated in Table 4.8, the rate is higher in horizontal direction than in vertical direction. A ratio of about 3.5 was obtained even under a low consolidation pressure of 25 kPa and the ratio increases as the consolidation pressure increases. A ratio of 5.89 was obtained for consolidation pressure of 200 kPa.

As stated in the preceding paragraph, the secondary compression started during the process of dissipation of pore water pressure, thus affect the rate of vertical and horizontal coefficient of consolidation. The findings show that effect of secondary consolidation on the primary consolidation is significant because secondary consolidation may start as early as 65% degree of consolidation or only 65% of excess pore water pressure is dissipated. The secondary compression started later when the water is allowed to flow in horizontal direction. This means that the

effect of secondary compression on primary consolidation can be minimized by providing vertical drain in fibrous peat deposit.

The ratio of secondary compression to the compression index is proofed to be almost constant with consolidation pressure as well as the direction of drainage. The study suggests a ratio of 0.08 which is slightly higher than published data (Ajlouni, 2002). This might be due to the high fiber content of the soil.

Initial permeability of the peat is very high and it is comparable to sand. However, the data also showed that the permeability is highly affected by compression or reduction in void ratio. The coefficient of permeability decreases drastically as consolidation increases. The initial permeability is 1.2×10^{-4} m/s, while the coefficient of permeability under consolidation pressure of 200 kPa is found as 5.07×10^{-10} m/s. The lower coefficient of permeability was assessed from the results of consolidation test through c_v values. For this case, the coefficient of permeability calculated based on the coefficient of rate of consolidation are 7.39×10^{-11} m/s 3.35×10^{-11} m/s for the consolidation pressure of 100 and 200 kPa respectively.

Permeability of the fibrous peat soil is affected by the arrangement fiber in the soil mass. Scanning Electron micrograph was taken on samples of fibrous peat cut in vertical and horizontal direction under various consolidation pressures. It is the objective of the research to evaluate the effect of fiber orientation and to compare the vertical and horizontal coefficient of permeability, (k_h and k_v) of fibrous peat soil under a range of consolidation pressure. Comparison of the results of SEM on samples cut in vertical and horizontal direction demonstrates the difference in the fiber arrangement in both direction and the effect of application of consolidation pressure on the fiber arrangement. It is clear that the effect of consolidation pressure can be reduced if the water is allowed to flow in horizontal direction. The ratio of k_h/k_v increases from 0.79 for initial condition to about 5 under consolidation pressure of 200 kPa.

The final objective of the study was to outline the use of knowledge of horizontal coefficient of consolidation, c_h on the development of soil improvement method for construction on fibrous peat soil. In general, the results of the study indicate that the utilization of vertical drainage on the perimeter improves the compressibility of fibrous peat soil in terms of both primary consolidation and secondary compression. The coefficient of rate of consolidation increases significantly by application of the perimeter drainage and it is not much affected by the application of consolidation pressure. The rate of secondary consolidation is also improved by the application of vertical drainage even though the time needed to finish consolidation is much slower due to the length of drainage path. This can be improved by designing an optimum distance of vertical drainage. The effect of secondary consolidation on primary consolidation stage can also be improved by the utilization of vertical drain.

The results of this study suggested that sand column or other means of vertical drainage could be an effective method of soil improvement for fibrous peat soil. Besides reducing the compressibility of the soil and increasing the rate of primary consolidation, the drainage can have a positive effect on increasing the shear strength of the soil, thus; the height of fill can be improved. The method should be combined with confinement because the most critical problem involving peat soil is lateral spreading of the soil. This method has been applied successfully for peat soil deposits in Japan and many other countries.

CHAPTER 5

CONCLUSIONS AND RECOMMENDATION FOR FUTURE STUDY

5.1 Conclusions

The first objective of the study is to determine the horizontal coefficient of consolidation on Rowe consolidation test, and how it compared with the vertical coefficient of consolidation. It is found that the coefficient of rate of consolidation is higher in the horizontal direction than in the vertical direction.

The effect of secondary consolidation on the primary consolidation is significant, thus: it is recommended to perform large strain consolidation test on Rowe cell. The secondary compression is less dominant when the soil is subjected to horizontal drainage, thus utilization of vertical drainage will reduce the secondary compression. Furthermore the study indicated that the coefficient of secondary consolidation decreases when water is allowed to flow in horizontal direction. The c_α/c_c ratio obtained from this study is 0.08 which is in higher end of the range suggested by previous researchers.

Application of consolidation pressure has the effect of decreasing the coefficient of consolidation; however the horizontal rate of consolidation decreases in a slower rate than the vertical coefficient of consolidation due to the rearrangement of the fiber in the soil. The ratio of c_h/c_v is increasing from 3.5 to 6.0 for consolidation pressure of 25 to 200 kPa.

The fourth objective of the research is to evaluate the effect of fiber orientation and to compare the vertical and horizontal coefficient of permeability, (k_h and k_v) of fibrous peat soil under a range of consolidation pressure. Results show that the ratio of k_h/k_v increases from 0.79 for initial condition to about 5 under consolidation pressure of 200 kPa. Thus the permeability of the soil in horizontal direction is not greatly affected by the application of consolidation pressure.

The final objective of the research was to outline the use of knowledge of horizontal coefficient of consolidation, c_h on the development of soil improvement method for construction on fibrous peat soil. The results shows that utilization of perimeter drainage has a positive effect on speeding up the primary consolidation process, thus the post-construction estimation of the settlement could be made based only on the secondary compression.

5.2 Recommendation for Future Study

The research conducted in this study has been limited to the laboratory evaluation of compressibility characteristics of fibrous peat soil. Results have shown that utilization of perimeter or any form of vertical drainage could be a good improvement method when construction is to take place on fibrous peat deposit. The method has been applied successfully for peat soil deposits in Japan and many other countries. The method has the advantage of increasing shear strength and at the same time increasing the rate of primary consolidation process.

Further study involving field investigation on the fibrous peat soil needs to be done to justify the laboratory investigation on the soil from this study and to test the suitability of the method. An evaluation on the increase in shear strength due to application of consolidation pressure and draining process is recommended as an extension of this research because the shear strength of the soil determine the amount of fill that could be placed to induce consolidation and compression.

REFERENCES

Adams, J. (1965). The Engineering Behavior of a Canadian Muskeg. *Proc., 6th Int. Conf. Soil Mech. Found. Engrg*. Montreal, Canada, 1: 3-7.

Ajlouni, M.A. (2000) *Geotechnical Properties of Peat and RelatedEengineering Problems.* Thesis. University of Illinois at Urbana-Champaign.

American Society for Testing and Materials. (1994) *Annual Book of ASTM Standard*. Vol. 04.08 and 04.09

Asaoka, A. (1978). Observational Procedure of Settlement Prediction. *Soils and Foundation*, 18(4):87-101.

British Standards Institution. (1981). *Methods of Test for Soils for Civil Engineering Purposes*. London, BS 1377.

Clarke, B. G., Carter, J. P. and Wroth, C. P. (1979). In Situ Determination of the ConsolidationCharacteristics of Saturated Clays.*Proc. 7th Eur. Conf. Soil Mech.*, Brighton, 2:207-211 .

Colley, B. E. (1950). Construction of Highways Over Peat and Muck Areas. *American Highway*, 29(1): 3-7.

Colleselli, F., Cortellazzo, G., and Cola, S., (2000). Laboratory Testing of Italian Peat Soils, *Geotechnics of High Water Content Materials*, *ASTM STP 1374*, Edil, T.B., and Fox, P.J. (Eds.), American Society for Testing and Materials, West Conshohocken, PA.

Dhowian, A. W. and Edil, T. B. (1980). Consolidation Behavior of Peats. *Geotech. Testing J*., 3(3): 105-114.

Edil, T.B. and A. W. Dhowian. (1981). At-rest Lateral Pressure of Peat Soils. *Conf. on Sedimentation and Consolidation Model*, ASCE, San Fransisco, 411 – 424.

Edil, T.B. (2001) Site Characterization in Peat and Organic Soils. In *Proceeding of the International Conference on In Situ Measurement of Soil Properties and Case Histories*, 49-59, Bali, Indonesia.

Edil, T.B. (2003). Recent Advances in Geotechnical Characterization and Construction Over Peats and Organic Soils. *Putrajaya (Malaysia): 2nd International Conferences in Soft Soil Engineering and Technology*.

Escario, V. and Uriel, S. (1961). Detremining the Coefficient of Consolidation and Horizontal Permeability by Radial Drainage. 5th ICSMFE, 1:83-87.

Fox, P.J., and Edil, T.B. (1966). Effects of Stress and Temperature on Secondary Compression of Peat. *Canadian Geotechnical Journal*. 33(3): 405-415.

Hanrahan, E. T. (1954). An Investigation of Some Physical Properties of Peat." *Geotechnique*, London, England, 4(2): 108-123.

Hartlen, J. and J. Wolski. (1996). Embankments on Organic Soils. *Developemnet in Geotechnical Engineering, Elsevier*. 425.

Head, K.H., (1981). *Manual of Soil Laboratory Testing*, Volume 1,2, and 3. Pentech Press, London.

Head, K.H. (1982). *Manual of Soil Laboratory Testing,* Volume 2*:* Permeability, Shear Strength and Compressibility Tests. London: Pentech Press Limited.

Head, K.H. (1986). *Manual of Soil Laboratory Testing*, Volume 3: Effective Stress Tests. London: Pentech Press Limited.

Hillis, S. F.and C. O. Brawner, (1961). The Compressibility of Peat with references to Construction of Major Highways in B. C. *Proc. 7th Muskeg Res. Conf.*, Ottawa.

Huat, Bujang, B.K., (2004) *Organic and Peat Soil Engineering*. Univ. Putra Malaysia Press.

Hobbs, N. B. (1986). Mire Morphology and the Properties and Behaviour of Some British and Foreign Peats. Q. *I Eng. Geol.,* London, 19(1): 7-80.

Holtz, R.D. and Kovacs, W.D. (1981). *An Introduction to Geotechnical Engineering*. Prentice-Hall, Inc., Englewood Cliffs, New Jersey.

Karlsson, R. and Hansbo, S. (1981). (In Collaboration with the Laboratory Committee of the Swedish Geotechnical Society). Soil Classification and Identification. Swedish Council for Building Research. D8:81. Stockholm.

Kogure, K., Yamaguchi, H., and Shogaki, T. (1993). *Physical and Pore Properties of Fibrous Peat Deposit*. Singapore: 11th Southeast Asian Geotechnical Conference. 1993.

Lan, l.T. (1992). *A Model for One-dimensional Compression of Peat*. Ph.D. thesis. University of Wisconsin, Madison, U.S.A.

Landva, A. O., Pheeney, P. E. and Mersereau, D. E. (1983). Undisturbed Sampling of peat. *Testing of Peat and Organic Soils, ASTM STP 820*, 141-156.

Landva,A.O. and La Rochelle, P. (1983). Compressibility and Shear Characteristics of Radforth Peats, *Testing of Peat and Organic Soils, ASTM STP*, 820: 157-191.

Lea, N., D. and Browner, C. 0. (1963). Highway Design and Construction Over Peat Deposits in the Lower British Colombia. *Highway Research Record,* (7): 1-32.

Leonards, G.A. and P. Girault. (1961). A Study of The One-dimensional Consolidation Test.*Proceeding 9th ICSMFE*, Paris, 1:116-130.

Mesri, G., Stark, T. D. and Chen, C. S. (1994). C_c/C_α Concept Applied to Compression of Peat. Discussion, J. of *Geotech. Engrg.,* ASCE, 118(8): 764-766.

Mesri, G., T.D. Statark, M.A. Ajlouni and C. S. Chen (1997). Secondary Compression of Peat With or Without Surcharging. *J. Geotech. Geoev. Engr*. 123(5): 411-421.

Miyakawa, J. (1960). Soils Engineering Research on Peats Alluvia. Reports 1-3. Civil Enggrg. Research Institute. Hokkaido Development Bureau Bulletin No. 20

Mokhtar, N.E. (1998). Perbedaan Perilaku Teknis Tanah Lempung dan Tanah Gambut (Peat Soil), *Jurnal Geoteknik*, Himpunan Ahli Teknik Tanah Indonesia, 3(1): 16-34.

Muskeg Engineering Handbook. (1969). I.C. Macfarlane. Univ of Toronto Press.

Nurly Gofar and Yulindasari Sutejo. (2005). Engineering Properties of Fibrous Peat, *Proc. Seminar Penyelidikan Kej. Awam (SEPKA)*, Johor Bahru. 119-129.

Noto, Shigeyuki. (1991). *Peat Engineering Handbook*. Civil Engineering Research Institute, Hokkaido development Agency, Prime Minister's Office, Japan.

Robinson, R. G. (1997). Determination of Radial Coefficient of Consolidation by the Inflection Point Method, *Geotechnique*, 47(5): 1079-1081.

Robinson, R. G. (2003). A Study on the Beginning of Secondary Compression of Soils. *Journal of Testing and Evaluation*. 31(5): 1-10.

Rowe, P.W. and Barden, L. (1966). A New Consolidation Cell. *Geotechnique*. 16: 162-169.

Tortensson, B. A. (1975). The Pore Pressure Sounding Instrument. *Proceeding ASCE Speciality Conference on In Situ Measurement of Soil Properties*. Raleigh 2. New York. American Society of Civil Engineering. 48-54.

Wilkinson,W. B. (1968). Constan Head In Situ Permeability Tests in Clay Strata. *Geotechnique*. 18: 172-194.

APPENDIX A

Classification of Peat

Table A.1 Classification of Peat Based on Degree of Decomposition (von Post, 1922)

Condition of peat before squeezing				Condition of peat on sequeezing		
Degree of Humification	**Soil color**	**Degree of decomposition**	**Plant structure**	**Squeezed solution**	**Material extruded (passing between fingers)**	**Nature of Residue**
H1	White or yellow	None	Easily identified	Clear, color-less water	Nothing	Not pasty
H2	Very pale brown	Insignificant	Easily identified	Yellowish water/pale brown-yellow	Nothing	Not pasty
H3	Pale brown	Very slight	Still identified	Dark brown, muddy water not peat	Nothing	Not pasty
H4	Pale brown	Slight	Not easily identified	Very dark brown muddy water	Some peat	Some what pasty
H5	Brown	Moderate	Recogniza ble but vague	Very dark brown muddy water	Some peat	Strongly pasty
H6	Brown	Moderately strong	Indistinct (more distinct after squeezing)	Very dark brown muddy water	About one-third of peat squeezed out	Very strongly pasty
H7	Dark brown	Strong	Faintly recognizab le	Very dark brown muddy water	About one-half of peat squeezed out	Very strongly pasty
H8	Dark brown	Very strong	Very indistinct	Very dark brown pasty water	About two-third squeezed out	Very strongly pasty
H9	Very dark brown	Nearly complete	Almost recognizab le	Very dark brown muddy water	Nearly all the peat squeezed out as fairly uniform paste	Very strongly pasty
H10	Black	Complete	Not discernible	Very dark brown muddy paste	All the peat passes between the fingers;no free water visible	N/A

Table A.2 Clasification of Peat based on organic and fiber content

Classification peat soil based on ASTM standards	
Fiber Content (ASTM D1997)	Fibric : Peat with greater than 67 % fibers
	Hemic : Peat with between 33 % and 67 % fibers
	Sapric : Peat with less than 67 % fibers
Ash Content (ASTM D2974)	Low Ash : Peat with less than 5 % ash
	Medium Ash : Peat with between 5% and 15 % ash
	High Ash : Peat with more than 15 % ash
Acidity (ASTM D2976)	Highly Acidic : Peat with a pH less than 4.5
	Moderately Acidic : Peat with a pH between 4.5 and 5.5
	Moderately Acidic : Peat with a pH between 4.5 and 5.5
	Slighly Acidic : Peat with a pH greater than 5.5 and less than 7
	Basic : Peat with a pH equal or greater than 7

APPENDIX B

SCANNING ELECTRON MICROGRAPH OF PEAT SAMPLES (SEM)

1. Apparatus

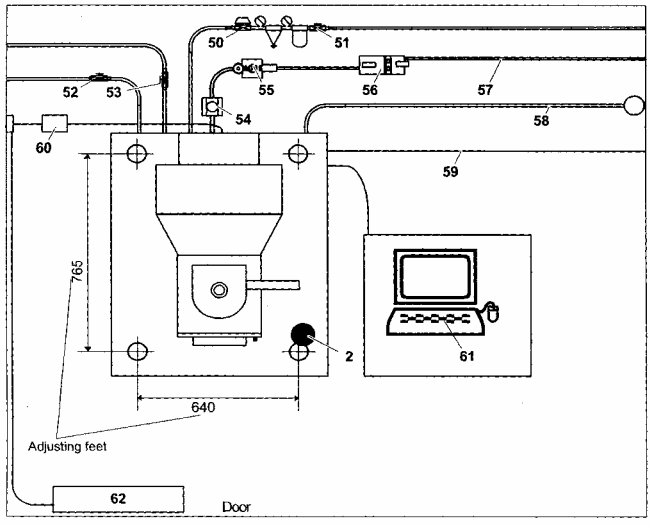

Figure B1: Assembly Plan for SEM test,
(21) Emergency shutdown button, (56) Rotary pump, (50) Water solenoid valve, (57) Exhaust hose, (51) Water main valve, (58) Discharge line, (52) Compressed air-Main valve, (59) Grounding, (53) Nitrogen-Main valve, (60) Switchbox, (54) Dynamic vibration-damper, (61) Computer with keyboard and mouse, (55) Static damper with adsorption trap, (62) Miniature circuit breaker, Ground fault circuit interrupter-emergency shutdown – switch.

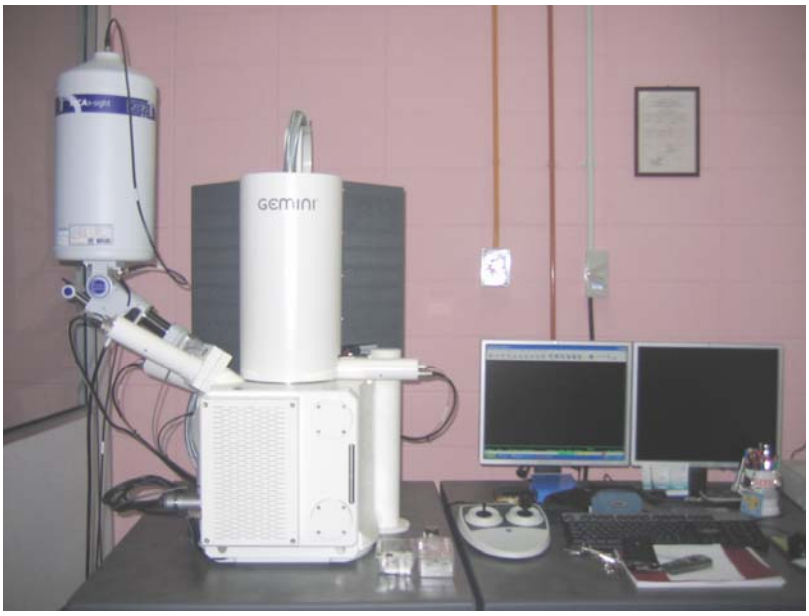

Figure B2: The equipment for SEM test.

2. Procedure Scanning Electron Microscope (SEM)

The procedure for Scanning Electron Microphotograph (SEM) using G34-SUPRA 35 VP en 01 Carl Zeisss SMT – Nano Technology System Division as follows :

1. Switching the instrument on.
   The emergency shutdown button must be unlocked, and the master's switch must be switched on. Then open the cooling water valve, the nitrogen valve, the cover on the yellow STANDBY-button and press the button. If the SEM is equipped with a water solenoid valve, it will be opened automatically. More over, to make the entire instrument's electronics on, press the green ON button.
2. Starting the Smart SEM program.
   Double-click on the *Smart SEM* icon with the left mouse button. While the program loads, the screen will also show you which systems. In the User Name field, enter your user name. In the Password field, enter your password. Click OK or press Enter on the keyboard.
3. Loading the specimen chamber.
   Take hold of the door handle and carefully open the chamber door. The chamber is filled with nitrogen. Next, load specimen containers into specimen holder and tighten laterally with an Allen wrench. Load samples into specimen containers. Place the prepared specimen holder on the table. The specimen table can be moved in three directions, tipped, and rotated around the beam axis. After that close the chamber door by pressing lightly on the front with the palm of your hand, or use the door handle.
4. Evacuating the specimen chamber.
   When the specied vacuum has been reached, you will see the message "Vac Status ready", and the red X next to the "Vac" icon in the bottom toolbar will change to a green check mark.
5. Activating the electron beam.
   Left-click on "GUN" and "EHT" (on the bottom toolbar). Subsequently the cathode will heat up, electrons will be emitted, the acceleration voltage will

be on, and the image on the screen will turn lighter. If the focus is (by chance) already correct, the contours of the specimen will appear.

6. Focusing the electron beam.

   The objective focuses the electron beam on the surface of the specimen. The specimen must be placed in the correct position under the electron beam before you bring it into focus. If the image is not sharp enough, you will need to make further adjustments.

7. Modifying the image.

   The Smart SEM program has many functions to help you obtain the desired results. Information of interest can be accessed via Windows help, program help, or context-based help.

8. VP-Mode.

   When examining non- or only slightly conductive preparations, charges can be induced on their surfaces, which are difficult or impossible to divert and which result in an altered image. In VP-Mode, these surface charges are avoided or reduced and high-quality images can be produced, even from such preparations.

9. Finishing examination of a specimen.

   You can save or print out an image if it meets your quality requirements. If you did not order a printer with your instrument, you can move the file to another computer with a printer and print it out from there.

10. Placing the SEM in standby mode.

    Standby mode is the normal status for the SEM once you have finished examining a specimen. The cathode will continue to heat, and the vacuum pump will evacuate the electro-optic column and the specimen chamber.

11. Switching off the SEM.

    The SEM must be shut down for maintenance, repairs, if the instrument will not be used for an extended period of time or in case of an emergency.

12. Shutting down the SEM completely.

3. Results of Scanning Electron Microscope (SEM) in Horizontal Section

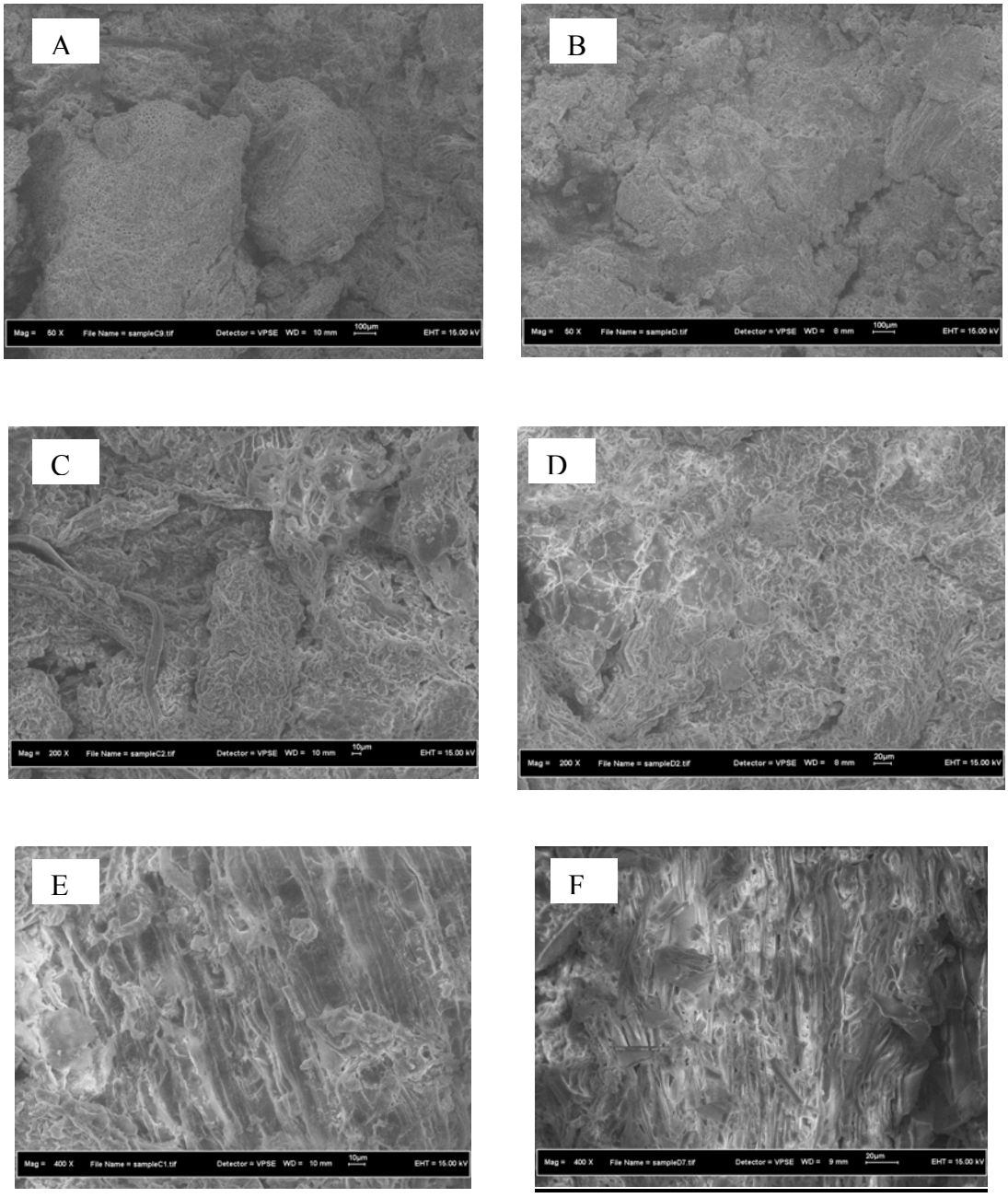

Figure B3: Scanning Electron Microphotographs (SEM) of Kampung Bahru, Pontian, West Johore Peat. (A) Horizontal Section before Compression x50, (B) Horizontal Section after Compression under 200kPa x50, (C) Horizontal Section before Compression x200, (D) Horizontal Section after Compression under 200kPa x200, (E) Horizontal Section before Compression x400, (F) Horizontal Section after Compression under 200kPa x400.

4. Results of Scanning Electron Microscope (SEM) in Vertical Section

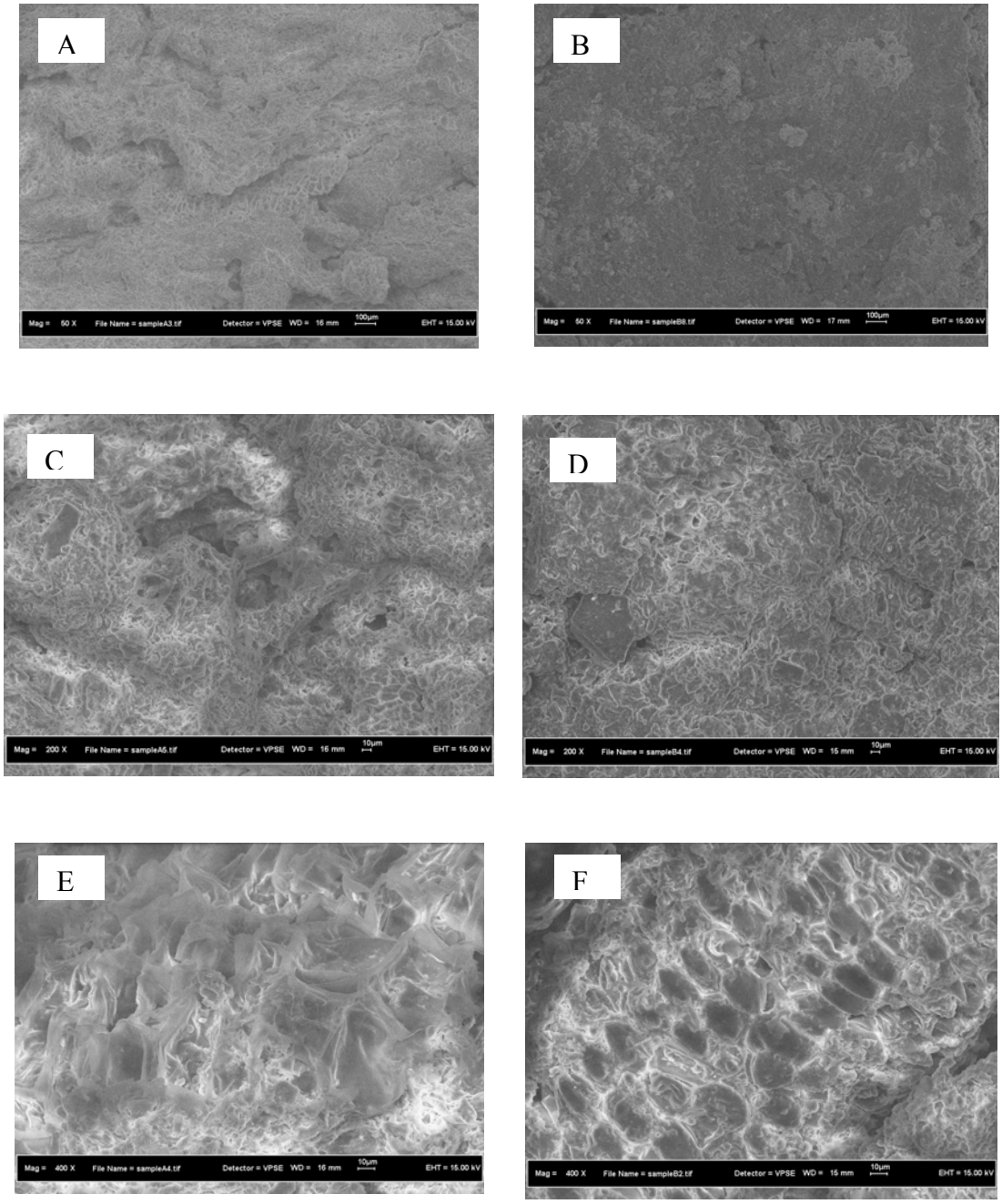

Figure B4: Scanning Electron Microphotographs (SEM) of Kampung Bahru, Pontian, West Johore Peat. (A) Vertical Section before Compression x50, (B) Vertical Section after Compression under 200kPa x50, (C) Vertical Section before Compression x200, (D) Vertical Section after Compression under 200kPa x200, (E) Vertical Section before Compression x400, (F) Vertical Section after Compression under 200kPa x400.

APPENDIX C

Procedures for Hydraulic Consolidation Test

1. Apparatus

Figure C1: Two independently controlled water pressure systems, giving maximum pressure up to 1000 kPa used for hydraulic consolidation and permeability tests in laboratory

Figure C2: Power supply and readout unit for the electric pore pressure transducer

Figure C3: Volume change gauge

Figure C4: Sintered bronze disc of 4 mm thickness

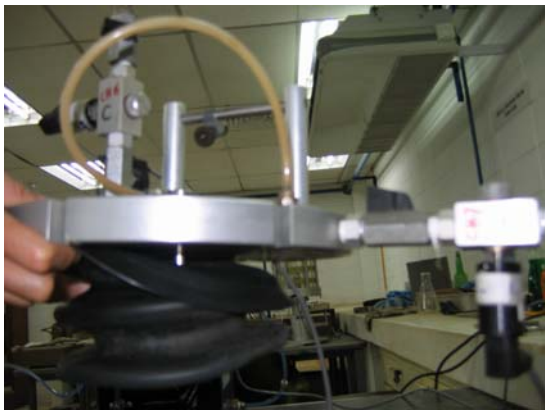

Figure C5: Rowe cell top attached to diaphragm

Figure C6: Rowe cell body of 151.4 mm internal diameter

Figure C7: Rowe cell base

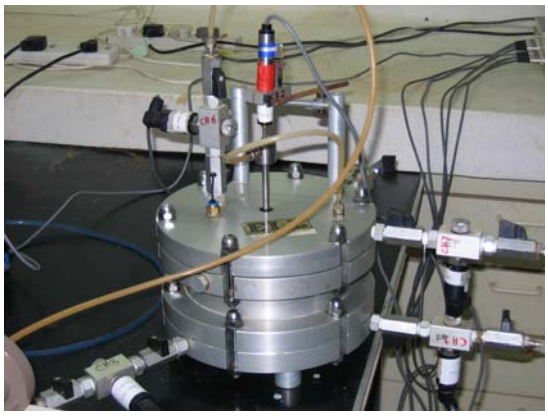

Figure C8: Bolt tightened Rowe cell connected to linear transducer

Figure C9: A burette connected to Rowe consolidometer for hydraulic permeability test

2. Cell assembly and Connections

Equipment & accessories needed for the large strain consolidation test are as follows:

1. Rowe cell (diameter 150 mm)
2. Sintered bronze porous disc 3 mm thick with typical permeability 4 x 10^{-4} m/s (the porous metal disc should be boiled after every test and carefully inspected in order to prevent a gradual build-up of fine particles).
3. Dial gage for measuring vertical settlement
4. Spare porous insert for measuring pore water pressure
5. Spare O Ring base seal
6. Spare Diaphragm
7. Flange sealing ring
8. Data Acquisition system for measurement of
    a. Diaphragm pressure
    b. Back pressure
    c. Pore water pressure
    d. Vertical settlement
    e. Volume of water draining out
    f. Time
9. Consumables: Silicone grease

The arrangement of the Rowe cell and connections are described in the following steps:

1. After covering the base with a film of water, place a saturated porous disc of sintered bronze on the cell base without entrapping any air.

2. Fit the cutting rings containing soil sample on top of the Rowe cell body (Figure C10). Place the sample into the Rowe cell body by slowly and steadily pushing the soil sample vertically downwards using a porous disc (Figure C.11).

3. Flood the space at the top of the cell above the sample with de-aired water.

Figure C.10: Cutting rings containing soil sample are fitted on top of the Rowe cell

Figure C.11: A porous disc is used to slowly and steadily push the soil sample vertically downward into the Rowe cell body

4. Place a saturated drainage disc through the water onto the sample by lowering into position using the lifting handle. Avoid trapping air under the plate. Ensure that there is a uniform clearance all round between the disc or discs and the cell wall.

5. Connect a tube to valve F and immerse the other end in a beaker containing de-aired water. The tube should be completely filled with de-aired water making sure that there are no entrapped air bubbles.

6. Support the cell top at three points so that it is level, and with more than enough clearance underneath for the settlement spindle attached to the diaphragm to be fully extended downwards. The cell top should be supported near its edge so that the flange of the diaphragm is not restrained. Fill the diaphragm with water using rubber tubing about one-third the volume. The way distilled water is filled into the diaphragm can be diagrammatically observed in Figure C.12 and realistically observed in Figure C.13. Open valve C.

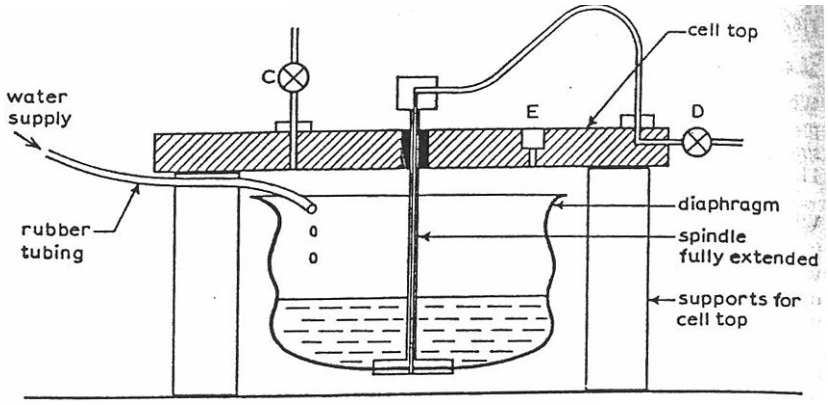

Figure C.12: Schematic diagram of filling of distilled water into the diaphragm (Head, 1986)

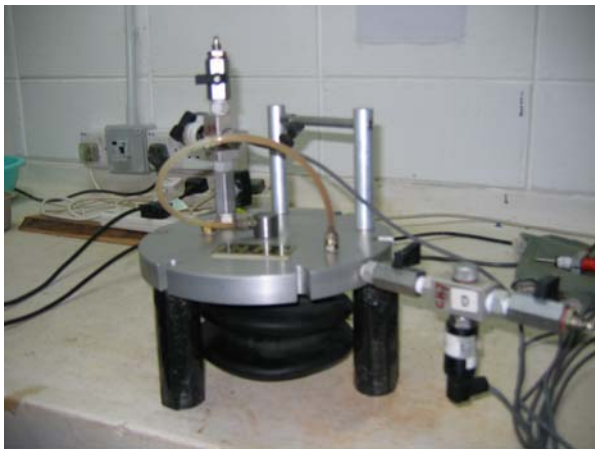

Figure C.13: Realistic view of filling of distilled water into the diaphragm

7. Place three or four spacer blocks, about 30 mm high, on the periphery of the cell body flange. Lift the cell top, keeping it level, and lower it onto the spacers, allowing the diaphragm to enter the cell body. Bring the bolt holes in the cell top into alignment with those in the body flange.

8. Use rubber tube to add more water to the inside of the diaphragm so that the weight of water brings the diaphragm down and its periphery is supported by the cell body. Check that the cell body is completely filled with water. The whole of the extending portion of the diaphragm should be inside the cell body, and the diaphragm flange should lie perfectly flat on the cell body flange.

9. Hold the cell top while the supporting blocks are removed, then carefully lower it to seat onto the diaphragm flange without entrapping air or causing ruckling or pinching (Figure C.14). Align the bolt holes. When correctly seated, the gap between top and body should be uniform all round and equal to a diaphragm thickness. Open valve F to permit escape of excess water from under the diaphragm.

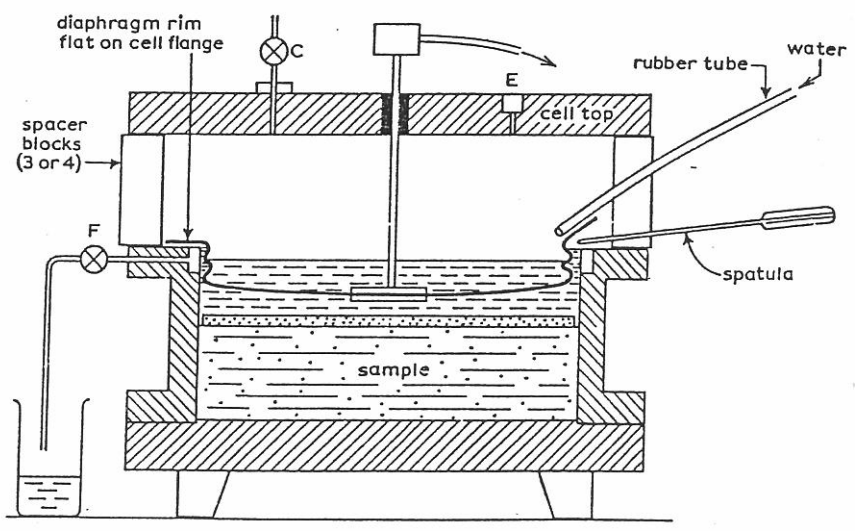

Figure C.14: Diaphragm inserted into Rowe cell body (Head, 1986)

10. Tighten the bolts systematically (Figure C.15). Ensure that the diaphragm remains properly seated, and that the gap between the metal ranges remains constant all round the perimeter.

11. Open valve D, and press the settlement stem steadily downwards until the diaphragm is firmly bedded on top of the plate covering the sample. Close valve D when no more water emerges.

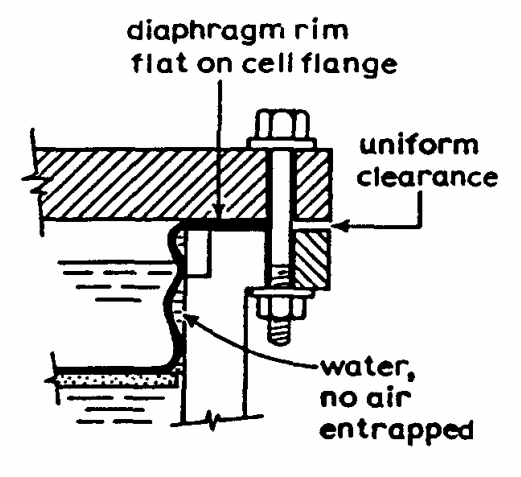

Figure C.15: Diaphragm is correctly seated (Head, 1986)

12. Connect valve C to a header tank of distilled water having a free surface about 1.5 m above the sample.

13. Completely fill the space above the diaphragm with water through valve C with bleed screw E opened. Tilt the cell so that the last pocket of air can be displaced through E. Maintain the supply of water at C when subsequently replacing the bleed screw.

14. Maintain pressure at C, and as the diaphragm expands allow the remaining surplus water from above the sample to emerge through valve F. Open valve D for a moment to allow the escape of any further water from immediately beneath the diaphragm.

    Escape of water from F due to diaphragm expansion may take some considerable time because of the barrier formed by the folds of the diaphragm pressing against the cell wall.

15. Close valve F when it is evident that the diaphragm has fully extended. Observe the pore water pressure at the base of the sample, and when it has reached a constant value record it as the initial pore water pressure, u_o. This corresponds to the initial pressure p_o under the head of water connected to C. If the height from the top of the sample to the level of water in the header tank is h mm, then:

$$p_o = \frac{h \times 9.81}{1000} = \frac{h}{102} \text{ (kPa)}$$

16. Maintain the pressure at C.

17. Connect the lead from the back pressure system to valve D without entrapping any air. Open valve F for a while to let out the bubble from back pressure line.

3. Test Procedures for Two-Way Vertical Drainage

The final arrangement of Rowe cell for two-way vertical drainage is diagrammatically shown in Figure C.16.

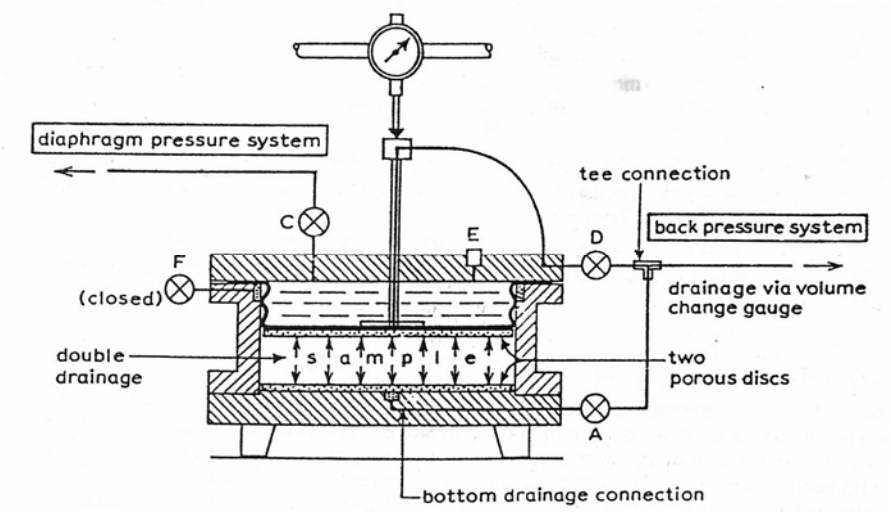

Figure C.16 Arrangement of Rowe cell for consolidation test with two-way vertical drainage (Head, 1986)

The designation of the hydraulic consolidation test with vertical drainage (two-way) is shown in Figure C.17. In this type of test, drainage takes place from both top and bottom faces of the sample. A porous drainage disc is placed under the sample, and is connected to the same back pressure system as the top drainage line for the consolidation stages. In this type of test, drainage takes place vertically upwards and downwards while pore pressure is measured at the center of the base.

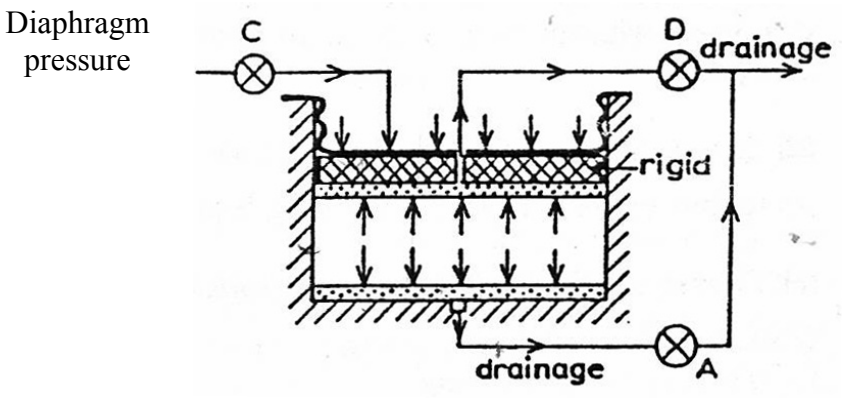

Figure C.17: Two-way vertical drainage and loading condition for hydraulic consolidation test in Rowe cell with 'equal strain' loading (Head, 1986)

The test is described under the following stages: (A) Preliminaries, (B) Saturation, (C) Loading Stage, (D) Consolidation Stage, (E) Further Load Increments, (F) Unloading, (G) Conclusion of Test, and (H) Measurements and Removal of the Sample.

A. Preliminaries

1. Close valve B to isolate the pore pressure transducer from the flushing system throughout the test.
2. Set the vertical movement dial gauge at a convenient initial reading near the upper limit of its travel, but allow for some upward movement if saturation is to be applied.
3. Record the reading as the zero (datum) value under the seating pressure p_o.
4. Set the back pressure to the required initial value, with valve D closed. The back pressure should be greater than the initial pore pressure (u_o) but it should be 10 kPa less than the first increment of cell pressure.
5. Record the initial reading of the volume gauge when steady.

B. Saturation

Saturation by the application of increments of back pressure is desirable for undisturbed samples taken from above water table. For this type of test, application of 10 kPa back pressure is used.

Saturation is generally accepted as being complete when the value of the pore pressure parameter B reaches about 0.96.

C. Loading Stage

1. With the drainage lines valve A and valve D closed and valve C open, increase the diaphragm pressure steadily to the first increment. Open valve A valve D when set.
   First increment of diaphragm pressure is taken as 50 kPa for this type of test.
2. Open valve F to allow excess water to escape from behind the diaphragm for a short time just to allow excess water from the top of the sample.
3. Wait until the pore pressure reaches a steady value equal to diaphragm pressure. If the sample is virtually saturated the increase in pore pressure should almost equal the pressure increment applied to the sample.
4. Record any settlement indicated by the dial gauge before starting consolidation.

D. Consolidation Stage

Consolidation is started by opening the drainage outlets (valve A and valve D in Figure C.9) and at the same instant starting the clock. Read the following data:

a. Vertical settlement
b. Pore water pressure
c. Volume change on back pressure line
d. Diaphragm pressure (check)

The primary consolidation phase is completed when the pore pressure has fallen to the value of the back pressure. Wait for secondary consolidation to take place.

E. Further Load Increments

1. Increase the diaphragm pressure to give the next value of effective stress. Allow excess water to drain from behind the diaphragm (valve F) if necessary.
2. The pore pressure should then be allowed to reach equilibrium before proceedings to the next consolidation stage.
3. Repeat the above steps for 100 kPa and 200 kPa consolidation pressures.

F. Unloading

Unloading is needed for evaluation of the effect of surcharge on the compressibility characteristics of peat. In this case, the sample was loaded to the pre-consolidation pressure (estimated based on oedometer test data, 30 kPa) and loaded to 100 kPa. At the end of consolidation test under 100 kPa, the soil was unloaded back to 30 kPa. For unloading stage, diaphragm pressure is reduced with valve D closed. It should be followed by swelling stage with valve D open, during which upward movement, volume increase and pore-pressure readings are taken in the same way as consolidation process. The pore-pressure should be allowed to reach equilibrium at the end of each stage before proceeding to the next stage of loading. The following stage of loading in this case is 100 kPa and 150 kPa.

G. Conclusion of Test

1. Reduce the pressure to the initial seating pressure, p_o
2. When equilibrium has been achieved, record the final settlement, volume change and pore pressure readings.
3. Close valve A and open valves C, D and F, allowing surplus water to escape. Unbolt and remove the cell top and place it on the bench supports.

H. Measurement and Removal of Sample

1. Remove the porous disc to expose the sample surface. Measure the diameter and height of the sample.

2. Remove the cell body from the base and remove the sample intact from the cell. Split the sample in two along a diameter.
3. Take two or more representative sample from one half of the sample for moisture content measurements.
4. Allow the other half to air-dry to reveal the fabric and any preferential drainage paths, which may have affected the test behavior.
5. Allow at least 4 hour before taking picture of the sample.

The cell components should be cleaned and dried before putting away, giving careful attention to the sealing ring at the base. Porous bronze and ceramic discs and inserts should be boiled and brushed; used porous plastic should be discarded. Connecting ports and valves should be washed out to remove any soil particles. Any corrosion growth on exposed metal surfaces should be scraped off, and the surface made smooth and lightly oiled.

4. Test Procedures for Radial Outward Drainage

The arrangement of Rowe Cell for consolidation test with radial outward drainage is shown in Figure C.18. This arrangement for equal strain loading.

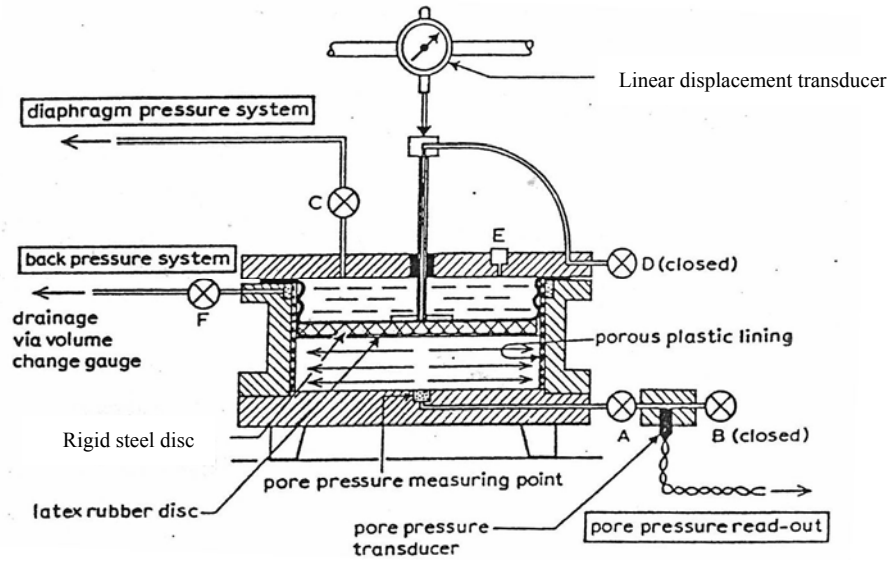

Figure C.18: Arrangement of Rowe cell for consolidation test with radial drainage to periphery; pore pressure measurement from centre of base of sample (Head, 1986)

The designation of the hydraulic consolidation test with radial drainage periphery is shown in Figure C.19. The procedure for fitting a porous plastic peripheral drain to the Rowe cell is described below.

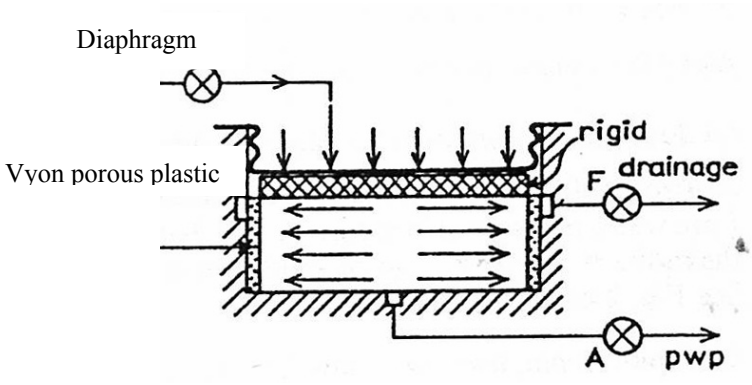

Figure C.19: Radial drainage to periphery, and loading condition for hydraulic consolidation test in Rowe cell with 'equal strain' loading (Head, 1986)

The test is described under the following stages: (A) General Preparation, (B) Fitting Peripheral Drain, and (C) Preparation of Sample.

A. General Preparation

The cell base is made ready and the ceramic insert, which is situated at the centre, is prepared for measuring pore water pressure. The transducer block, with valve B and the connection to the pore pressure panel, is fitted on to valve A. Since only one back pressure system is available, the back pressure system with volume change gauge is connected to valve F for periphery. The port connecting to ceramic inserts at the centre should be de-aired. The connection to valve D is not used. The undisturbed sample is prepared and set up in the Rowe cell.

B. Fitting Peripheral Drain

1. Cut a strip of the plastic material of width equal to the depth of the cell body, and about 20 mm longer than its internal circumference. Cut the ends square using a sharp blade and metal straight-edge.

2. Fit the plastic tightly against the wall of the cell body. Mark the end of the overlap with a sharp pencil (Figure C.20).

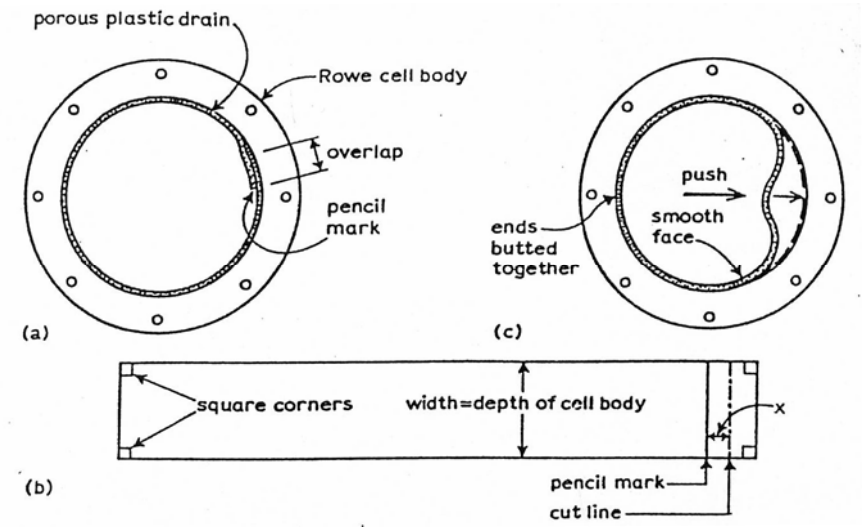

Figure C.20: Fitting porous plastic liner in Rowe cell: (a) initial fitting and marking, (b) locating line of cut, (c) final fitting (Head, 1986)

3. Lay the plastic material on a flat surface and mark another line exactly parallel to the first (i.e. square to the edges) at the following distance outside it (denoted by x in Figure C.20): For the 151.4 mm diameter Rowe cell: 3 mm.
4. Make a clean square cut on this line.
5. Fit the plastic in the cell body again, smooth face inwards and trimmed ends butting. Allow the additional length to be taken up in the form of a loop opposite the joint (Figure C.20).
6. Push the loop outwards and the plastic material will spring against the wall of the cell. Check that it fits tightly, with no gaps.
7. Immediately before inserting the sample, remove the porous plastic for saturating and de-airing in boiling water, then replace it in the cell. The inside face of porous plastic must not be greased, because grease will prevent drainage. Peripheral drain fitted into the Rowe cell body is shown in Figure C.21.

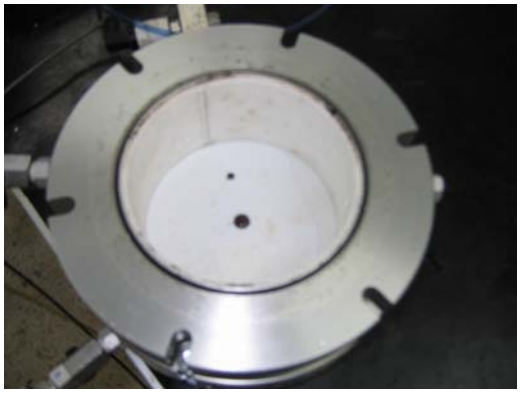

Figure C.21: Peripheral drain fitted into the Rowe cell body

C. Preparation of Sample

With exception of periphery drain and central drain installations, the procedure of preparing and setting up the sample in the cell for radial drainage to periphery and to centre is the same as that of vertical drainage (two-way).

1. For 'equal strain' test, an impermeable steel disc is placed through the water on to the soil sample, without entrapping air.
2. Fit and assemble the cell top to the body as described by the procedure for vertical drainage (two-way).

Details differ from the arrangement for two-way vertical consolidation test in the following ways:

1. The sample is surrounded by a drainage layer of porous plastic material.
2. The top surface of the sample is covered by an impermeable steel disc.
3. A back pressure system with volume gauge is connected to the rim drain at the top of the cell, via valve F.
4. Pore water pressure is measured at the base of the sample from the centre. The pore pressure transducer housing block is connected to valve A which replaces the blanking plug at that cell outlet (Figure C.18).
5. The top drainage line is not used and valve D remains closed.
   In this case, the thickness of horizontal consolidating layer is taken as half of the diameter of the soil sample that is 74.2 mm. With equal strain loading and sample saturation by applying back pressure, the diaphragm pressure line is the same as

used for the one-way vertical consolidation test. With exception of periphery Vyon porous plastic drain and installation, sample preparation is the same as that of one-way vertical consolidation test.

6. Graphical plots

   As consolidation proceeds, plot the following graphs from the observed data.

   a. Settlement (ΔH mm) against log time. This graph should be kept up to date during each stage so that the approach to 100% primary consolidation can be monitored. This graph can be used to obtain C_h, t_p, C_α, and t_s.
   b. Calculate void ratio at the end of each loading stage and plot the void ratio against effective pressure on a log scale. This graph could be used to obtain, C_c and C_r. Pre-consolidation pressure can also be obtained if possible.

Note for hydraulic radial consolidation test with radial drainage to periphery:

- $T_{50} = 0.0866$; $T_{90} = 0.288$;
- Use pore water pressure measurement to estimate 100% consolidation

$$c_h = 0.131 \frac{T_{r\theta} H^2}{t}$$

where, H is in mm and t is in minutes.

5. Hydraulic Permeability Test

Permeability measurements are carried out on a sample in a Rowe cell with laminar flow of water in the vertical direction (downwards) and with radial flow horizontally (inwards).

The procedures for preparing samples for each type of permeability test are outlined below.

1. Two-Way Vertical Permeability Test

The arrangement of Rowe cell for the permeability test with vertical drainage is shown in Figure C.22.

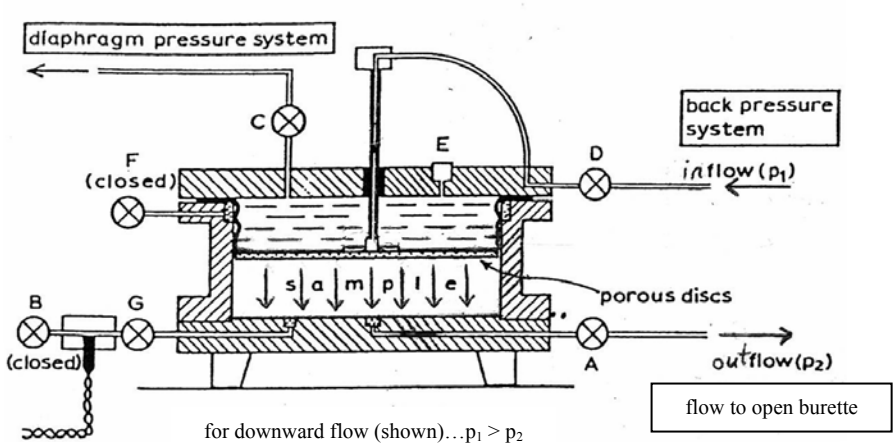

Figure C.22: Arrangement of Rowe cell for permeability test with vertical flow (downwards) (Head, 1986)

The designation of the hydraulic permeability test with vertical flow of water downwards is shown in Figure C.23.

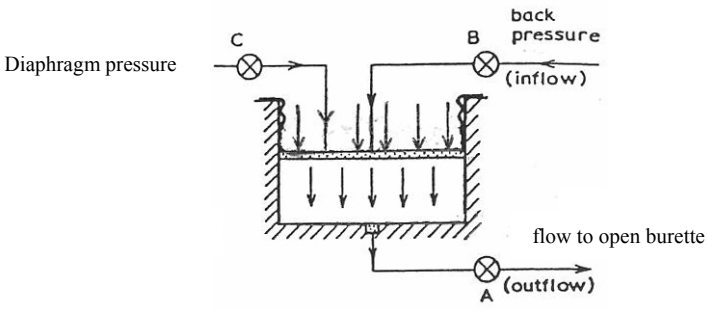

Figure C.23: Downward vertical flow condition for hydraulic permeability test in Rowe cell (Head, 1986).

The preparation of the sample and assembly of the cell are summarized as follows:

1. Fit a bottom drainage disc on the cell base.
2. Set up the sample in the cell by the method similar to that of Rowe cell consolidation test with vertical drainage (two-way).
3. Fit a porous stone on top of the sample.
4. Assemble the cell top.

Two independently controlled constant-pressure systems are required for the permeability test. One system is connected to valve C (Figure C.22) to provide pressure on the diaphragm. One back pressure system is connected to valve D, and valve A is connected to an open burette.

Pore pressure readings are not required, except as a check on the B value if incremental saturation is applied before starting the test. Valve F remains closed. The difference between the inlet and outlet pressures should be appropriate to the vertical permeability of the soil, and should be determined by trial until a reasonable rate of flow is obtained. The pressures are adjusted to give downward flow.

Permeability tests are carried out in Rowe consolidation cell under 'equal strain' conditions of known effective stress, with downward flow of water.

The arrangement of the cell and ancillary equipment is shown in Figure C.22. Three independent constant pressure systems are required, one for applying the vertical stress, the other two on inlet and outlet flow lines but since, only two independent constant pressure systems are available, valve A at the base of the Rowe cell is connected to an open burette.

Since saturation by incremental back pressure is to be carried out initially, the pore pressure transducer housing should be connected to valve A. During the saturation stage, valve A should remain closed and water admitted to the sample through valve D as usual. Since only two constant pressure systems are available, the outlet from the sample is connected to an open burette via valve A whereas; the inlet to the sample is connected to a back pressure system via valve D. That means the direction of flow of water in the sample upon consolidation is downwards.

The arrangement shown in Figure C.22 allows water to flow vertically through the sample under the application of a differential pressure between the base and top, while the sample is subjected to a vertical stress from the diaphragm pressure as in a consolidation test. Since the flow is to an open burette, the outlet pressure is zero if the free water surface in the burette is maintained at the same level as the sample face from which the water emerges.

The sample is first consolidated to the required effective stress by the application of diaphragm loading. Consolidation should be virtually completed, i.e. the excess pore pressure should be at least 95% dissipated before starting a permeability test.

The procedure for two-way vertical permeability test using Rowe cell is as follows:

1. The test is first carried out by adjusting the pressure difference across the sample to provide a reasonable rate of flow through it. The hydraulic gradient required to induce flow should be ascertained by trial, starting with equal pressures on the inlet and outlet lines and progressively increasing the inlet pressure, which must never exceed the diaphragm pressure. Since only one back pressure system is used, the outlet drainage is connected to an open burette as shown in Figure C.12.

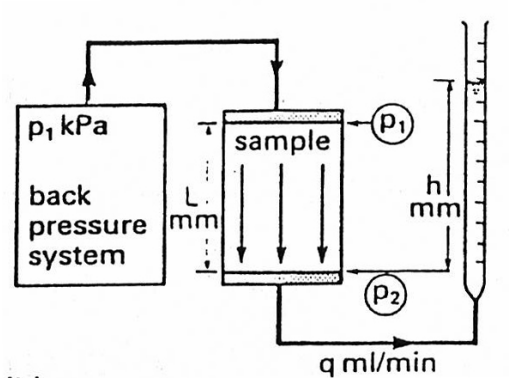

Figure C.24: Arrangement for hydraulic vertical permeability test using one back pressure system for downward flow (Head, 1986)

2. When a steady rate of flow has been established, measure the time required for a given volume to pass through. The volume of water is measured from an open burette incorporated in the outlet of the soil sample via valve A.
3. Calculate the cumulative flow, Q (ml) up to the time of each reading, and plot a graph of Q against time, t (minutes), as the test proceeds. Continue the test until it can be seen that a steady rate of flow is reached, i.e. the graph is linear.
4. From the linear part of the graph, measure the slope to calculate the rate of flow, q (ml/minute); i.e. $q = \delta Q / \delta t$ (ml/minute).

5. Since the rate of flow is relatively small, the effect of head losses in the pipelines and connections can be neglected and the pressure difference across the soil sample is equal to $p_1 - p_2 = \Delta p$ where, $p_2 = 0$ since the free water surface in the burette is maintained at the same level as the sample face from which the water emerges.

The vertical coefficient of permeability is calculated from the following equation:

$$\mathbf{k_v} = \frac{\mathbf{q_v}}{\mathbf{60Ai}} = \frac{\mathbf{q_v\, H}}{\mathbf{60A \times 102\Delta p}} = \frac{\mathbf{q_v\, H}}{\mathbf{6120A\Delta p}} \quad \text{(m/s)}$$

where, q_v is rate of vertical flow (ml/minute), t is time in minutes, A is the area of sample (mm^2) , I is the hydraulic gradient = (102 p_1 - h)/H, Δp is the pressure difference (kPa) = $p_1 - p_2$, H is the height of sample (mm), p_1 and p_2 are inlet and outlet pressure (kPa), h is the head loss due to the height of water in the burette, and k_v is the vertical coefficient of permeability (m/s).

2. Radial Outward Drainage Permeability Test

The arrangement of Rowe cell for permeability test with radial outward drainage is shown in Figure C.25.

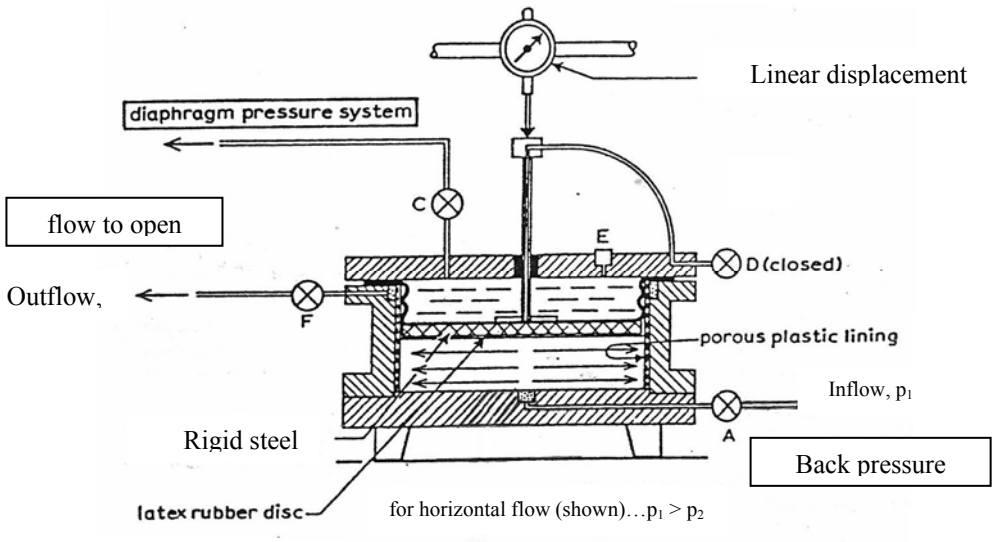

Figure C.25: Arrangement of Rowe cell for permeability test with radial outward drainage (Head, 1986)

The designation of hydraulic permeability test with radial outward drainage is shown in Figure C.26.

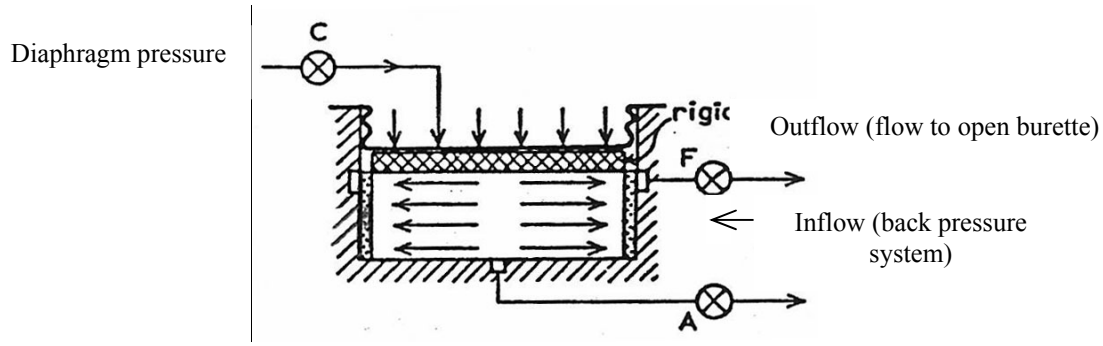

Figure C.26: Radial outward flow condition for permeability test in Rowe cell (Head, 1986)

Sample preparation and assembly of the cell are summarized as follows:

1. Fit a peripheral drain in the cell.
2. Set up the sample in the cell by the method similar to that of Rowe cell consolidation test with vertical drainage (two-way).
3. Form a central sand drain.
4. Place a porous disc sealed with impervious rubber membrane on the sample.
5. Assemble the cell top.

Three independent controlled pressure systems are required, including the one for applying the diaphragm pressure, connected to valve C. The second pressure system is connected to valve F, and the third to valve A. The system on the inlet should incorporate a volume-change gauge. Pore pressure readings are not necessary. Valve D remains close. Permeability measurements are made with the flow horizontally outwards, for which the pressure at B is greater than at F. The difference between these two pressures should be appropriate to the horizontal permeability of the soil, and should be determined by trial until a reasonable rate of flow is obtained.

Radial permeability is measured with the flow of water radially inwards where, equal strain loading condition is applied. The arrangement of the cell and ancillary equipment for both kinds of test is shown in Figure C.25. The top surface

of the sample is sealed with impermeable steel disc. Two independent constant pressure systems are used, as for a vertical permeability test. A diaphragm pressure system is connected to valve C; a back pressure system is connected to the rim drain valve at F, and the central base outlet at A is connected to an open burette. Valve D remains closed.

Since, saturation by incremental back pressure is carried out in order to determine the B value; pore pressure transducer housing is connected to valve G. During saturation, water is admitted to the periphery of the sample from the back pressure through valve F. Valve A and valve B must be closed. When saturation is achieved, valve A that is connected to the open burette, is opened.

Under a constant diaphragm pressure, back pressure is applied to valve F (rim drain) as an inlet pressure, whereas outlet pressure is provided by an open burette connected to valve A. Pore water pressure is measured by the pore pressure transducer connected to valve G with valve B and valve D closed.

The sample is first consolidated to the required effective stress and the consolidation procedure is the same as described in that of Rowe cell vertical permeability test.

Rowe cell radial outward drainage permeability test procedure is as follows:

1. The pressure difference across the sample is adjusted to give a reasonable rate of flow by progressively increasing the inlet pressure without allowing it to equal or exceed the diaphragm pressure.
2. Measure the rate of flow, when a steady state has been achieved.
3. Calculate the horizontal (radial) permeability from the equation below:

$$k_h = \frac{q_h}{60Ai} = \frac{q_h\, r}{60A \times 102\Delta p} = \frac{q_h\, r}{6120A\Delta p} \quad \text{(m/s)}$$

where, q_h is rate of horizontal flow (ml/minute), t is time (minutes), A is $2\pi rH$ (mm^2), I is hydraulic gradient is $(102\ p_1 - h)/r$, Δp is pressure difference (kPa) = $p_1 - p_2$, r is radius of sample (mm), H is height of sample (mm), p_1 is inlet pressure (kPa), p_2 is outlet pressure (kPa) = $(9.81h)/1000$, h is head loss due to the height of water in the burette, k_h is horizontal coefficient of permeability (m/s).

APPENDIX D

RESULTS OF CONSOLIDATION TEST ON ROWE CELL
AND
ANALYSIS OF TIME COMPRESSION CURVE

CONSOLIDATION TEST WITH TWO-WAY VERTICAL DRAINAGE

1. Procedures For Analysis of Time-Compression Curve Based on Robinson's (2003) Method.

Step 1: Log time-compression curves from consolidation test.

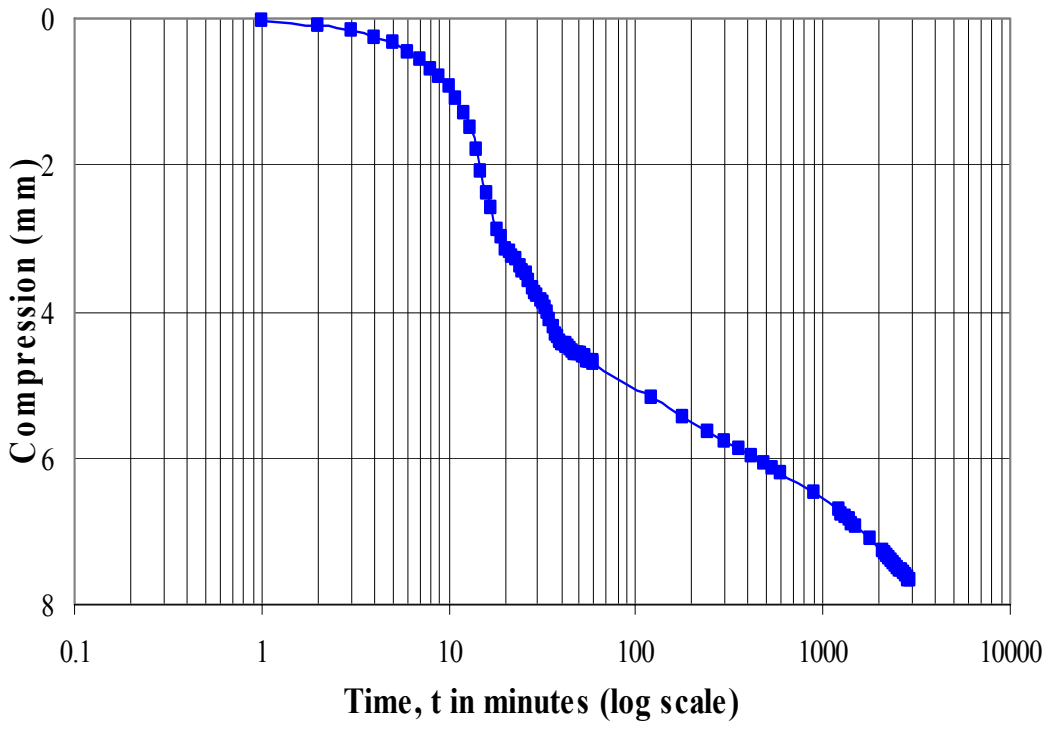

Step 2. Log time-pore water pressure curve

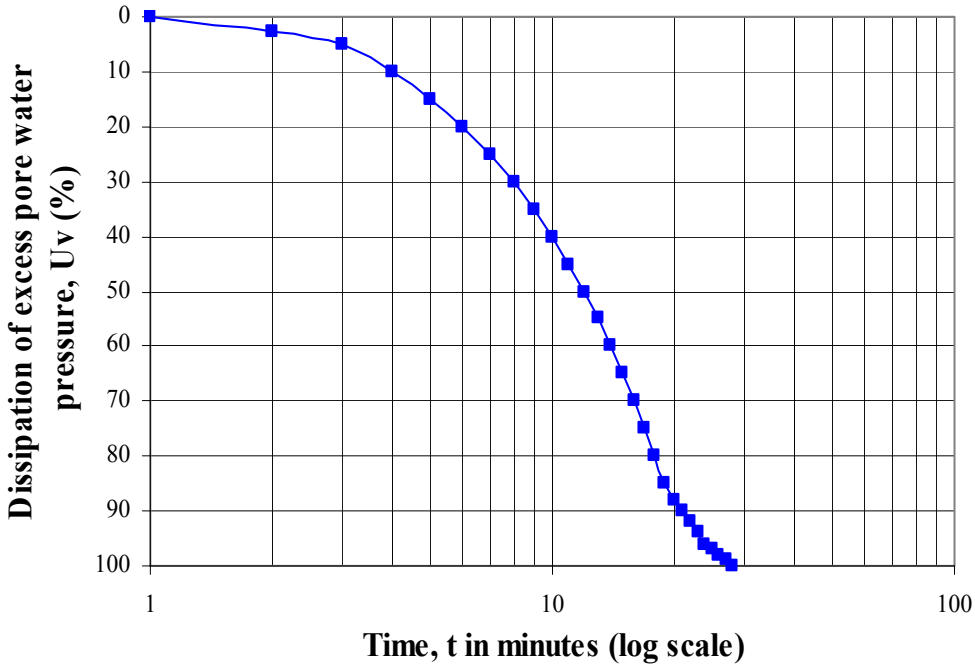

Step 3: Degree of consolidation - compression curve

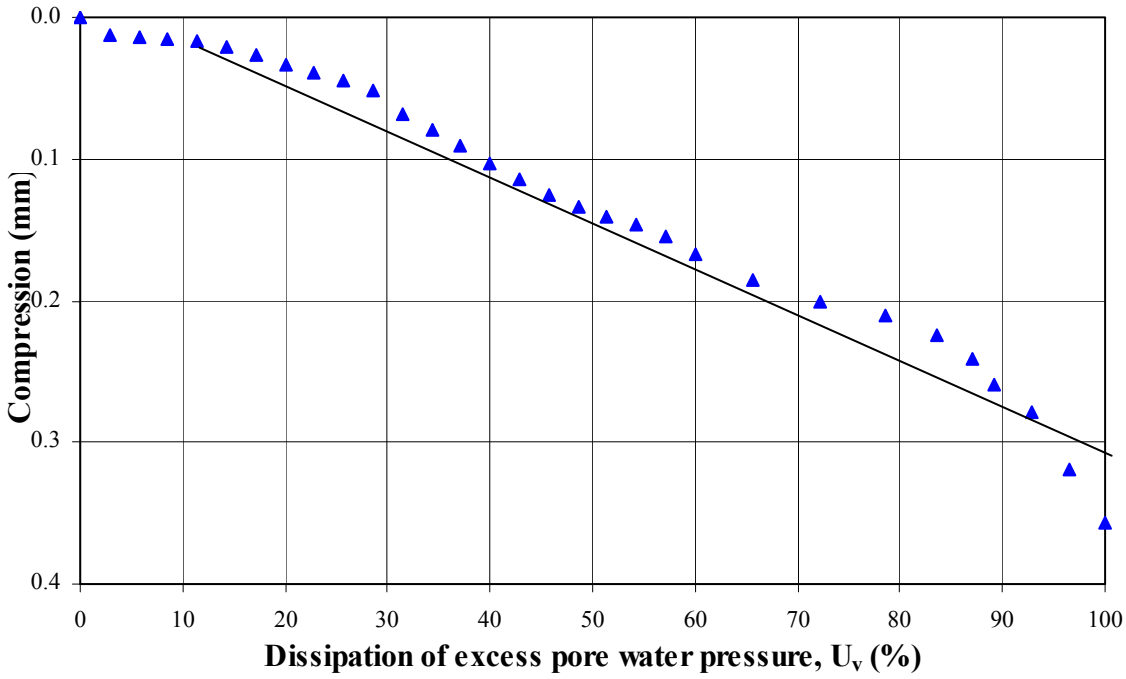

Step 4: Time – total settlement curve

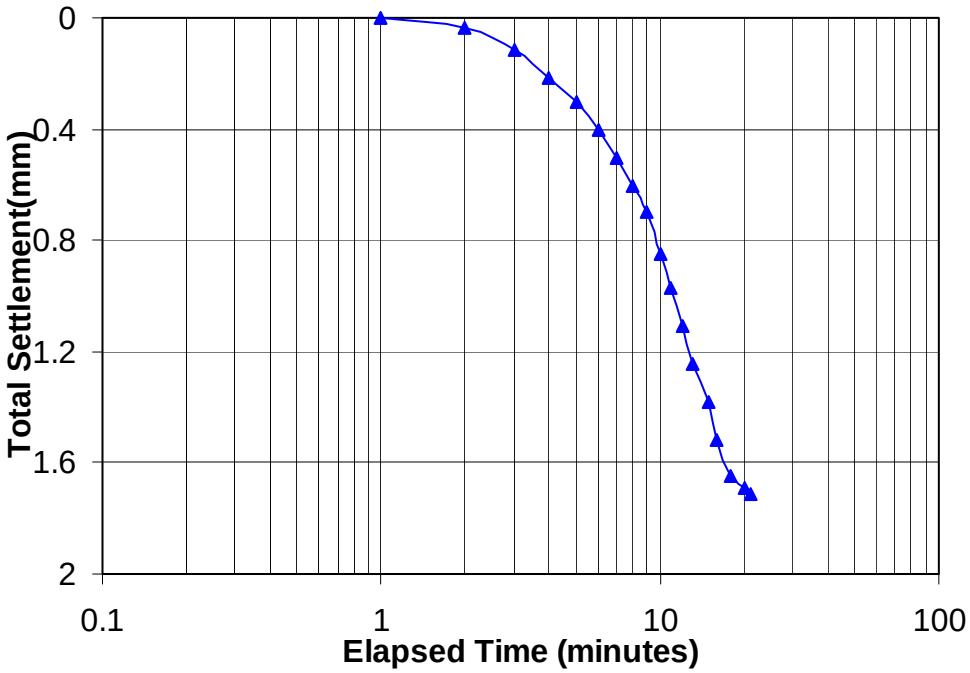

Step 5: Time – primary settlement curve (after removal of the secondary compression)

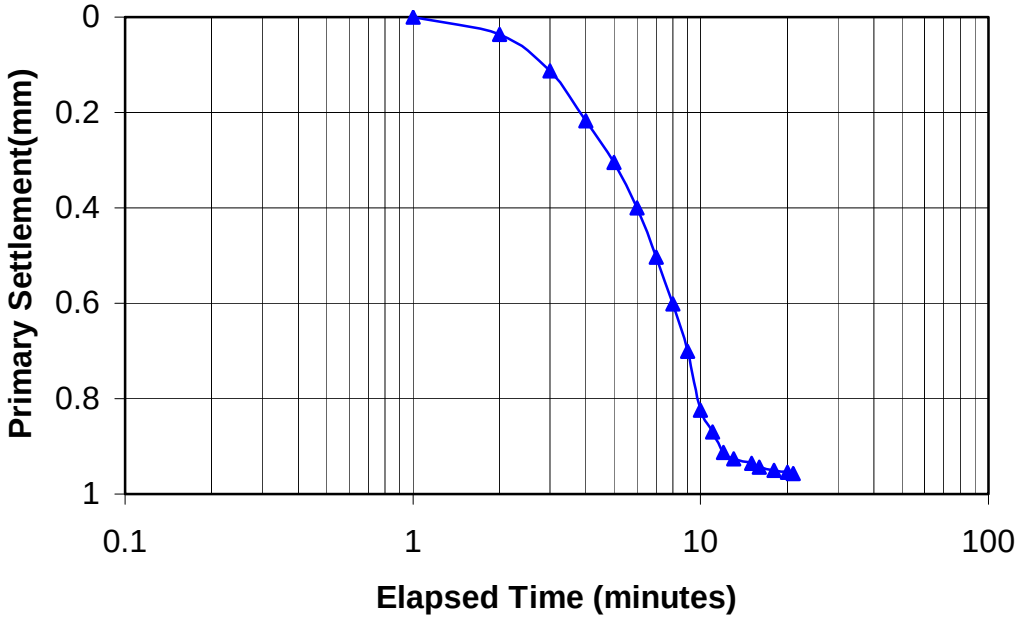

Step 6: Secondary compression-time curve

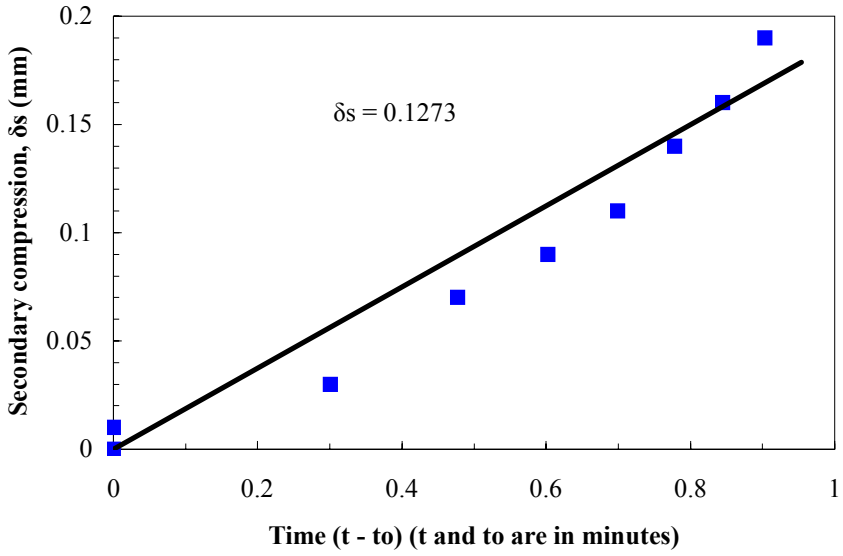

2. Analysis of Consolidation Parameters

Consolidation Pressure		25 kPa	50 kPa	100 kPa	200 kPa
Test 1	$t_{p\,(100)}$ (minutes)	25	24	23	22
	U_v (%)	60	60	58	55
	t_p (minutes)	16.5	14	9.5	6
	c_v (m^2/year)	0.948	0.931	0.849	0.795
	c_α	0.503	0.606	0.726	0.864
Test 2	$t_{p\,(100)}$ (minutes)	30	28	20	20
	U_v (%)	68	65	70	70
	t_p (minutes)	22	19	10	9
	c_v (m^2/year)	2.035	1.525	1.458	0.884
	c_α	0.117	0.127	0.148	0.455
Test 3	$t_{p\,(100)}$ (minutes)	25	21	20	20
	U_v (%)	50	50	64	70
	t_p (minutes)	13	9	9	9
	c_v (m^2/year)	1.691	1.513	1.407	0.967
	c_α	0.118	0.124	0.193	0.248
Test 4	$t_{p\,(100)}$ (minutes)	26	25	24	24
	U_v (%)	60	58	60	65
	t_p (minutes)	14	13	17	18
	c_v (m^2/year)	1.663	1.589	1.064	0.534
	c_α	0.102	0.103	0.12	0.175
Test 5	$t_{p\,(100)}$ (minutes)	31	30	28	27
	U_v (%)	23	22	19	18
	t_p (minutes)	68	72	70	67
	c_v (m^2/year)	1.020	0.960	0.805	0.593
	c_α	0.108	0.115	0.128	0.132

Consolidation Pressure		25 kPa	50 kPa	100 kPa	200 kPa
Average	$t_{p\,(100)}$ (minutes)	27.40	25.60	23.0	22.6
	U_v (%)	64.60	60.10	56.10	53.10
	t_p (minutes)	17.70	15.40	12.90	12.00
	c_v (m^2/year)	1.471	1.304	1.117	0.755
	c_α	0.190	0.215	0.263	0.375

3. Calculation of Permeability

Consolidation Pressure		25 kPa	50 kPa	100 kPa	200 kPa
Test 1	a_v	0.007	0.021	0.019	0.013
	m_v (1/kPa)	0.00082	0.00230	0.00208	0.00144
	c_h (m^2/year)	0.948	0.931	0.849	0.796
	k_h (m/s)	$0.26\text{x}10^{-10}$	$6.80\text{x}10^{-10}$	$0.56\text{x}10^{-10}$	$0.36\text{x}10^{-10}$
Test 2	a_v	0.019	0.029	0.019	0.010
	m_v (1/kPa)	0.00203	0.00310	0.00204	0.00113
	c_h (m^2/year)	2.035	1.525	1.458	0.884
	k_h (m/s)	$1.31\text{x}10^{-10}$	$15.0\text{x}10^{-10}$	$0.94\text{x}10^{-10}$	$0.32\text{x}10^{-10}$
Test 3	a_v	0.013	0.042	0.023	0.016
	m_v (1/kPa)	0.00122	0.00410	0.00219	0.00154
	c_h (m^2/year)	1.691	1.513	1.407	0.967
	k_h (m/s)	$0.65\text{x}10^{-10}$	$19.7\text{x}10^{-10}$	$0.98\text{x}10^{-10}$	$0.47\text{x}10^{-10}$
Test 4	a_v	0.032	0.043	0.022	0.011
	m_v (1/kPa)	0.00374	0.00506	0.00256	0.00125
	c_h (m^2/year)	1.663	1.589	1.064	0.534
	k_h (m/s)	$1.97\text{x}10^{-3}$	$25.5\text{x}10^{-10}$	$0.86\text{x}10^{-10}$	$0.21\text{x}10^{-10}$
Test 5	a_v	0.012	0.020	0.014	0.017
	m_v (1/kPa)	0.00117	0.00199	0.00138	0.00165
	c_h (m^2/year)	1.020	0.960	0.805	0.593
	k_h (m/s)	$0.38\text{x}10^{-10}$	$6.10\text{x}10^{-10}$	$0.35\text{x}10^{-10}$	$0.31\text{x}10^{-10}$
Average	**a_v**	**0.017**	**0.031**	**0.019**	**0.013**
	m_v (1/kPa)	**0.00179**	**0.00331**	**0.00205**	**0.00140**
	c_h (m^2/year)	**1.471**	**1.304**	**1.117**	**0.755**
	k_h (m/s)	**$0.91\text{x}10^{-10}$**	**$1.46\text{x}10^{-10}$**	**$0.74\text{x}10^{-10}$**	**$0.33\text{x}10^{-10}$**

APPENDIX E

RESULTS OF CONSOLIDATION TEST ON ROWE CELL AND ANALYSIS OF TIME COMPRESSION CURVE

CONSOLIDATION TEST WITH HORIZONTAL DRAINAGE

1. Procedures for Analysis of Time-Compression Curve Based on Robinson'S (2003) Method.

Step 1: Log time-compression curves from consolidation test.

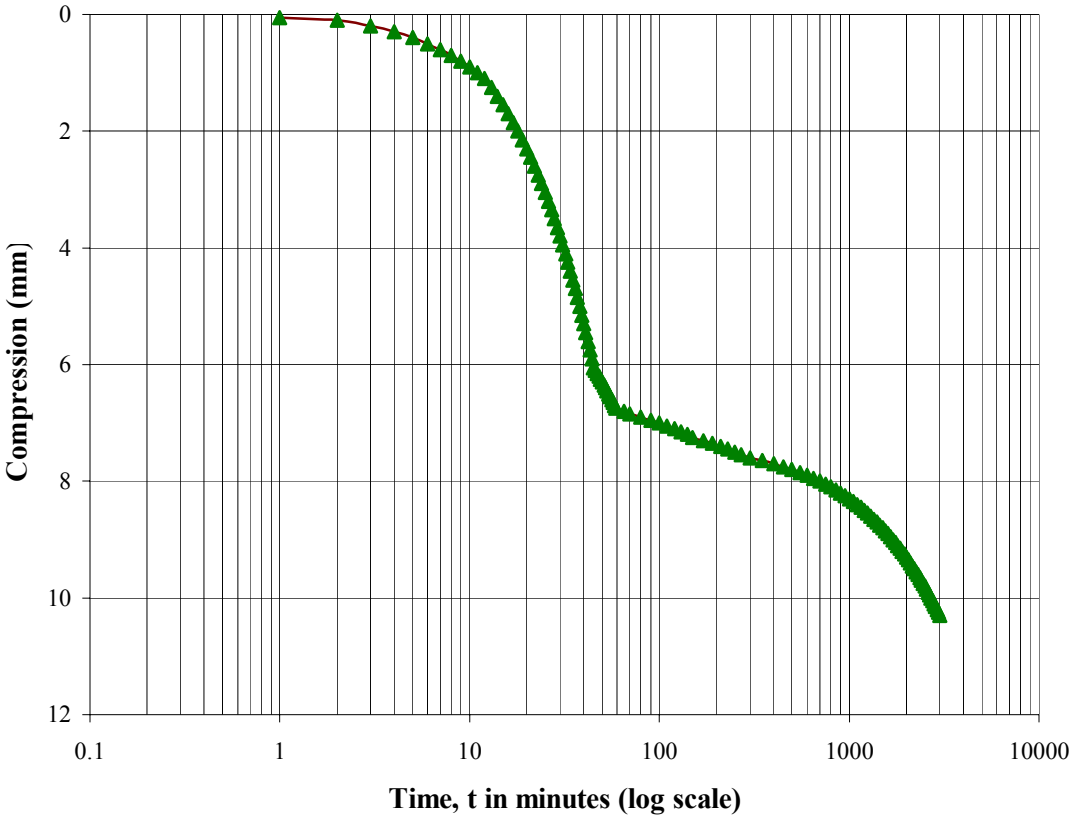

Step 2. Log time-pore water pressure curve

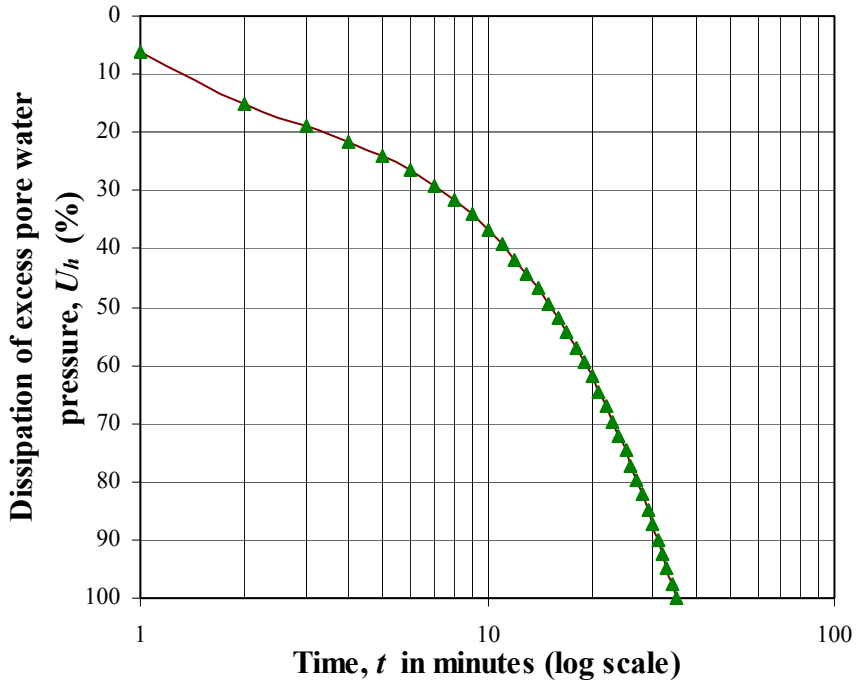

Step 3: Degree of consolidation - compression curve

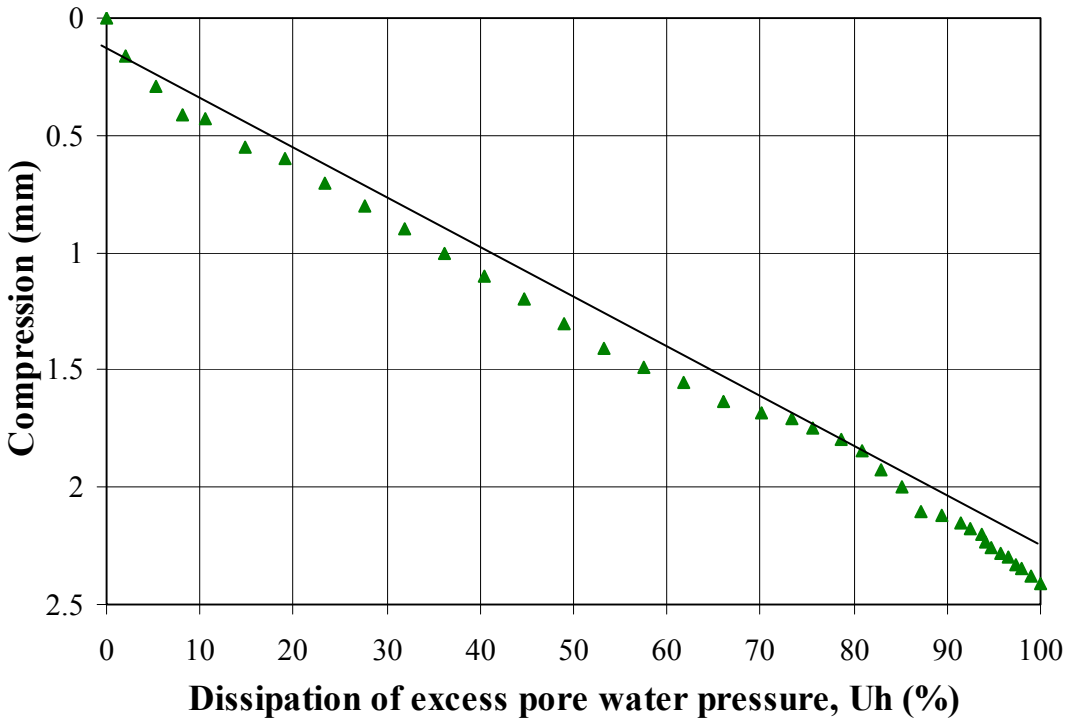

Step 4: Time – total settlement curve

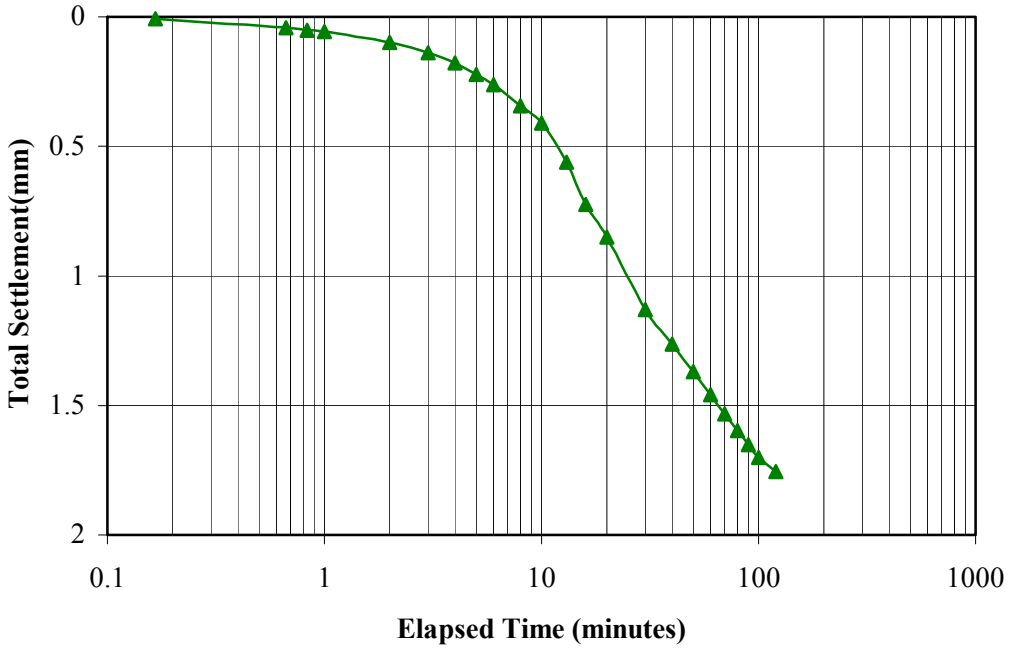

Step 5: Time – primary settlement curve (after removal of the secondary compression)

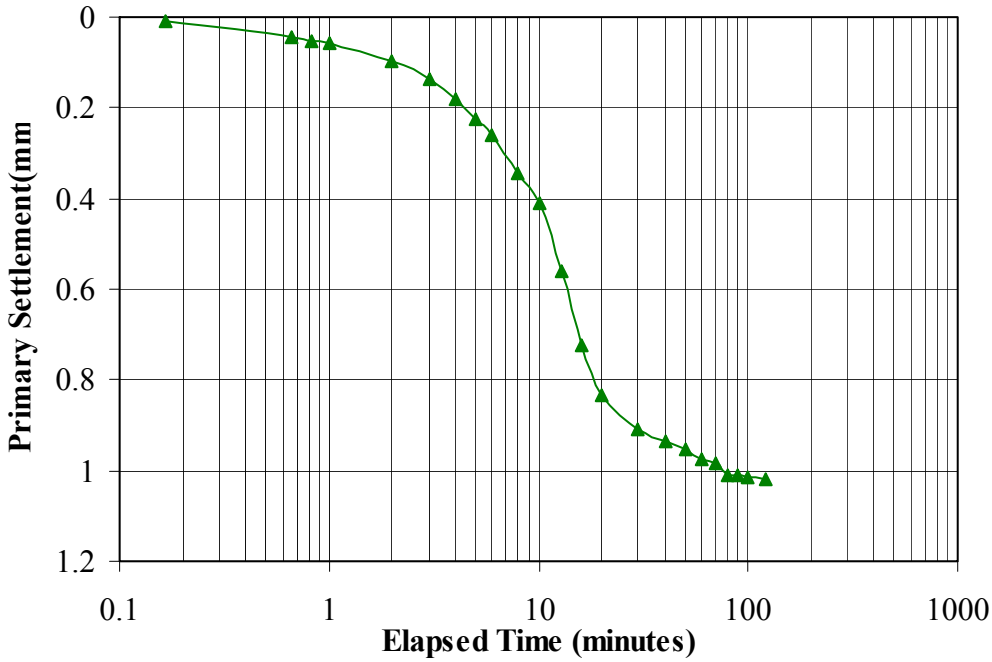

Step 6: Secondary compression-time curve

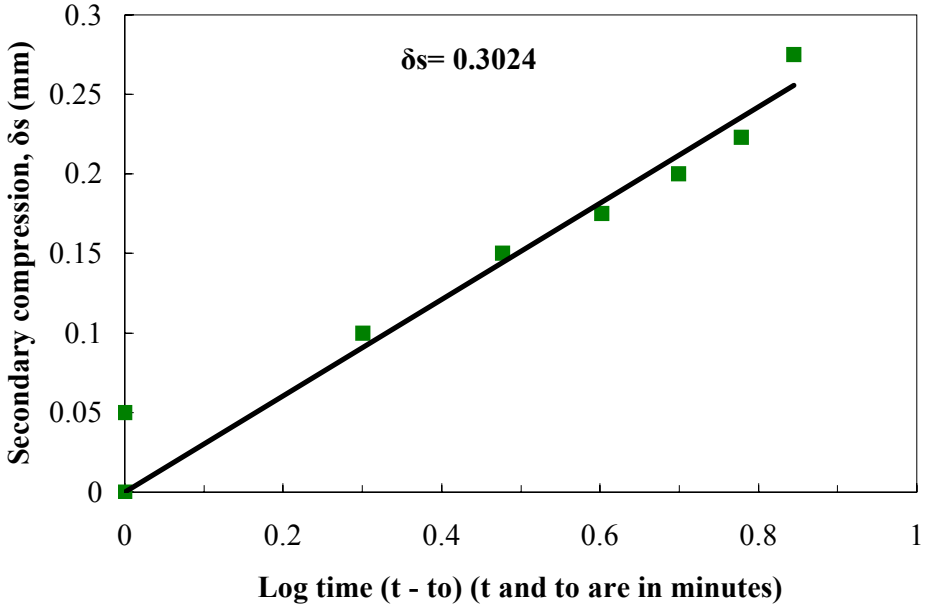

2. Analysis of Consolidation Parameters

Consolidation Pressure		**25 kPa**	**50 kPa**	**100 kPa**	**200 kPa**
Test 1	$t_{p\,(100)}$ (minutes)	44	39	36	32
	U_h (%)	82	70	60	65
	t_p (minutes)	42	35	28	20
	c_v (m^2/year)	5.143	5.085	4.980	4.565
	c_α	0.101	0.104	0.122	0.152
Test 2	$t_{p\,(100)}$ (minutes)	41	35	32	30
	U_h (%)	80	80	70	60
	t_p (minutes)	34	28	20	18
	c_v (m^2/year)	4.121	3.912	3.703	3.630
	c_α	0.199	0.3024	0.337	0.424
Test 3	$t_{p\,(100)}$ (minutes)	39	37	35	32
	U_h (%)	80	80	70	65
	t_p (minutes)	24	22	20	20
	c_v (m^2/year)	6.384	6.200	5.956	5.243
	c_α	0.399	0.358	0.646	0.952
Average	**$t_{p\,(100)}$ (minutes)**	**41.3**	**37.0**	**34.3**	**31.3**
	U_h (%)	**80.60**	**76.50**	**66.20**	**61.40**
	t_p (minutes)	**33.33**	**28.33**	**22.67**	**19.33**
	c_v (m^2/year)	**5.216**	**5.066**	**4.880**	**4.479**
	c_α	**0.233**	**0.255**	**0.368**	**0.509**

3. Calculation of Permeability

Consolidation Pressure		**25 kPa**	**50 kPa**	**100 kPa**	**200 kPa**
Test 1	a_v	0.018	0.028	0.014	0.010
	m_v (1/kPa)	0.00171	0.00263	0.00132	0.00095
	c_h (m^2/year)	5.143	5.085	4.980	4.565
	k_h (m/s)	$0.27x10^{-10}$	$4.24x10^{-10}$	$2.08x10^{-10}$	$1.38x10^{-10}$
Test 2	a_v	0.030	0.035	0.019	0.012
	m_v (1/kPa)	0.00264	0.00310	0.00169	0.00105
	c_h (m^2/year)	4.121	3.912	3.703	3.630
	k_h (m/s)	$0.34x10^{-10}$	$3.90x10^{-10}$	$1.99x10^{-10}$	$1.21x10^{-10}$
Test 3	a_v	0.010	0.015	0.011	0.007
	m_v (1/kPa)	0.00106	0.00155	0.00120	0.00074
	c_h (m^2/year)	6.384	6.200	5.956	5.243
	k_h (m/s)	$0.21x10^{-10}$	$3.05x10^{-10}$	$2.27x10^{-10}$	$1.24x10^{-10}$
Average	**a_v**	**0.019**	**0.026**	**0.015**	**0.010**
	m_v (1/kPa)	**0.00180**	**0.00243**	**0.00140**	**0.00091**
	c_h (m^2/year)	**5.216**	**5.066**	**4.880**	**4.479**
	k_h (m/s)	**$0.28x10^{-10}$**	**$3.73x10^{-10}$**	**$2.11x10^{-10}$**	**$1.28x10^{-10}$**

APPENDIX F

Results of Permeability Tests

1. Constan Head Permeability

A. Apparatus

Figure F1: The piston sample using for permeability test

Figure F1: The equipment for permeability test

Figure F3: Constan Head Permeability Test

B. Procedure of Constan Head Permeability

The apparatus for constant head permeability such a: (a) Permeameter cell, fitted with loading piston,perforated plates, flow tube connections, piezometer nipples and connections, air bleed valve, sealing rings, (b) Glass piezometer tubes, (c) Rubber tubing, (d) Uniform fine gravel, or glass balls, for end filter layers, (e) Two disc of wire gauze, of the same diameter as the internal cell diameter, (f) Two porous stone or sintered bronze disc of the same diameter, (g) Measuring cylinders: 500 ml and 100 ml, (h) Constant head reservoir, (i) Outlet reservoir with overflow to maintain a constant water level, (j) Supply of clean water, (k) Small tools: funnel, tamping rod, scoop, etc., (l) Thermometer, (m) Stop-clock (minutes timer).

The general arrangement diagram of the test system is shown in figure F4.

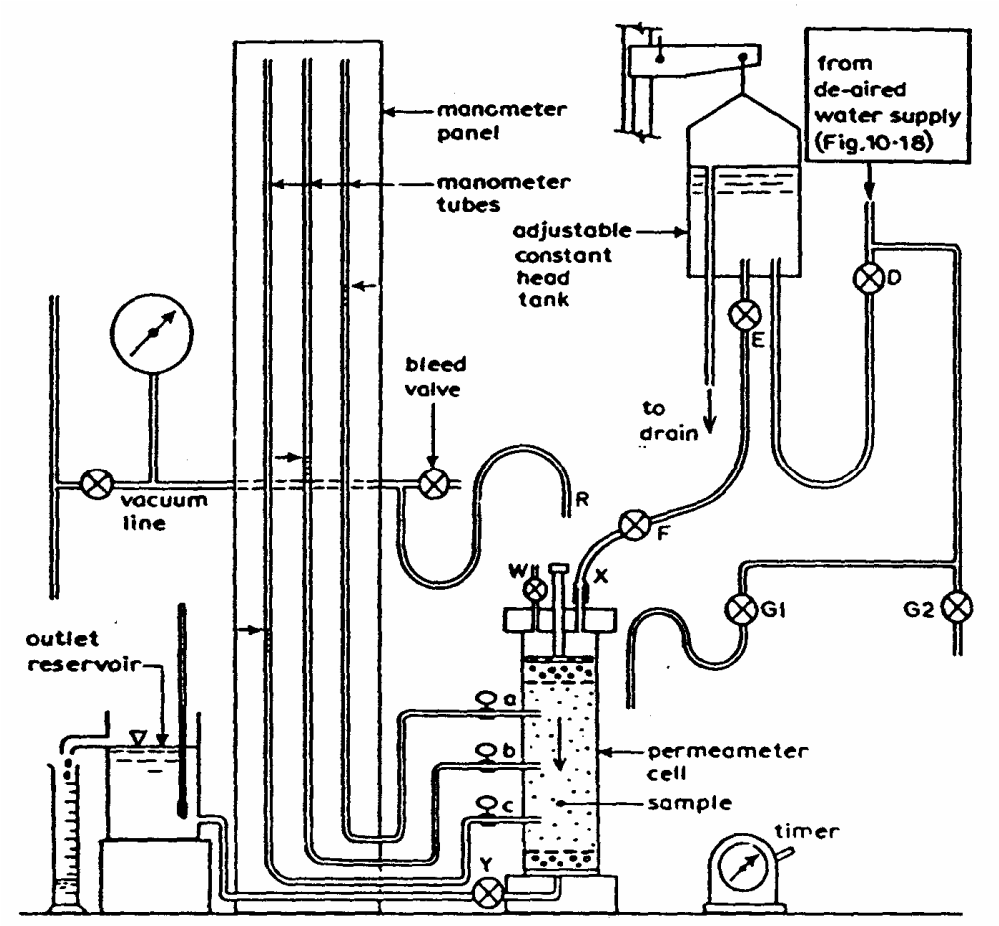

Figure F4: General Arrangement for Constant Head Permebility Test (downward flow) (Head, 1981)

The test procedure for constant head permeability:

1. Preparation of ancillary apparatus.
2. Preparation of permeameter cell.
3. Selection of sample.
4. Preparation of test sample.
5. Placing sample in cell.
6. Assembling cell.
7. Connections to cell.
8. Saturation of sample.
9. Connections for test.
10. Running the test.
11. Repeat tests.
12. Dismantling cell.
13. Calculations.

For the calculations, a quantity of water Q ml flows through a sample in a time of t min, the mean rate of flow q is equal Q/t ml/min or Q/60t ml/s. The hydraulic gradient i between two adjacent manometer points a distance L mm apart, giving manometer levels h_1, h_2 mm above a datum, is calculated from the equation :

$$\mathbf{i} = \frac{\mathbf{h_1 - h_2}}{\mathbf{L}}$$

If the area of cross-section of the sample is equal to A mm2, the permeability K_T (m/s) of the sample at T°C is calculated from equation :

$$K_T = \frac{\mathbf{Q}}{\mathbf{60\ Ait}}$$

C. Results of Constant Head Permeability Test

A. Horizontal Samples

1. Sample No.1

Date of testing the sample: 31st May 2005
Measuring beaker capacity: 200 ml
Mass of sample + mould: 2333 g
Mass of mould: 1373 g
Mass of sample: 960 g

Hydraulic gradient, i	*Horizontal rate of flow, q (ml/ min.)*	*Horizontal rate of flow, q (m^3/ s)*	*Horizontal flow velocity, v (m/ s)*
3.34	10.31	0.00000017	0.00001970
4.99	13.85	0.00000023	0.00002646
6.64	20.47	0.00000034	0.00003910
7.47	22.02	0.00000037	0.00004206
7.88	27.07	0.00000045	0.00005171
8.29	24.99	0.00000042	0.00004774

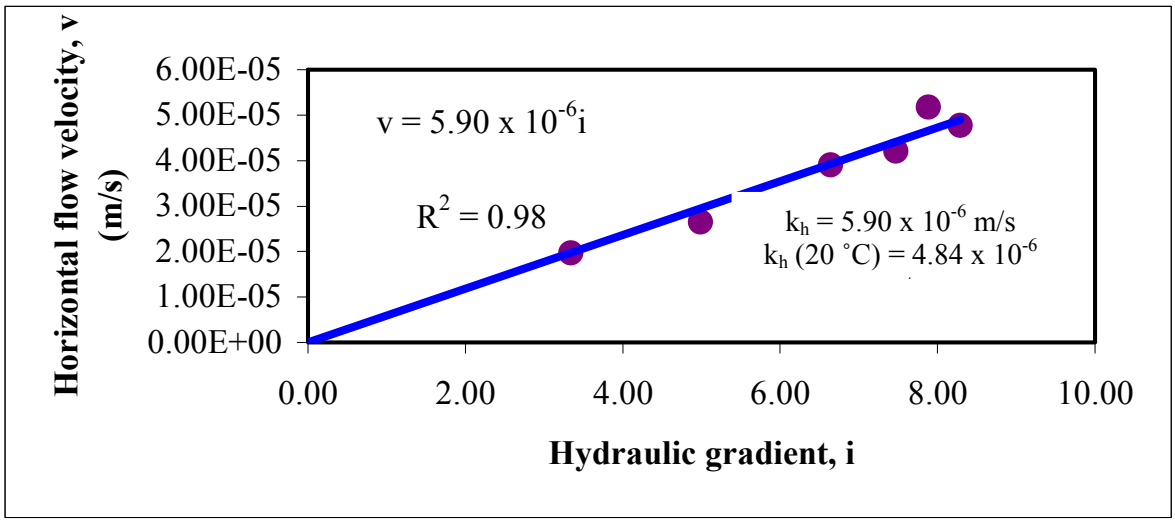

2. Sample No.2

Date of testing the sample: 2nd June 2005
Measuring beaker capacity: 200 ml
Mass of sample + mould: 2403 g
Mass of mould: 1375 g
Mass of sample: 1028 g

Hydraulic gradient, i	***Horizontal rate of flow, q (ml/ min.)***	***Horizontal rate of flow, q (m^3/ s)***	***Horizontal flow velocity, v (m/ s)***
3.34	15.70	0.00000026	0.00002999
4.99	24.23	0.00000040	0.00004628
6.64	33.72	0.00000056	0.00006441
7.47	36.23	0.00000060	0.00006921
7.88	37.12	0.00000062	0.00007091
8.29	37.34	0.00000062	0.00007133

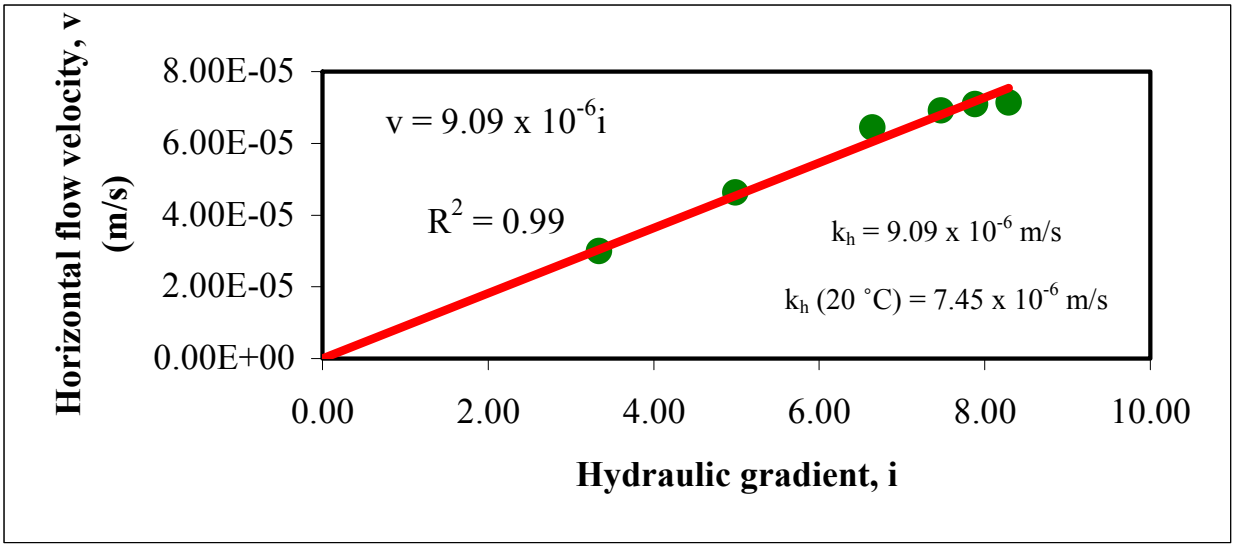

3. Sample No.3

Date of testing the sample: 3rd June 2005
Measuring beaker capacity: 1000 ml
Mass of sample + mould: 2305 g
Mass of mould: 1345 g
Mass of sample: 960 g

Hydraulic gradient, i	*Horizontal rate of flow, q (ml/ min.)*	*Horizontal rate of flow, q (m^3/ s)*	*Horizontal flow velocity, v (m/ s)*
2.10	409.21	0.00000682	0.00078167
2.52	432.22	0.00000720	0.00082562
2.93	445.24	0.00000742	0.00085050
3.34	456.69	0.00000761	0.00087237
3.75	452.19	0.00000754	0.00086377
4.17	460.27	0.00000767	0.00087921
4.58	475.22	0.00000792	0.00090776
4.99	481.21	0.00000802	0.00091921
5.40	613.45	0.00001022	0.00117181
5.82	630.69	0.00001051	0.00120474

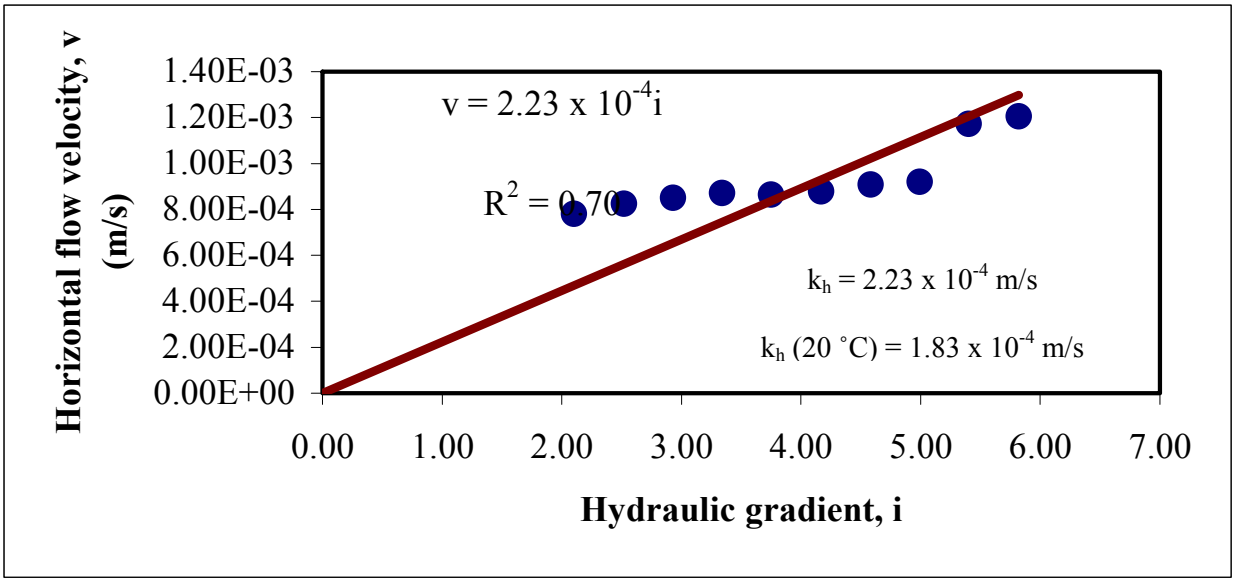

4. Sample No.4

Date of testing the sample: 3rd June 2005
Measuring beaker capacity: 1000 ml
Mass of sample + mould: 2403 g
Mass of mould: 1371 g
Mass of sample: 1032 g

Hydraulic gradient, i	*Horizontal rate of flow, q (ml/ min.)*	*Horizontal rate of flow, q (m^3/ s)*	*Horizontal flow velocity, v (m/ s)*
2.10	397.35	0.00000662	0.00075902
2.52	422.52	0.00000704	0.00080710
2.93	433.68	0.00000723	0.00082841
3.34	468.03	0.00000780	0.00089403
3.75	447.73	0.00000746	0.00085525
4.17	456.08	0.00000760	0.00087120
4.58	463.13	0.00000772	0.00088467
4.99	557.96	0.00000930	0.00106581
5.40	593.14	0.00000989	0.00113301
5.82	626.42	0.00001044	0.00119658

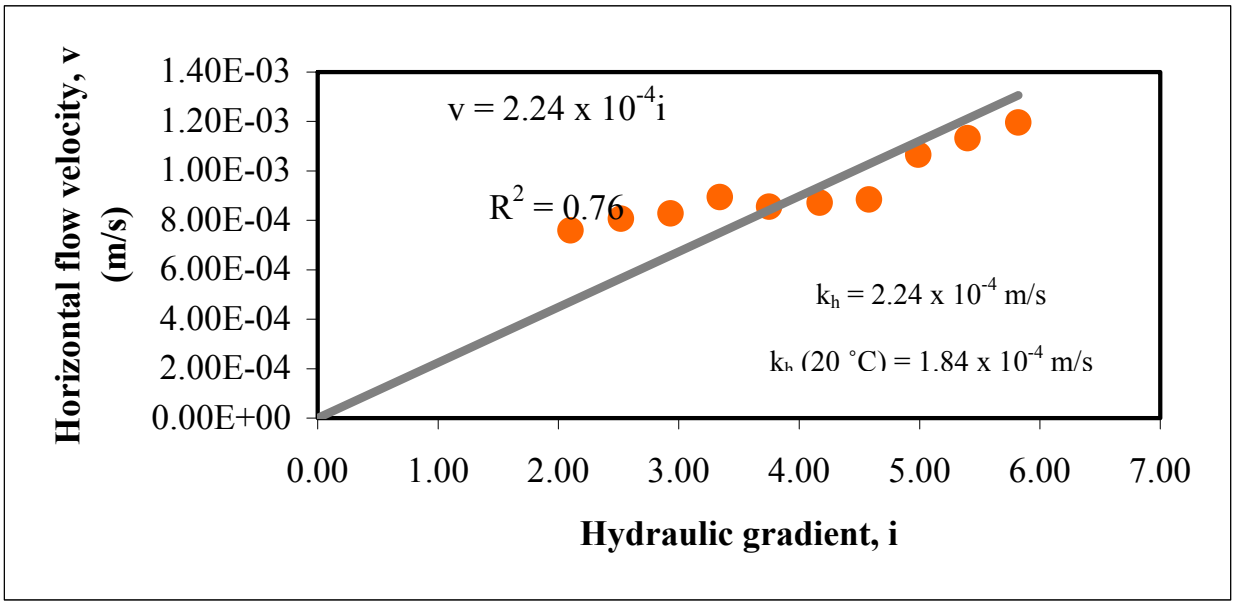

Average horizontal coefficient of permeability at 29 °C, k_h = 1.15 x 10^{-4} m/s

Average horizontal coefficient of permeability at 20 ˚C, k_h (20 ˚C) = 9.48 x 10^{-5} m/s

B. Vertical Samples

1. Sample No.5

Date of testing the sample: 28th May 2005
Measuring beaker capacity: 1000 ml
Mass of sample + mould: 2295 g
Mass of mould: 1349 g
Mass of sample: 946 g

Hydraulic gradient, i	***Vertical rate of flow, q (ml/ min.)***	***Vertical rate of flow, q (m^3/ s)***	***Vertical flow velocity, v (m/ s)***
3.34	85.67	0.00000143	0.00016365
4.99	142.92	0.00000238	0.00027301
6.64	214.62	0.00000358	0.00040997
7.47	237.77	0.00000396	0.00045419
7.88	255.03	0.00000425	0.00048716
8.29	274.67	0.00000458	0.00052467

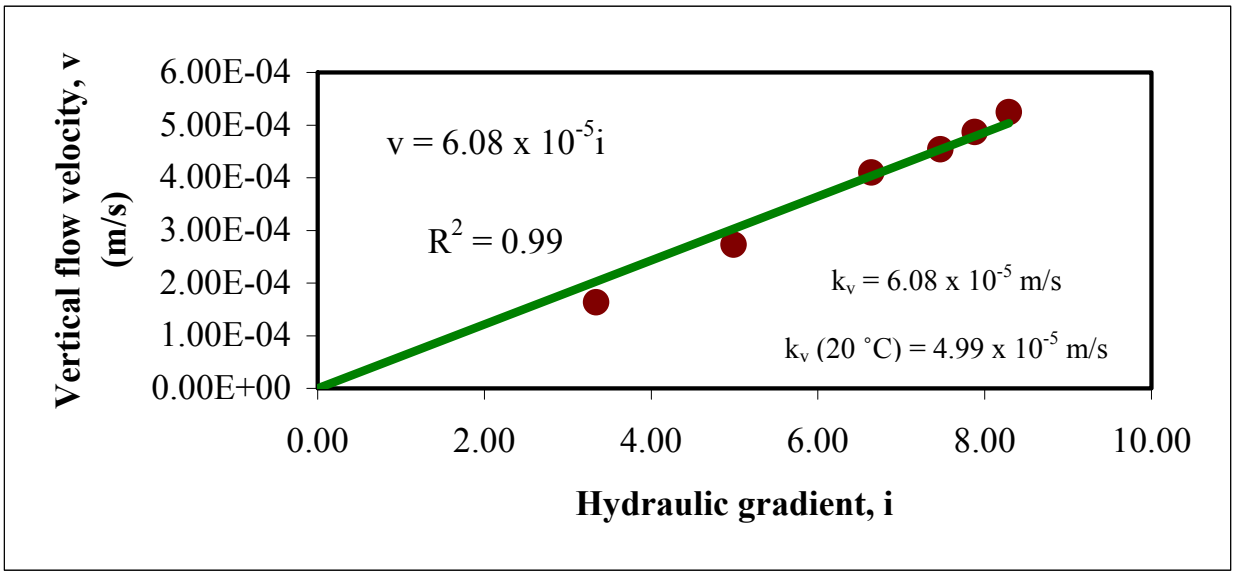

2. Sample No.6

Date of testing the sample: 2nd June 2005
Measuring beaker capacity: 1000 ml
Mass of sample + mould: 1941 g
Mass of mould: 985 g
Mass of sample: 956 g

Hydraulic gradient, i	***Vertical rate of flow, q (ml/ min.)***	***Vertical rate of flow, q (m^3/ s)***	***Vertical flow velocity, v (m/ s)***
2.10	422.82	0.00000705	0.00080767
2.52	432.12	0.00000720	0.00082543
2.93	441.78	0.00000736	0.00084389
3.34	462.57	0.00000771	0.00088360
3.75	462.80	0.00000771	0.00088404
4.17	504.63	0.00000841	0.00096394

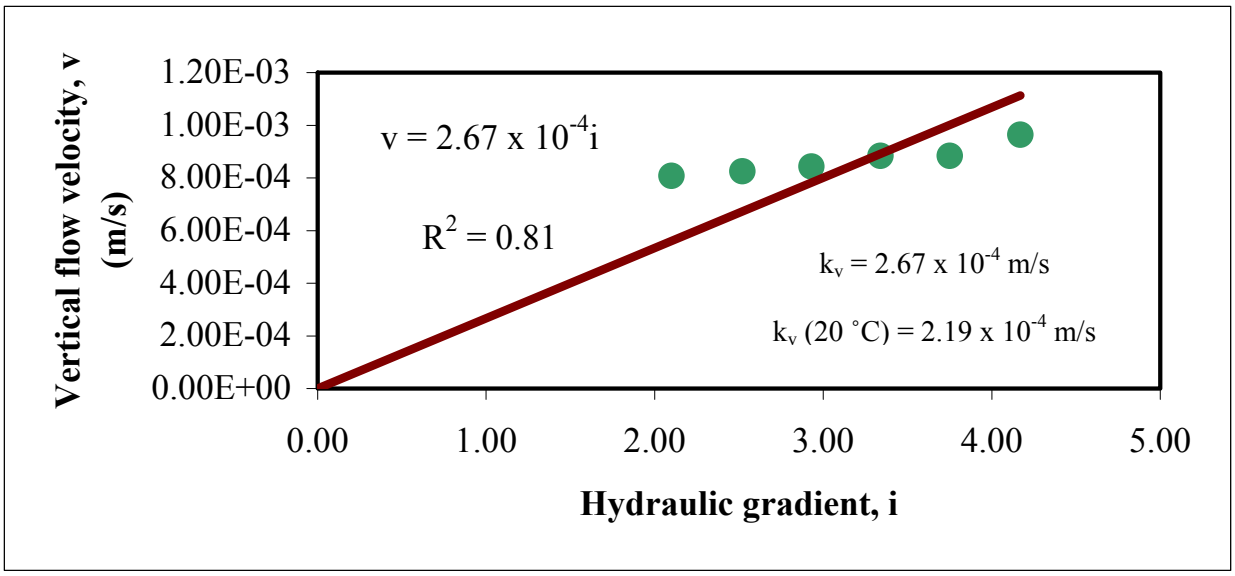

3. Sample No.7

Date of testing the sample: 2nd June 2005
Measuring beaker capacity: 1000 ml
Mass of sample + mould: 2334 g
Mass of mould: 1345 g
Mass of sample: 989 g

Hydraulic gradient, i	*Vertical rate of flow, q (ml/ min.)*	***Vertical rate of flow,q (m^3/ s)***	***Vertical flow velocity, v (m/ s)***
3.34	254.20	0.00000424	0.00048557
4.99	337.89	0.00000563	0.00064544
6.64	398.64	0.00000664	0.00076148
7.47	430.84	0.00000718	0.00082299
7.88	432.29	0.00000720	0.00082576
8.29	437.65	0.00000729	0.00083600

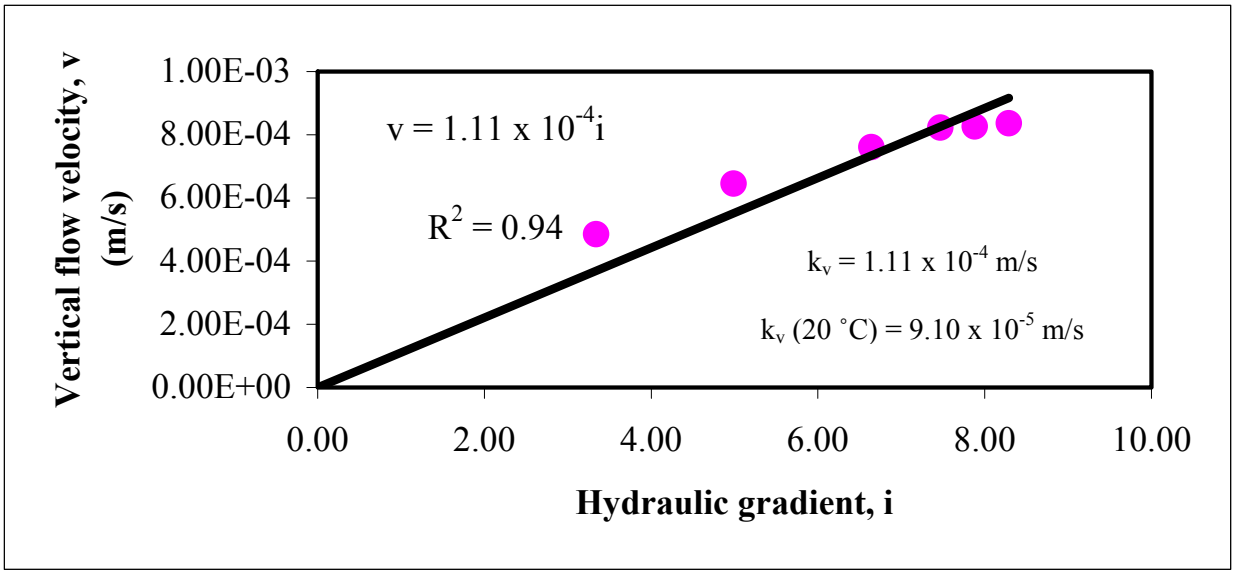

Average vertical coefficient of permeability at 29 ˚C, k_v = 1.46 x 10^{-4} m/s

Average vertical coefficient of permeability at 20 ˚C, k_v (20 ˚C) = 1.20 x 10^{-4} m/s

Conclusion: **k_h / k_v = 0.79**
k_h < k_v

Data Summary of Constant Head Permeability Test of fibrous peat soil samples obtained from Kampung Bahru, Pontian, Johor

Date of sampling: ***21st – 23rd May 2005***
Water temperature: ***29 ˚C***
Flow: ***Downwards***
Sample diameter: ***105.40 mm***
Sample length: ***121.20 mm***
Sample area: ***8725.11 mm^2***
Sample volume: ***1057483.80 mm^3***
Mould internal diameter: ***105.40 mm***
Mould external diameter: ***113.50 mm***
External diameter of piston tube: ***108.00 mm***
Internal diameter of piston tube: ***105.40 mm***
Length of piston tube: ***457.00 mm***

Data of coefficient of permeability at 20°C, *k (20℃)* versus void ratio, *e* of Pontian Fibrous Peat Soil Samples

A. Horizontal samples

Horizontal sample no.	Total mass of initial soil sample, M_T (kg)	Total volume of initial sample, V_T (m^3)	Bulk density, ρ (kg/m^3)	Moisture content, *w* (%)	Dry density, ρ_d (kg/m^3)	Initial void ratio, e_o	Horizontal coefficient of permeability at 20°C, k_h (20°C) (m/s)
1	0.960	0.0010574838	907.82	460.50	161.97	8.36	0.00000484
2	1.028	0.0010574838	972.12	522.64	156.13	8.71	0.00000745
3	0.960	0.0010574838	907.82	609.60	127.93	10.85	0.00018300
4	1.032	0.0010574838	975.90	664.76	127.61	10.88	0.00018400

B. Vertical samples

Vertical sample no.	Total mass of initial soil sample, M_T (kg)	Total volume of initial sample, V_T (m^3)	Bulk density, ρ (kg/m^3)	Moisture content, *w* (%)	Dry density, ρ_d (kg/m^3)	Initial void ratio, e_o	Vertical coefficient of permeability at 20°C, k_v (20°C) (m/s)
1	0.946	0.0010574838	894.58	526.68	142.75	9.62	0.00004990
2	0.956	0.0010574838	904.03	578.02	133.33	10.37	0.00021900
3	0.989	0.0010574838	935.24	679.16	120.03	11.63	0.00091000

2. Hydraulic Permeability Test

Note: Please refer to Appendix C for Procedure for Hydraulic permeability test on Rowe Cell

Type of permeability test	Hydraulic permeability test	Consolidation Pressure (kPa)	Coefficient of permeability at 20° C
Double Vertical Drainage	Test 1	200	k_v (20°C) = 2.36 x 10^{-10} m/s
	Test 2	200	k_v (20°C) = 8.82 x 10^{-10} m/s
	Test 3	200	k_v (20°C) = 4.02 x 10^{-10} m/s
Average			**k_v (20°C) = 5.07 x 10^{-10} m/s**

Type of permeability test	Hydraulic permeability test	Consolidation Pressure (kPa)	Coefficient of permeability at 20° C
Double Vertical Drainage	Test 1	100	k_v (20°C) = 2.10 x 10^{-9} m/s
	Test 2	100	k_v (20°C) = 1.32 x 10^{-9} m/s
	Test 3	100	k_v (20°C) = 3.83 x 10^{-9} m/s
Average			k_v (20°C) = 2.71 x 10^{-9} m/s

Type of permeability test	Hydraulic permeability test	Consolidation Pressure (kPa)	Coefficient of permeability at 20° C
Horizontal Drainage	Test 1	200	k_h (20°C) = 4.29 x 10^{-9} m/s
	Test 2	200	k_h (20°C) = 2.42 x 10^{-9} m/s
	Test 3	200	k_h (20°C) = 1.08 x 10^{-9} m/s
Average			k_h (20°C) = 2.60 x 10^{-9} m/s

Sample Calculation for two-way vertical permeability test 3:

Formula : $\mathbf{k_v = \frac{q_v}{60Ai} = \frac{q_v H}{60A \times 102\Delta p} = \frac{q_v H}{6120A\Delta p}}$

$$q_v = \frac{\delta Q}{\delta t} = \frac{70}{23} = 3.043 \text{ ml/minute}$$

H = 2.4 cm = 24 mm

$$A = \frac{\pi D^2}{4} = \frac{\pi (151.4)^2}{4} = 18002.865 \text{ mm}^2$$

p_1 = 180 kPa

h = 70 x 6 = 420 mm

$$p_2 = \frac{9.81 h}{100} = \frac{9.81 \times 420}{100} = 4.120 \text{ kPa}$$

$\Delta P = p_1 - p_2 = 180 - 4.120 = 175.880$ kPa

$$k_v = \frac{q_v H}{6120 A \Delta P} = \frac{3.043 \times 420}{6120 \times 18002.865 \times 175.880} = 3.765 \times 10^{-9} \text{ m/s}$$

k_v (29^oC) = 3.765×10^{-9} m/s

k_v (20^oC) = (3.765×10^{-9}) x Rt = (3.765×10^{-9}) x (0.91) = 3.43×10^{-9} m/s

where,

q_v is rate of horizontal flow (ml/minute),

t is time (minutes),

A is the area of sample (mm^2),

i is the hydraulic gradient = (102 p_1 - h)/H,

Δp is the pressure difference (kPa) = $p_1 - p_2$,

H is height of sample (mm),

p_1 and p_2 are inlet and outlet pressure (kPa),

h is the head loss due to the height of water in the burette,

Rt is correction factor refer to figure 4 BS 1377 part 5, and

k_v is the vertical coefficient of permeability (m/s)